Electronic Supplementary Material (ESI) for Dalton Transactions.

Supporting Information for

Cycloaddition of isoselenocyanates to sodium and magnesium metallacycles

Vladimir A. Dodonov,[a] Olga A. Kushnerova,[a] Roman V. Rumyantsev,[a] Alexander S. Novikov,[b] Vladimir K. Osmanov[c] and Igor L. Fedushkin*[a]

[a] *G.A. Razuvaev Institute of Organometallic Chemistry of Russian Academy of Sciences, Tropinina str. 49, Nizhny Novgorod 603137, Russia. Email: igorfed@iomc.ras.ru*
[b] *Institute of Chemistry, Saint Petersburg State University Universitetskaya Nab., 7/9, Saint Petersburg 199034, Russia. Email:a.s.novikov@spbu.ru*
[c] *Nizhny Novgorod State Technical University. Minina str. 24, N. Novgorod 603155, Russia. tantalovk@yandex.ru*

Experimental Section

All the manipulations with air- and moisture-sensitive compounds were carried out in vacuum or under argon using standard Schlenk technique or under argon atmosphere in a drybox. Solvents (toluene, 1,2-dimethoxyethane, pyridine, THF, CH_2Cl_2, $CHCl_3$, hexane and pentane) were dried using appropriate methods and were distilled under argon or condensed in vacuo prior to use. THF-d_8 and benzene-d_6 were dried over Na/K alloy. [(dpp-bian)GaNa$(DME)_2$],[1] [(H-dpp-bian)Na$(DME)_2$],[2] [(dpp-bian)Ga−Ga(dpp-bian)],[3] [(dpp-bian)Mg$(THF)_3$][4] were prepared according to literature procedures. Deuterated [(D-dpp-bian)Na$(DME)_2$] was prepared according the literature procedure,[2] where D_2O instead of H_2O was used as the reagent. Isoselenocyanates were synthesied by a slightly modified procedure[5] was used with additional recrystallization from hexane. Other chemicals were purchased from commercial sources and used without further purification. The IR spectra were recorded on FSM-1201 spectrometer in Nujol, the NMR spectra – on Bruker AvanceNEO300 (300 MHz) or Advance III (400 MHz) spectrometers and were referenced to the residual ^1H or ^{13}C signals of deuterated solvents. Chemical shifts are given in ppm. Abbreviations used: Ar - aromatic, naph - naphthalene, tol - tolyl, pyr – pyridine, d - doublet, m - multiplet, t - triplet, s - singlet, br - broad, hept - heptet. The ESR spectra were obtained on a Bruker EMX spectrometer (9.75 GHz), the signals were referred to the signal of diphenylpicrylhydrazyl (g=2.0037). HFC constants were obtained by simulation with the WinEPR SimFonia Software and Easyspin toolbox.[6] Elemental analyses were carried out on Elementar VarioEL III instrument.

General procedure for synthesis of isoselenocyanates.

A mixture of amine (0.15 mol), $CHCl_3$ (24 g, 16.2 mL, 0.20 mol), CH_2Cl_2 (100 mL), Aliquat 336 (2 g, 0.005 mol), and 50% aq NaOH (68.4 g, 45 mL, 0.86 mol) was vigorously stirred; an exothermic effect was observed. When the effect had ceased, the mixture was vigorously stirred and refluxed for 3 h. The mixture was cooled to r.t., and black, finely powdered, elemental selenium (15 g, 0.19 mol) was added. The reagents were vigorously stirred at refluxed for the 3 h. The mixture was cooled to r.t., then water (150 mL) and CH_2Cl_2 (150 mL) were added, and the unreacted selenium was filtered off under reduced pressure using a Büchner funnel and filter paper. The organic layer was separated and dried (anhydr. $MgSO_4$). The drying agent was filtered off, and the solvent was evaporated under reduced pressure. The residue was extracted with hexane 3 times with 150 ml. The extracts were combined and evaporated under reduced pressure to 60 ml and cooled to -20ºC. The precipitated crystals of substances were washed with hexane cooled to -20ºC and dryed in vacuum.

Orthomethylphenyl isoselenocyanates: yield 34%. Crystals suitable for X-ray diffraction analysis were obtained by recrystallization from hexane. IR (nujol, cm^{-1}): 465 M, 500 M, 527 M, 544 S, 627 S, 704 S, 752 VS, 860 S, 939 M, 1038 S, 1111 S, 1157 M, 1192 S, 1229 M, 1291 M, 1379 S, 1458 VS, 1483 VS, 1578 S, 1599 S, 2078 VS, 2116 VS. ^{1}H NMR (300 MHz, C_6D_6) 6.74 – 6.65 (m, 1H), 6.63 – 6.57 (m, 2H), 6.54 (dd, J = 8.3, 1.6 Hz, 1H), 1.83 (s, 3H). ^{13}C NMR (75 MHz, C_6D_6) 135.2, 130.2, 129.2, 127.5, 126.5, 125.7, 17.6. ^{77}Se NMR (76 MHz, C_6D_6) -305.64. Elemental analysis C_8H_7NSe (196.11), calc. C 48.99, H 3.59, N 7.14 %; found C 48.68, H 3.34, N 7.43 %.

Orthomethoxyphenyl isoselenocyanates: yield 41%. IR (nujol, cm^{-1}): 457 W, 536 W, 561 M, 613 M, 752 VS, 772 W, 849 M, 860 W, 934 M, 949 W, 1013 S, 1040 M, 1109 S, 1156 M, 1184 M, 1215 M, 1258 S, 1279 S, 1300 S, 1377 M, 1435 M, 1491 S, 1590 M, 2100 VS, 2136 VS. ^{1}H NMR (400 MHz, THF-d_8) 7.31 (td, J = 7.9, 1.6 Hz, 1H), 7.24 (dd, J = 7.9, 1.7 Hz, 1H), 7.06 (d, J = 8.3 Hz, 1H), 6.92 (td, J = 7.6, 1.1 Hz, 1H), 3.91 (s, 3H). ^{13}C NMR (101 MHz, THF-d_8) 156.3, 133.3, 129.2, 125.9, 120.5, 119.0, 111.7, 55.5. ^{77}Se NMR (76 MHz, THF-d_8) -302.3. Elemental analysis C_8H_7NOSe (212.11), calc. C 45.30, H 3.33, N 6.60 %; found C 45.47, H 3.14, N 6.35 %.

Orthochlorophenyl isoselenocyanates: yield 42%. IR (nujol, cm^{-1}): 442 W, 509 M, 525 W, 540 W, 561 W, 623 M, 694 M, 752 VS, 856 M, 941 W, 1030 M, 1042 M, 1065 S, 1094 W, 1115 M, 1128 M, 1157 W, 1308 W, 1348 W, 1418 M, 1443 S, 1584 S, 1626 M, 2064 VS, 2108 VS. ^{1}H NMR (400 MHz, C_6D_6) 6.83 (dd, J = 7.6, 2.0 Hz, 1H), 6.63 – 6.49 (m, 2H), 6.49 – 6.39 (m, 1H). ^{13}C NMR (75 MHz, C_6D_6) 134.9, 131.5, 129.7, 128.2, 127.2, 126.7. ^{77}Se NMR (76 MHz, C_6D_6) -282.3. Elemental analysis C_7H_4ClNSe (216.53), calc. C 38.83, H 1.86, N 6.47 %; found C 38.98, H 2.02, N 6.65 %.

Reaction of [(dpp-bian)HNa(DME)$_2$] with 1-isoselenocyanato-2-methoxybenzene.

0.106 g (0.497 mmol) of 2-(MeO)C_6H_4NCSe was added to a blue solution of 0.335 g (0.497 mmol) of [(dpp-bian)HNa(Et_2O)$_2$] in 5 ml of DME at 0 °C. The solution color changed to pale brown within 5 min. The resulting solution was layered with 10 ml of pentane. The vessel was sealed and left unshaken for two days at -20 °C. That gave light orange crystals of compound **2**. Yield 0.316 g, 77%. IR (nujol, cm^{-1}) 453 vw, 480 vw, 490 vw, 540 w, 556 w, 590 w, 604 w, 666 w, 677 vw, 739 s, 745 s, 758 s, 777 s, 806 s, 826 m, 858 m, 905 m, 936 s, 953 m, 961 m, 982 w, 1017 s, 1047 m, 1076 s, 1115 s, 1159 m, 1190 m, 1240 s, 1256 m, 1287 w, 1304 w, 1325 w, 1333 w, 1362 m, 1439 s, 1480 s, 1514 s, 1590 m, 1622 m, 1644 s, 3174 w. ^{1}H NMR (400 MHz, THF-d_8) 7.92 (s, 1H), 7.76 (d, J = 8.0 Hz, 1H), 7.56 (s, 1H), 7.54 (d, J = 8.3 Hz, 1H), 7.30 – 7.19 (m, 3H), 7.16 (t, J = 7.6 Hz, 1H), 7.14 (t, J = 7.8 Hz, 1H), 7.12 (d, J = 7.3 Hz, 1H), 6.92 (t, J = 7.7 Hz, 1H), 6.88 – 6.80 (m, 3H), 6.68 (d, J = 7.6 Hz, 1H), 6.58 (d, J = 7.5 Hz, 1H), 6.55 (d, J = 7.2 Hz, 1H), 4.13 (br s, 1H), 3.57 (hept, J = 6.8 Hz, 1H), 3.07 (br s, 1H), 2.96 (hept, J = 6.8 Hz, 1H), 1.44 (d, J = 6.7 Hz, 3H), 1.23 (d, J = 6.8 Hz, 3H), 1.22 (d, J = 6.8 Hz, 3H), 1.08 (d, J = 6.9 Hz, 3H), 1.04 (d, *J* = 6.8 Hz, 3H), 0.85 (d, *J* = 6.7 Hz, 3H), 0.80 (d, *J* = 6.5 Hz, 3H), -0.32 (d, *J* = 6.4 Hz, 3H). ^{13}C NMR (75 MHz, THF-d_8) 191.0, 178.9, 150.4, 146.6, 145.5, 144.1, 143.9, 143.8, 143.4, 143.3, 139.2, 136.5, 133.0, 130.7, 128.3, 126.9, 125.9, 124.5, 124.3, 123.7, 123.5, 123.3, 122.8, 122.8, 122.7, 122.4, 122.3, 121.6, 120.5, 111.9, 83.4, 55.4, 28.6, 28.2, 27.4, 26.7, 24.9, 24.4, 24.3, 24.1, 23.8, 23.7, 23.7, 20.7. ^{15}N NMR (40 MHz, THF-d_8, indirect observation) 64.1. ^{77}Se NMR (76 MHz, C_6D_6) -301.0. NMR assignment table is given below. Elemental analysis $C_{48}H_{58}N_3O_3NaSe$ (826.92), calc. C 69.72, H 7.07, N 5.08 %; found C 69.53, H 6.87, N 5.28 %.

Reaction of [(dpp-bian)HNa(DME)$_2$] with 1-isoselenocyanato-2-methylbenzene.

0.088 g (0.446 mmol) of 2-MeC$_6$H$_4$NCSe was added to a blue solution of 0.300 g (0.446 mmol) of [(dpp-bian)HNa(Et$_2$O)$_2$] in 5 ml of DME at 0°C. The solution color changed to brown within 5 min. The resulting solution cooled down to -20°C. After 10 min violet and yellow-brown layers are formed. The upper violet layer was removed. The residue washed twice with cold DME. The yellow-brown residue was dryed in vacuum to give yellow-brown solid of compound **3**. Yield 0.342 g, 85%. Removal of volatiles from violet layer resulted in violet solid (0.034 g), NMR and IR spectral characteristics correspond to [(dpp-bian)H$_2$].[2] IR (nujol, cm^{-1}) 465 VS, 521 W, 538 W, 556 W, 604 VW, 631 VW, 694 VS, 750 S, 766 M, 783 M, 833 M, 855 M, 895 M, 938 W, 978 M, 1030 S, 1067 M, 1082 S, 1111 S, 1140 M, 1157 W, 1179 M, 1194 M, 1210 W, 1252 M, 1296 W, 1304 W, 1329 W, 1360 M, 1495 VS, 1524 W, 1568 S, 1588 M, 1605 S, 1620 W, 1645 M, 3162 M. ^{1}H NMR (400 MHz, C_6D_6) 7.65 (s, 1H, NH), 7.45 (d, J = 7.9 Hz, 1H, CH-naph), 7.33 (dd, J = 7.7, 1.2 Hz, 1H, CH-naph), 7.29 – 7.24 (m, 2H, CH-Ar), 7.24 – 7.18 (m, 2H, CH-Ar), 7.18 – 7.12 (m, 2H, CH-Tol), 7.08 – 7.02 (m, 1H, CH-Ar), 7.02 – 6.99 (m, 1H, CH-naph), 6.99 – 6.97 (m, 1H, CH-Tol), 6.83 - 6.77 (m, 1H, CH-naph), 6.80 – 6.75 (m, 1H, CH-naph), 6.77 – 6.72 (m, 1H, CH-Ar), 6.67 (d, J = 7.2 Hz, 1H, CH-naph), 4.65 (hept, J = 6.8 Hz, 1H, CH-iPr), 3.81 (hept, J = 6.8 Hz, 1H, CH-iPr), 3.11 (hept, J = 6.8 Hz, 1H, CH-iPr), 3.03 (hept, J = 6.8 Hz, 1H, CH-iPr), 1.89 (s, 3H, CH3-Tol), 1.58 (d, J = 6.9 Hz, 3H, CH3-iPr), 1.57 (d, J = 6.7 Hz, 3H, CH3-iPr), 1.42 (d, J = 6.7 Hz, 3H, CH3-iPr), 1.18 (d, J = 6.8 Hz, 3H, CH3-iPr), 1.14 (d, J = 6.9 Hz, 3H, CH3-iPr), 1.10 (d, J = 6.8 Hz, 3H, CH3-iPr), 1.00 (d, J = 6.7 Hz, 3H, CH3-iPr), -0.16 (d, J = 6.8 Hz, 3H, CH3-iPr). ^{13}C NMR (101 MHz, C_6D_6) 180.9 (N=C-Se), 178.3 (C=NAr), 153.2 (C-Tol), 146.0 (C-Ar), 144.9 (C-naph), 143.4 (C-Ar), 143.3 (C-Ar), 142.4 (C-naph), 142.3 (C-naph), 139.2 (C-Ar), 136.7 (C-Ar), 131.1 (C-naph), 130.5 (C-Ar), 129.6 (CH-Tol), 129.3, 129.2 (CH-Ar), 127.3 (CH-naph), 126.3 (CH-naph), 125.0 (CH-Tol), 125.0 (CH-Ar), 124.3 (CH-naph), 123.8 (CH-Ar), 123.7 (CH-naph), 123.4 (CH-naph), 123.1 (CH-Ar), 122.9 (CH-Ar), 122.1 (CH-Ar), 119.4 (CH-naph), 81.5 (C-N(H)), 29.2 (CH-iPr), 28.9 (CH-iPr), 27.7 (CH-iPr), 27.2 (CH-iPr), 26.2 (CH3-iPr), 26.0 (CH3-iPr), 25.6 (CH3-iPr), 25.0 (CH3-iPr), 24.5 (CH3-iPr), 24.2 (CH3-iPr), 23.9 (CH3-iPr), 20.9 (CH3-iPr), 18.3 (CH3-Tol). ^{15}N NMR (40.55 MHz, C_6D_6, indirect observation) 70.6. ^{77}Se NMR (76 MHz, C_6D_6) 57.5.

Reaction of [(dpp-bian)GaNa(DME)$_2$] with 1-isoselenocyanato-2-methoxybenzene.

0.213 g (1.0 mmol) of Ph(OMe)NCSe was added to a solution of [(dpp-bian)GaNa(DME)$_3$] (1 mmol) in DME (15 ml). Solution color changed to green. Within 15 min yellow-green needle crystals of **5** precipitated. Yield 0.86 g, 83%. IR (nujol, cm^{-1}): 463 VW, 548 VW, 594 W, 721 M, 750 M, 760 M, 770 M, 787 M, 802 W, 820 W, 835 W, 926 W, 936 W, 1038 W, 1082 W, 1113 W, 1142 VW, 1192 W, 1252 W, 1275 W, 1321 M, 1350 W, 1364 M, 1503 W, 1539 M, 1591 W. Elemental analysis $C_{104}H_{160}Ga_2N_4Na_2O_{16}Se_2$ (2065.74), calc. C 60.47, H 7.81, N 2.71 %; found C 60.77, H 7.54, N 2.51 %.

Reaction of [(dpp-bian)GaNa(DME)$_2$] with 2,3-dimethyl-1,3-butadiene and 1-isoselenocyanato-2-methoxybenzene.

0.082 g (1 mmol) of 2,3-dimethyl-1,3-butadiene was added to a yellow-green solution of 1 mmol of [(dpp-bian)GaNa(DME)$_2$] in 5 ml of DME. The resulting mixture was heated within 4 hours at 80 °C. No visible changes were observed. Solution of 0.212 g (1 mmol) of 1-isoselenocyanato-2-methoxybenzene in 3 ml of DME was added to the mixture. The mixture was left unshaken for 2 days. That resulted in mixture of orange crystals and brown crystals, that were manually separated in glovebox and identified by X-ray diffraction analysis as compound **2** and compound **6** correspondingly. Total yield was 0.290 g.

Reaction of digallane [(dpp-bian)Ga−Ga(dpp-bian)] with 2,3-dimethyl-1,3-butadiene. 0.164 g (2.0 mmol) of 2,3-dimethyl-1,3-butadiene was added to a solution of 1 mmol of digallane in 10 ml of toluene. The vessel was sealed and was heated for 48h at 120 °C. Solution color changed to brown. All volatiles were removed in vacuum. The residue was dissolved in 5 ml of DME. Concenration to 2 ml gave brown crystals of compound **6**. Yield 0.352 g, 54%. IR (cm^{-1}) 455 w, 546 w, 615 w, 633 w, 669 w, 768 s, 785 w, 804 m, 820 m, 874 w, 891 w, 938 w, 1038 w, 1057 w, 1084 w, 1107 w, 1136 m, 1161 w, 1186 m, 1211 w, 1256 m, 1325 m, 1362 m, 1543 m. EPR (THF, 295 K) $a_i(2\times{}^{14}N) = 0.51$, $a_i({}^{69}Ga) = 1.85$, $a_i({}^{71}Ga) = 2.34$, $a_i(4\times{}^{1}H) = 0.11$ mT, $g = 2.0025$. Elemental analysis $C_{42}H_{50}N_2Ga$ (652.56), calc. C 77.30, H 7.27, N 4.29 %; found C 77.09, H 7.44, N 4.44 %.

Reaction of [(dpp-bian)GaNa(DME)$_2$] with 2,3-dimethyl-1,3-butadiene. 0.164 g (2.0 mmol) of 1,3-dimethylbutadiene was added to a solution of [(dpp-bian)GaNa(DME)$_2$] (1 mmol) in DME (10 ml). It was heated up at 80°C for 1 day. Slow concentration gave dark green crystals of compound **9**. Yield 0.446 g, 47 %. IR (nujol, cm^{-1}): 463 VW, 517 W, 550 VW, 613 W, 625 W, 646 W, 683 W, 748 W, 766 S, 799 M, 810 M, 839 W, 858 S, 876 W, 893 M, 926 M, 936 M, 959 W, 997 W, 1019 M, 1030 M, 1084 VS, 1105 S, 1123 S, 1134 M, 1159 W, 1177 S, 1190 M, 1210 W, 1217 W, 1260 M, 1319 S, 1343 VS, 1428 VS, 1518 S, 1588 W. ^1H NMR (400 MHz, THF-d_8, 223

K): 7.05 – 6.84 (m, 6H, CH-Ar), 6.57 – 6.40 (m, 4H, CH-naph), 5.46 (d, J = 6.6 Hz, 2H, CH-naph), 4.09 (hept, J = 6.8 Hz, 4H, CH-iPr), 1.62 (s, 6H, CH3-diene), 1.13 (d, J = 6.9 Hz, 12H, CH3-iPr), 1.05 (d, J = 6.9 Hz, 12H, CH3-iPr), 0.75 (s, 4H, CH2-diene). ^{13}C NMR (75 MHz, THF-d_8, 298 K): 136.3 (C-naph), 131.7 (C-diene), 126.9 (C-naph), 126.5 (CH-naph), 126.1 (CH-naph), 125.5 (C-Ar), 125.3 (C-Ar), 123.9 (CH-Ar), 123.3 (CH-naph), 122.0 (C-Ar), 121.5 (CH-naph), 119.0 (CH-Ar), 27.0 (CH-iPr), 24.7 (CH3-iPr), 24.2 (CH3-iPr), 21.2 (CH3-diene). Elemental analysis $C_{54}H_{80}GaN_2NaO_6$ (945.93), calc. C 68.56, H 8.52, N 2.96 %; found C 68.81, H 8.25, N 3.20 %.

Reaction of 6 with sodium. A mixture of 0.219 g (0.33 mmol) of [(dpp-bian)Ga(C6H10)], 0.008 g (0.33 mmol) of sodium in 5 ml of DME was stirred within 24 hours. The metal dissolved, solution color changed to green. Slow concentration gave dark green crystals of compound **9**. Yield 0.284 g, 91%.

Reaction of 9 with 1-isoselenocyanato-2-methoxybenzene.

0.057 g (0.278 mmol) 1-isoselenocyanato-2-methoxybenzene was added to a solution 0.263 g (0.278 mmol) of compound **9** in 5 ml DME. Solution color changed to yellow-brown. After storage for two days at -20 °C, the solution was layered with 5 ml of pentane. This resulted in mixture of two type of crystals: dark needle and orange prisms. After decantation, crystals were divided manually in drybox. Orange crystals of compound **2** were identified by NMR spectra, yield 0.035 g, 15.3 %. Dark crystals were identified by EPR spectra as compound **6**, yield 0.091 g 50.3 %.

Reaction of [(dpp-bian)Mg(THF)$_3$] with 1-isoselenocyanato-2-methoxybenzene.

0.212 g (1.0 mmol) of 2-(MeO)C_6H_4NCSe was added to a green solution of 0.741 g (1.0 mmol) of [(dpp-bian)Mg(THF)$_3$] in 10 ml of THF at -20°C. The solution color changed to brown. The solution was concentrated to 2 ml in vacuum. Storage within 20 min at -20°C gave yellow-green microcrystalline powder of **11**. Yield 0.615 g, 69%. Crystals suitable for X-ray diffraction analysis were obtained by recrystallization from pyridine at -40°C within 24h. IR (nujol, cm^{-1}): 455 W, 517 W, 550 W, 573 W, 602 W, 631 W, 679 M, 702 S, 739 M, 745 M, 774 M, 785 M, 804 M, 822 W, 918 W, 934 M, 970 M, 992 W, 1022 M, 1042 S, 1069 M, 1092 M, 1115 M, 1146 W, 1154 W, 1161 W, 1181 M, 1190 M, 1206 W, 1219 M, 1229 M, 1250 M, 1271 M, 1283 W, 1312 M, 1329 M, 1364 S, 1373 M, 1402 M, 1437 M, 1501 S, 1580 M, 1597 M, 1640 M. ^{1}H NMR (400 MHz, THF-d_8, 213 K) 9.48 (d, J = 7.9 Hz, 1H, CH-Ar), 7.78 (d, J = 8.1 Hz, 1H, CH-Ar), 7.50 (d, J = 8.2 Hz, 1H, CH-Ar), 7.28 (s, 2H, CH-Ar), 7.18 – 7.09 (m, 2H, CH-Ar), 7.05 (s, 1H, CH-Ar), 6.75 (t, J = 7.3 Hz, 1H, CH-Ar), 6.61 (d, J = 7.2 Hz, 1H, CH-Ar), 6.39 (d, J = 7.2 Hz, 1H, CH-Ar), 6.11 (d, J = 7.2 Hz, 1H, CH-Ar), 4.40 (hept, J = 6.9 Hz, 1H, CH3-iPr), 4.10 (s, 3H, OMe), 3.35 (hept, J = 7.0 Hz, 1H, CH-iPr), 2.96 (hept, J = 7.0 Hz, 2H, CH-iPr), 1.18 (d, J = 6.8 Hz, 9H, CH3-iPr), 0.86 (d, J = 7.0 Hz, 3H, CH3-iPr), 0.83 – 0.78 (m, 9H, CH3-iPr), -0.58 (d, J = 6.7 Hz, 3H, CH3-iPr). Elemental analysis $C_{64}H_{67}MgN_7OSe$ (1053.52), calc. C 72.96, H 6.41, N 9.31 %; found C 72.30, H 6.83, N 9.00 %.

Reaction of [(dpp-bian)Mg(THF)$_3$] with 1-isoselenocyanato-2-methylbenzene.

0.197 g (1.0 mmol) of 2-MeC_6H_4NCSe was added to a green solution of 0.741 g (1.0 mmol) of [(dpp-bian)Mg(THF)$_3$] in 10 ml of THF at -20°C. The solution color changed to brown-violet. The solution was concentrated to 2 ml in vacuum. Storage within 30 min at -20°C gave light-yellow-green crystals of **12**. Yield 0.615 g, 61%. IR (nujol, cm^{-1}): 465 VW, 538 W, 600 W, 629 M, 639 W, 666 W, 720 M, 752 VS, 781 S, 829 M, 835 M, 851 W, 901 W, 926 M, 938 M, 984 VW, 1042 M, 1073 S, 1113 S, 1138 M, 1159 W, 1192 M, 1221 M, 1254 M, 1275 W, 1327 M, 1483 M, 1593 S, 1642 S, 1665 S. ^{1}H NMR (400 MHz, THF-d$_8$, 243 K) 7.82 (d, J = 8.1 Hz, 1H, CH-Ar), 7.50 (d, J = 8.2 Hz, 1H, CH-Ar), 7.43 – 7.31 (m, 3H, CH-Tol), 7.29 (d, J = 7.9 Hz, 1H, CH-Ar), 7.19 (t, J = 7.7 Hz, 1H, CH-Ar), 7.11 (t, J = 7.7 Hz, 1H, CH-Ar), 7.05 (d, J = 7.5 Hz, 1H, CH-Ar), 6.87 (t, J = 7.1 Hz, 1H, CH-Ar), 6.83 (t, J = 7.1 Hz, 1H, CH-Ar), 6.74 (d, J = 7.4 Hz, 1H, CH-Tol), 6.68 (d, J = 7.4 Hz, 1H, CH-Ar), 6.63 (d, J = 7.3 Hz, 1H, CH-Ar), 6.43 (d, J = 7.2 Hz, 1H, CH-Ar), 6.30 (d, J = 7.1 Hz, 1H, CH-Ar), 5.14 (hept, J = 6.7 Hz, 1H, CH-iPr), 4.11 (hept, J = 6.7 Hz, 1H, CH-iPr), 3.29 (hept, J = 6.7 Hz, 2H, CH-iPr), 1.31 (s, 3H, CH3-Tol), 1.27 (d, J = 6.5 Hz, 3H, CH3-iPr), 1.24 (d, J = 6.9 Hz, 6H, CH3-iPr), 1.22 (d, J = 6.7 Hz, 3H, CH3-iPr), 0.92 (d, J = 6.7 Hz, 3H, CH3-iPr), 0.85 (d, J = 7.1 Hz, 3H, CH3-iPr), 0.83 (d, J = 7.0 Hz, 3H, CH3-iPr), -0.48 (d, J = 6.8 Hz, 3H, CH3-iPr). ^{13}C NMR (101 MHz, THF-d$_8$, 243 K, indirect observation) 154.8 (C-Ar), 154.6 (C-Ar), 151.7 (C-Ar), 149.9 (C-Ar), 149.5 (C-Ar), 145.1 (C-Ar), 144.3 (C-Ar), 141.1 (C-Ar), 138.4 (C-Ar), 129.9 (CH-Ar), 128.4 (CH-Tol), 127.2 (CH-Ar), 125.9 (CH-Tol), 125.7 (CH-Ar), 124.8 (CH-Tol), 124.3 (CH-Ar), 124.2 (CH-Ar), 124 (CH-Tol), 123.7 (CH-Ar), 122.1 (CH-Ar), 121.7 (CH-Ar), 121.5 (CH-Ar), 121.3 (CH-Ar), 119.5 (CH-Ar), 28.1 (CH-iPr), 27.8 (CH-iPr), 27.1 (CH-iPr), 26.2 (CH3-iPr), 25.7 (CH3-iPr), 25.2 (CH3-iPr), 24.5 (CH3-iPr), 23.8 (CH3-iPr), 23 (CH3-iPr), 21.7 (CH3-iPr), 17.5 (CH3-Tol). Elemental analysis $C_{60}H_{79}MgN_3O_4Se$ (1009.55), calc. C 71.38, H 7.89, N 4.16 %; found C 70.85, H 8.14, N 3.81 %.

Decomposition of complex 11, formation of complex 13.

0.212 g (1.0 mmol) of 2-(MeO)C_6H_4NCSe was added to a green solution of 0.741 g (1.0 mmol) of [(dpp-bian)Mg(THF)$_3$] in 10 ml of THF at -20°C. The solution color changed to brown. All volatiles were removed in vacuum. The residue was dissolved in 10 ml of pyridine. The vessel was sealed and left for 24h at room temperature. Solution color changed to bright red and **13** precipitated as red prismatic crystals. Yield 0.256 g, 40%. IR (nujol, cm^{-1}): 515 W, 550 W, 571 W, 629 W, 679 W, 702 M, 721 M, 737 M, 752 M, 772 W, 787 M, 835 W, 926 W, 938 W, 970 W, 1009 W, 1022 W, 1040 M, 1065 W, 1090 W, 1117 W, 1152 W, 1179 W, 1217 W, 1227 W, 1250 W, 1271 W, 1312 W, 1327 M, 1364 M, 1400 W, 1491 M, 1501 M, 1572 M, 1580 M, 1590 M, 1642 M, 1671 M. ^{1}H

NMR (400 MHz, THF-d_8, 243 K) 8.60 – 8.54 (m, 12H, CH-pyr), 8.52 (d, J = 7.2 Hz, 1H, CH-Ar), 8.07 (d, J = 8.2 Hz, 1H, CH-Ar), 7.77 – 7.70 (m, 6H, CH-pyr), 7.67 (d, J = 7.2 Hz, 2H, CH-Ar), 7.62 (d, J = 7.5 Hz, 3H, CH-Ar), 7.45 (d, J = 8.1 Hz, 1H, CH-Ar), 7.37 – 7.29 (m, 12H, CH-pyr), 7.24 (t, J = 8.1 Hz, 1H, CH-Ar), 7.18 (d, J = 7.7 Hz, 1H, CH-Ar), 6.92 (t, J = 7.6 Hz, 1H, CH-Ar), 6.83 (t, J = 7.6 Hz, 1H, CH-Ar), 6.75 (t, J = 7.9 Hz, 1H, CH-Ar), 6.66 (t, 1H, J = 7.6 Hz, CH-Ar), 6.41 (t, J = 7.7 Hz, 1H, CH-Ar), 5.92 (d, J = 7.3 Hz, 1H, CH-Ar), 3.95 (hept, J = 6.9 Hz, 1H, CH3-iPr), 3.16 (s, 3H, OCH3), 3.07 (hept, J = 6.9 Hz, 1H, CH-iPr), 1.38 (d, J = 6.7 Hz, 3H, CH3-iPr), 0.98 (d, J = 6.5 Hz, 3H, CH3-iPr), 0.81 (d, J = 6.9 Hz, 3H, CH3-iPr), 0.58 (d, J = 6.9 Hz, 3H, CH3-iPr). Elemental analysis $C_{74}H_{70}Mg_2N_6O_2Se_2$ (1281.91), calc. C 69.33, H 5.50, N 6.56 %; found C 68.90, H 5.18, N 6.91 %.

Table S1. NMR assignment table for compound **2**.

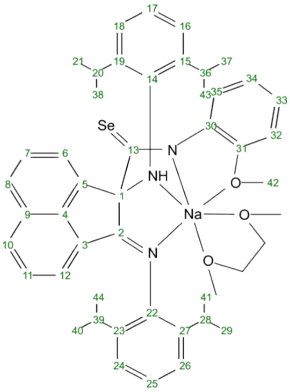

Atom	Chemical Shift	Atom	Chemical Shift	Atom	Chemical Shift
1 C	83.4	18 C	122.4	33 C	120.5
2 C	178.9	H	7.12	H	6.84
3 C	130.7	19 C	143.4	34 C	121.6
4 C	143.3	20 C	28.6	H	6.84
5 C	133.1	H	4.13	35 C	122.8
6 C	122.8	21 C	23.8	H	7.92
H	6.55	H3	1.44	36 C	28.2
7 C	125.9	22 C	146.6	H	2.96
H	7.16	23 C	136.5	37 C	20.7
8 C	128.3	24 C	123.7	H3	-0.32
H	7.76	H	7.26	38 C	23.7
9 C	143.9	25 C	124.4	H3	1.23
10 C	122.3	H	7.26	39 C	27.4
H	7.54	26 C	124.5	H	3.07
11 C	126.9	H	7.26	40 C	24.4
H	7.14	27 C	139.2	H3	1.22
12 C	123.5	28 C	26.7	41 C	23.7
H	6.58	H	3.57	H3	1.04
13 C	191.0	29 C	24.1	42 C	55.4
14 C	143.8	H3	0.85	H3	3.62
15 C	145.5	30 C	144.2	43 C	24.9
16 C	122.7	31 C	150.4	H3	0.80
H	6.68	32 C	111.8	44 C	24.4
17 C	123.3	H	6.84	H3	1.08
H	6.92				

X-ray Crystal Structure Determination

The X-ray diffraction data were collected on a Bruker D8 Quest Photon II (complexes **2**, **5**, **9**, **11**, **12**), an Oxford Xcalibur Eos (**2-MeOC$_6$H$_4$N=C=Se** and **6**) (Mo-K$_\alpha$ radiation, ω-scan technique, λ = 0.71073 Å) and a SuperNova Single source at offset/far Atlas (**13**) (Cu-K$_\alpha$ radiation, ω-scan technique, λ = 1.54184 Å) diffractometers. The intensity data were integrated by SAINT (**5**, **9**, **11** and **12**)[7] and CrysAlisPro (**2-MeOC$_6$H$_4$N=C=Se**, **2**, **6** and **13**)[8] programs. Absorption corrections were performed using the SADABS (**5**, **9**, **11** and **12**)[9] program and SCALE3 ABSPACK scaling algorithm (**2-MeOC$_6$H$_4$N=C=Se**, **2**, **6** and **13**).[10] All structures were solved by dual method[11] and refined on F_{hkl}^2 using SHELXTL package.[12] All non-hydrogen atoms were refined anisotropically. All hydrogen atoms, except H(1) in complex **2** and H(20A), H(23A), H(24A,B), H(25A,B) in **6**, were placed in calculated positions and were refined in the riding model ($U_{iso}(H) = 1.5U_{eq}(C)$ for CH$_3$-groups and $U_{iso}(H) = 1.2U_{eq}(C)$ for other groups). In turn, the listed hydrogen atoms were found from Fourier syntheses of electron density and were refined isotropically. To obtain an adequate geometry of some CH$_3$-groups in complex **6**, the DFIX instruction was used.

The crystal of **2-MeOC$_6$H$_4$N=C=Se** was twinned and therefore, a twin refinement using data in HKLF 5 format was performed (Component 2 rotated by 11.4927% around [-1.00 -0.04 0.07] (reciprocal) or [-0.99 -0.17 -0.01] (direct); BASF 0.11212). There are two uncoordinated disordered DME and THF molecules for each complex molecule in crystals **5** and **12**, respectively. The independent unit cell of complex **11** contains four pyridine molecules, one of which is disordered over two positions. Coordinated molecules of DME (**5**, **9**), THF (**12**), as well as the methyl (**11**) and isopropyl (**12**) groups are disordered in the structures of the corresponding compounds. The disordered fragments in the complexes investigated were modelled and refined with restraints of geometry (DFIX, SADI, FLAT) and thermal parameters (EADP and ISOR). The absolute structure parameter for complex **9** is -0.004(2).[13] Saturation of the metal coordination sphere (G-parameter) was calculated with Solid-G program.[14] I/σ(I) vs resolution and R_{merge} vs resolution plots were generated by Olex2.[15]

The crystal of complex **11** was a thin plate (0.20×0.10×0.04mm). The crystal also contains disordered solvent molecules. All these factors lead to the fact that the intensity of reflections quickly dies out with an increased resolution (Figures S5 and S6). The data were collected over a full sphere of reciprocal space up to 50º in 2θ: the individual frames were measured with an ω rotation of 0.3 and an acquisition time 30 s. Increasing the exposure time to obtain an acceptable resolution will result in an inadequately large number of saturated diffraction spots.

The crystal of complex **13** exhibited of reflections, that quickly dies out with an increased resolution. The data were collected over a full sphere of reciprocal space up to 150º in 2θ: the individual frames were measured with an ω rotation of 1° and an acquisition time 30 s. The chosen strategy of the experiment was the most optimal in terms of balancing too strong reflections (θ < 25°) and weak reflections (θ > 40°), to prevent missing strong reflections in the data set because of detector saturation (Figures S7 and S8).

The main crystallographic data and structure refinement details for compounds **2-MeOC$_6$H$_4$N=C=Se**, **2**, **5**, **6**, **9**, **11**, **12** and **13** are presented in Table S2. The crystallographic data have been deposed in the Cambridge Crystallographic Data Centre under the deposition codes CCDC 2142175 (**2**), 2092322 (**6**), 2127687 (**2-MeOC$_6$H$_4$N=C=Se**), 2127688 (**5**), 2127689 (**9**), 2127690 (**11**), 2127691 (**12**) and 2127692 (**13**). These data can also be obtained free of charge at ccdc.cam.ac.uk/structures/ from the Cambridge Crystallographic Data Centre.

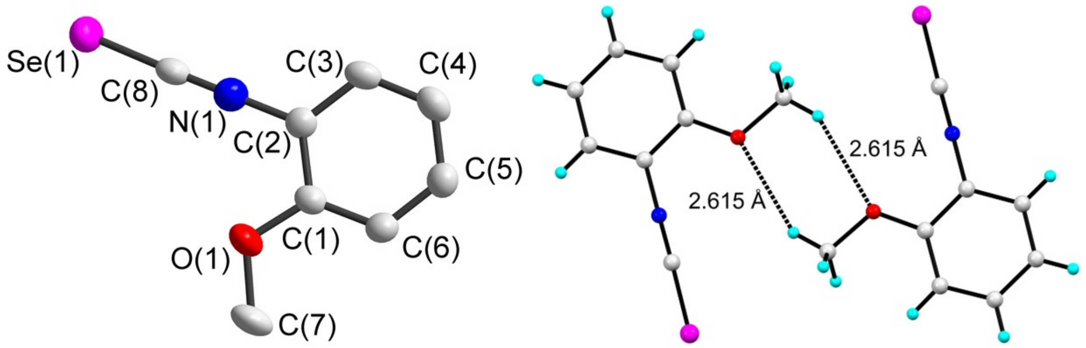

A B

Figure S1. Molecular structure (**a**) and dimeric pair (**b**) of **2-MeOC$_6$H$_4$N=C=Se**. The probability ellipsoids are drawn at the 30% level. The hydrogen atoms are omitted for clarity. Selected bond lengths (Å) and angles (°): N(1)-C(8) 1.156(8), N(1)-C(2) 1.368(8), O(1)-C(1) 1.354(7), O(1)-C(7) 1.436(8), Se(1)-C(8) 1.738(7), C(1)-C(2) 1.392(8); N(1)-C(8)-Se(1) 178.7(6), C(8)-N(1)-C(2) 174.5(7), C(1)-O(1)-C(7) 117.8(5).

The molecular structure of **2-MeOC$_6$H$_4$N=C=Se** is shown in Figure S1a. The molecule is almost flat. The average deviation of non-hydrogen atoms from the plane is 0.063 Å. The maximum deviation is observed for the selenium atom (0.126 Å). The geometric parameters are in agreement with reported similar structures.[16] The molecules form a dimeric pairs in a crystal (Fig. S1b). The O...H distance (2.615 Å) is characteristic to regular hydrogen bonds observed in a variety of organic compounds. [17]

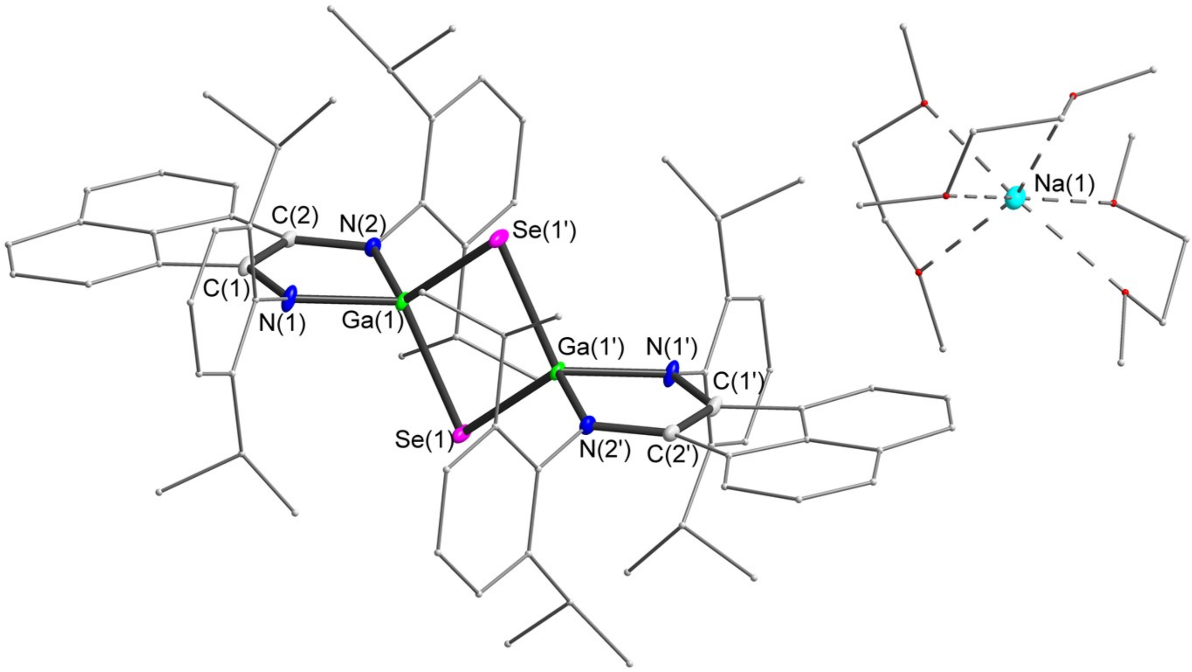

Figure S2. Molecular structure of **5**. Only one cationic part ([Na(DME)$_3$]$^+$) of the complex is shown. The probability ellipsoids are drawn at the 30 % level. The hydrogen atoms are omitted for clarity. Selected bond lengths (Å) and angles (°): Ga(1)-N(1) 1.9350(18), Ga(1)-N(2) 1.9443(17), Ga(1)-Se(1) 2.3557(3), Ga(1)-Se(1’) 2.3923(3), N(1)-C(1) 1.379(3), N(2)-C(2) 1.382(3), C(1)-C(2) 1.381(3), N(1)-Ga(1)-N(2) 87.65(7), N(1)-Ga(1)-Se(1) 119.02(5), N(2)-Ga(1)-Se(1) 118.60(5), N(1)-Ga(1)-Se(1’) 115.57(6), N(2)-Ga(1)-Se(1’) 117.18(5), Se(1)-Ga(1)-Se(1’) 100.079(11), Ga(1)-Se(1)-Ga(1’) 79.922(10). Symmetry transformations used to generate equivalent atoms (’): -x, -y+1, -z+1.

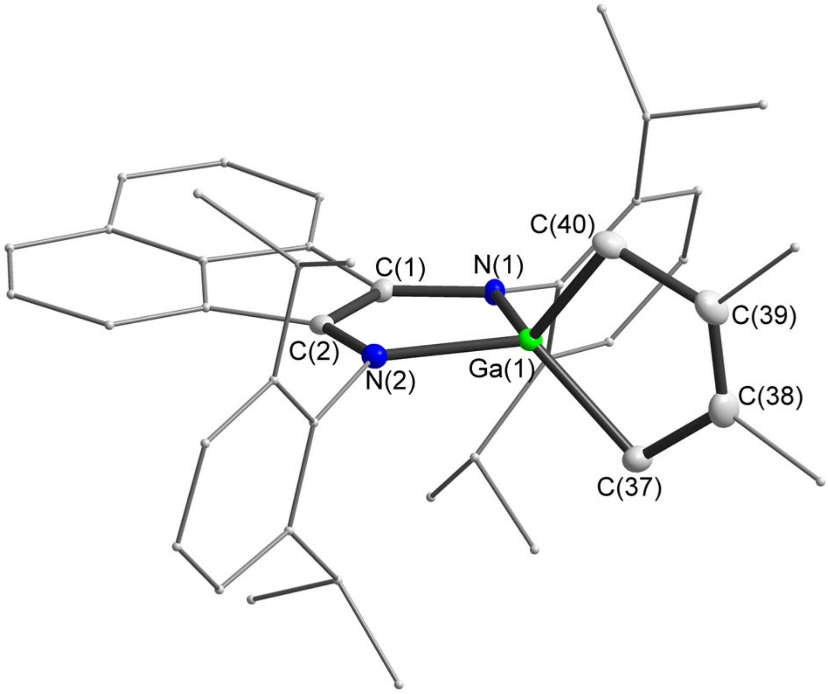

Figure S3. Molecular structure of anion of **9**. The probability ellipsoids are drawn at the 30 % level. The hydrogen atoms are omitted for clarity. Selected bond lengths (Å) and angles (°): The probability ellipsoids are drawn at the 30 % level. The hydrogen atoms are omitted for clarity. Selected bond lengths (Å) and angles (°): Ga(1)-N(2) 1.954(2), Ga(1)-N(1) 1.963(2), Ga(1)-C(37) 1.998(3), Ga(1)-C(40) 2.001(3), N(1)-C(1) 1.391(3), N(2)-C(2) 1.387(3), C(1)-C(2) 1.375(3), C(37)-C(38) 1.509(4), C(38)-C(39) 1.348(4), C(39)-C(40) 1.509(4); N(2)-Ga(1)-N(1) 87.28(8), N(2)-Ga(1)-C(37) 123.85(11), N(1)-Ga(1)-C(37) 118.89(11), N(2)-Ga(1)-C(40) 116.36(10), N(1)-Ga(1)-C(40) 122.29(10), C(37)-Ga(1)-C(40) 91.53(12).

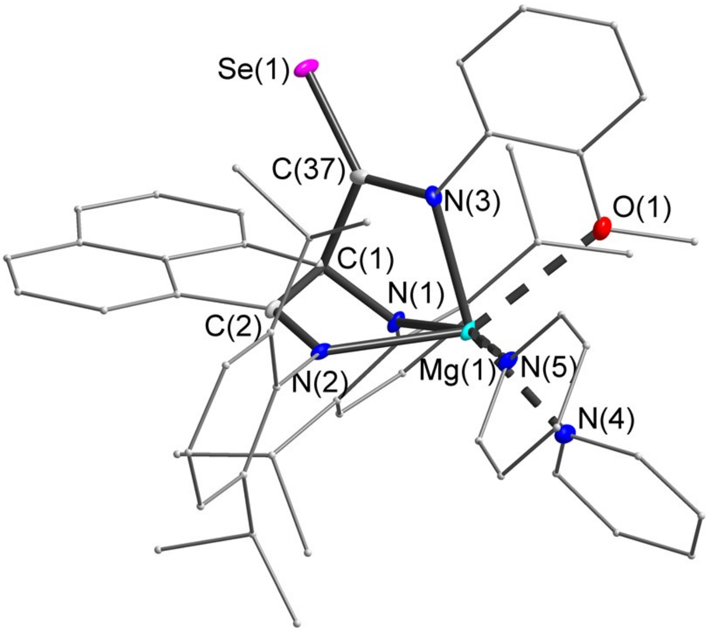

Figure S4. Molecular structure of anion of **11**. The probability ellipsoids are drawn at the 30 % level. The hydrogen atoms are omitted for clarity.

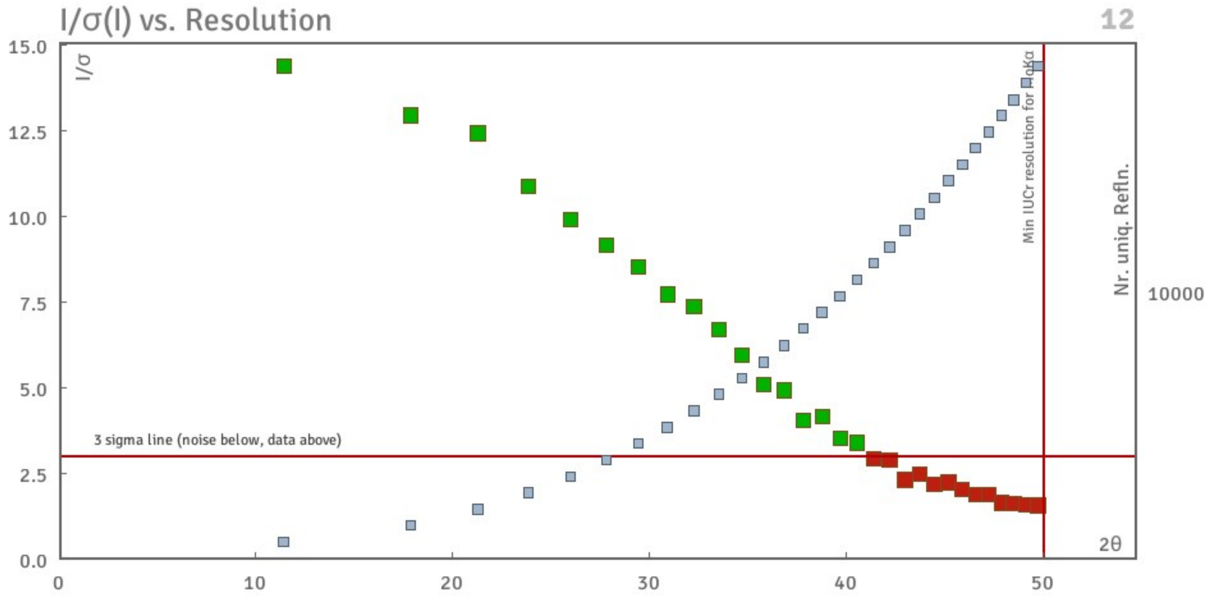

Figure S5. Intencity over sigma vs resolution plot for X-ray diffraction analysis of **11**.

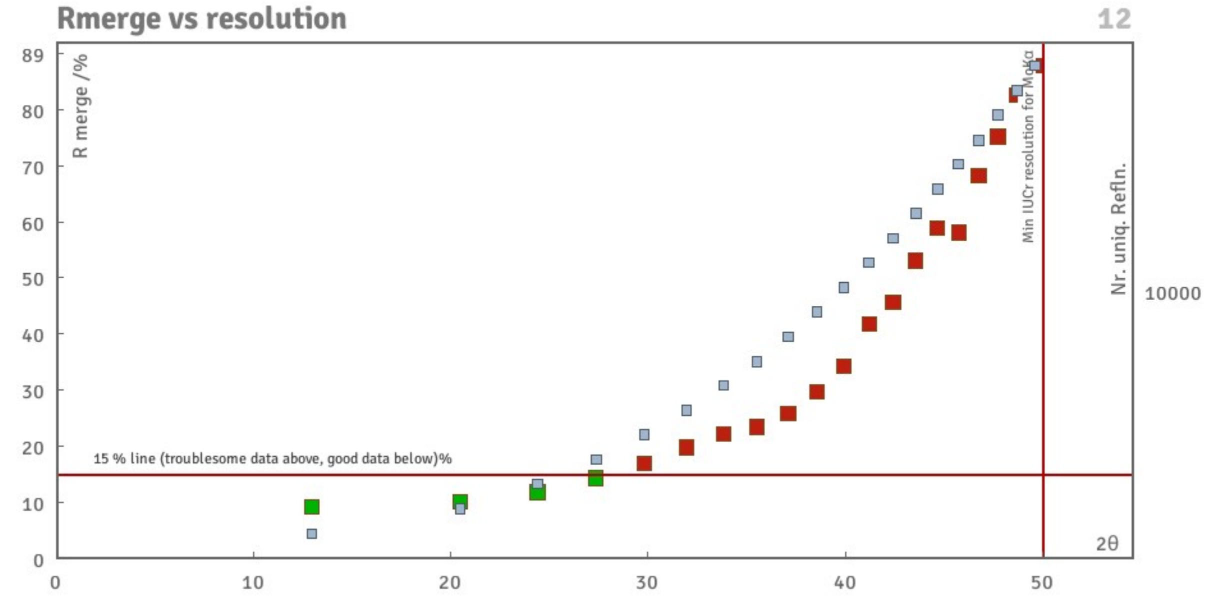

Figure S6. R_{merge} vs resolution plot for X-ray diffraction analysis of **11**.

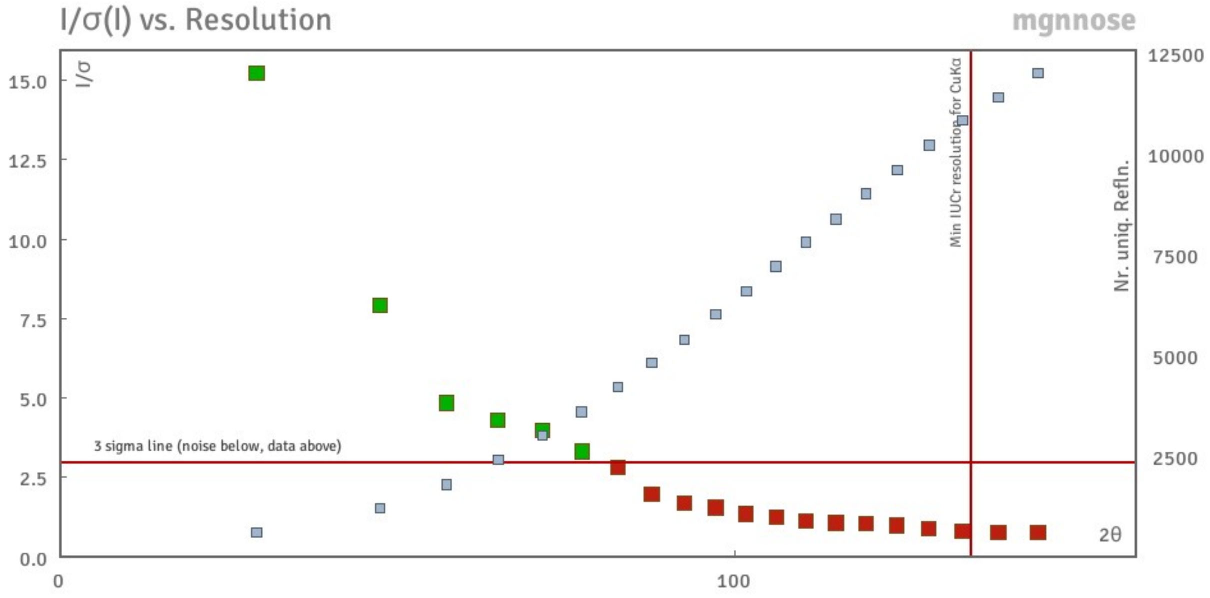

Figure S7. Intencity over sigma vs resolution plot for X-ray diffraction analysis of **13**.

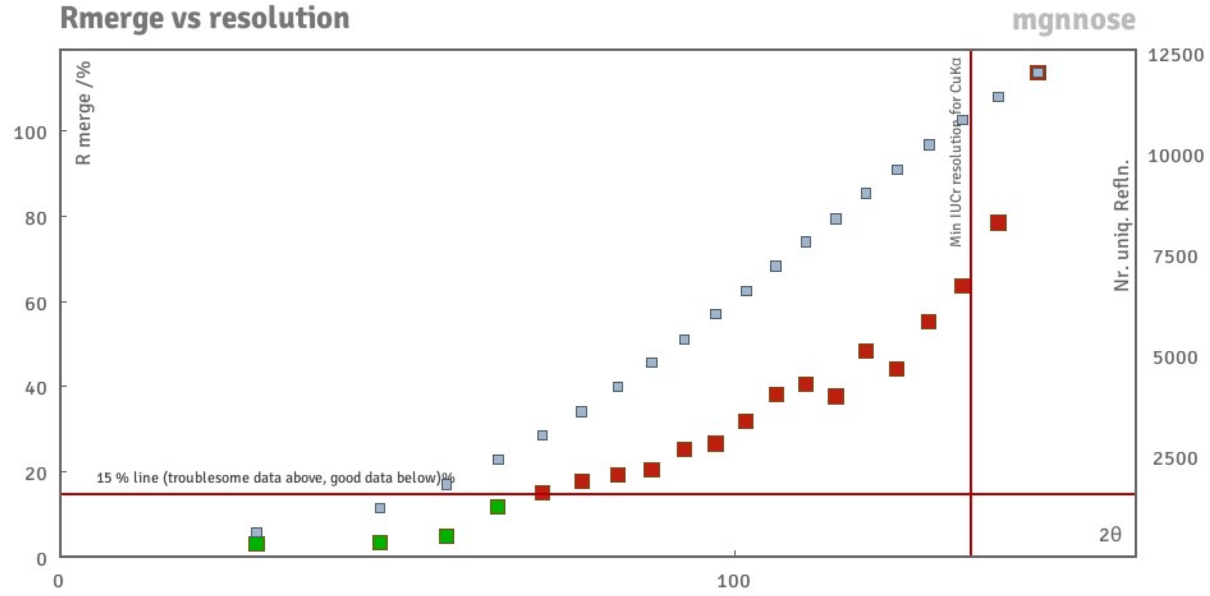

Figure S8. R_{merge} vs resolution plot for X-ray diffraction analysis of **13**.

Table S2. Crystallographic data and refinement details for compounds **2-MeOC$_6$H$_4$N=C=Se**, **2**, **5**, **6**, **9**, **11**, **12** and **13**.

Complex	**2-MeOC$_6$H$_4$N=C=Se**	**2**	**5**
Empirical formula	C_8H_7NOSe	$C_{48}H_{58}N_3NaO_3Se$	$C_{104}H_{160}Ga_2N_4Na_2O_{16}Se_2$
Formula weight	212.11	826.92	2065.69
Temperature [K]	298(2)	100(2)	100(2)
Crystal system	Monoclinic	Orthorhombic	Monoclinic
Space group	$P2_1/n$	Pbca	$P2_1/c$
Unit cell dimensions			
a[Å]	11.1882(8)	10.4126(2)	12.7954(7)
b[Å]	5.1560(4)	21.5074(5)	29.6704(15)
c[Å]	14.7709(11)	39.7104(8)	15.7466(8)
α[°]	90	90	90
β[°]	93.743(6)	90	113.3488(17)
γ[°]	90	90	90
Volume [Å^3]	850.26(11)	8893.0(4)	5488.6(5)
Z	4	8	2
Calculated density [Mg/m^3]	1.657	1.235	1.250
Absorption coefficient [mm^{-1}]	4.356	0.897	1.222
F(000)	416	3488	2184
Crystal size [mm^3]	0.72 × 0.58 × 0.40	0.35 × 0.30 × 0.25	0.54 × 0.22 × 0.20
θ [°]	2.215 – 26.024	2.154 – 25.026	2.211 – 29.129
Index ranges	$-13 \le h \le 13$ $-6 \le k \le 6$ $-18 \le l \le 18$	$-12 \le h \le 12$ $-25 \le k \le 25$ $-47 \le l \le 47$	$-17 \le h \le 17$ $-40 \le k \le 40$ $-21 \le l \le 21$
Reflections collected / unique	4282 / 4282	105117 / 7854	89307 / 14771
R(int)	0.0573	0.0734	0.0500
Data / restraints / parameters	4282 / 0 / 102	7854 / 0 / 520	14771 / 32 / 665
Final R indices [I>2sigma(I)]	R_1=0.0440, wR_2=0.1589	R_1=0.0450, wR_2=0.1023	R_1=0.0435, wR_2=0.0963
R indices (all data)	R_1=0.0768, wR_2=0.1690	R_1=0.0621, wR_2=0.1109	R_1=0.0641, wR_2=0.1051
S	1.012	1.039	1.036
Largest diff. peak and hole [e/Å^3]	0.452/-0.450	0.954/-0.499	1.056/-0.632

Table S2. *Continued.* Crystallographic data and refinement details for compounds **2-MeOC$_6$H$_4$N=C=Se**, **2**, **5**, **6**, **9**, **11**, **12** and **13**.

Complex	**6**	**9**	**11**
Empirical formula	$C_{42}H_{50}GaN_2$	$C_{54}H_{80}GaN_2NaO_6$	$C_{64}H_{67}MgN_7OSe$
Formula weight	652.56	945.91	1053.51
Temperature [K]	100(2)	100(2)	100(2)
Crystal system	Orthorhombic	Orthorhombic	Monoclinic
Space group	Pnma	$P2_12_12_1$	$P2_1/c$
Unit cell dimensions			
a[Å]	18.7199(5)	13.0889(4)	22.435(3)
b[Å]	18.2981(5)	19.0945(6)	22.776(3)
c[Å]	10.5069(3)	21.5669(7)	22.188(3)
α[°]	90	90	90
β[°]	90	90	104.728(4)
γ[°]	90	90	90
Volume [Å^3]	3599.00(17)	5390.1(3)	10965(3)
Z	4	4	8
Calculated density [Mg/m^3]	1.204	1.166	1.276
Absorption coefficient [mm^{-1}]	0.795	0.566	0.746
F(000)	1388	2032	4432
Crystal size [mm^3]	0.52 × 0.36 × 0.20	0.50 × 0.32 × 0.27	0.20 × 0.10 × 0.04
θ [°]	2.915 – 29.997	2.133 – 30.998	1.891 – 25.026
Index ranges	$-21 \le h \le 26$ $-25 \le k \le 19$ $-14 \le l \le 13$	$-18 \le h \le 18$ $-27 \le k \le 27$ $-31 \le l \le 31$	$-26 \le h \le 26$ $-27 \le k \le 27$ $-26 \le l \le 26$
Reflections collected / unique	17522 / 5401	95204 / 17170	116500 / 19353
R(int)	0.0345	0.0558	0.1883
Data / restraints / parameters	5401 / 6 / 238	17170 / 8 / 607	19353 / 200 / 1335
Final R indices [I>2sigma(I)]	R_1=0.0386, wR_2=0.0906	R_1=0.0446, wR_2=0.0851	R_1=0.1361, wR_2=0.3464
R indices (all data)	R_1=0.0657, wR_2=0.0987	R_1=0.0668, wR_2=0.0926	R_1=0.2098, wR_2=0.3959
S	1.033	1.037	1.058
Largest diff. peak and hole [e/Å^3]	0.536/-0.399	0.449/-0.634	4.551/-1.533

Table S2. *Continued*. Crystallographic data and refinement details for compounds **2-MeOC$_6$H$_4$N=C=Se**, **2**, **5**, **6**, **9**, **11**, **12** and **13**.

Complex	**12**	**13**
Empirical formula	$C_{60}H_{79}MgN_3O_4Se$	$C_{74}H_{70}Mg_2N_6O_2Se_2$
Formula weight	1009.53	1281.90
Temperature [K]	100(2)	150(2)
Crystal system	Monoclinic	Triclinic
Space group	$P2_1/n$	P-1
Unit cell dimensions		
a[Å]	12.9342(9)	13.5189(9)
b[Å]	24.5967(17)	14.4611(11)
c[Å]	17.0576(12)	18.747(2)
α[°]	90	76.429(8)
β[°]	93.274(2)	72.949(8)
γ[°]	90	63.250(7)
Volume [Å^3]	5417.8(7)	3106.2(5)
Z	4	2
Calculated density [Mg/m^3]	1.238	1.371
Absorption coefficient [mm^{-1}]	0.753	2.097
F(000)	2152	1328
Crystal size [mm^3]	0.33 × 0.17 × 0.04	0.20 × 0.15 × 0.10
θ [°]	2.043 – 26.372	2.483 – 74.102
Index ranges	$-15 \le h \le 16$ $-30 \le k \le 30$ $-21 \le l \le 21$	$-11 \le h \le 16$ $-15 \le k \le 17$ $-23 \le l \le 22$
Reflections collected / unique	67800 / 11079	22759 / 12208
R(int)	0.1008	0.1419
Data / restraints / parameters	11079 / 274 / 688	12208 / 0 / 785
Final R indices [I>2sigma(I)]	R_1=0.0754, wR_2=0.1667	R_1=0.0756, wR_2=0.1166
R indices (all data)	R_1=0.1170, wR_2=0.1832	R_1=0.1874, wR_2=0.1735
S	1.029	1.006
Largest diff. peak and hole [e/Å^3]	1.384/-0.793	0.924/-0.832

Table S3. Selected angles [°] in compounds **2**, **6**, **12** and **13**.

Angle [°]	**2**	Angle [°]	**6**
N(1)-Na(1)-O(1)	118.51(9)	N(1)-Ga(1)-N(1')	84.43(7)
N(1)-Na(1)-O(2)	137.26(9)	N(1)-Ga(1)-C(20)	119.94(6)
N(1)-Na(1)-O(3)	90.94(9)	N(1)-Ga(1)-C(23)	120.91(5)
N(1)-Na(1)-N(2)	70.82(8)	C(20)-Ga(1)-C(23)	93.72(10)
N(1)-Na(1)-N(3)	58.55(8)	Angle [°]	**12**
N(2)-Na(1)-O(1)	124.90(9)	N(1)-Mg(1)-O(1)	179.3(11)
N(2)-Na(1)-O(2)	92.86(9)	N(1)-Mg(1)-O(2)	95.76(13)
N(2)-Na(1)-O(3)	133.22(10)	N(1)-Mg(1)-N(2)	82.03(13)
N(2)-Na(1)-N(3)	84.39(8)	N(1)-Mg(1)-Se(1)	86.40(10)
N(3)-Na(1)-O(1)	64.44(7)	N(2)-Mg(1)-O(1)	97.3(10)
N(3)-Na(1)-O(2)	161.67(10)	N(2)-Mg(1)-O(2)	143.15(13)
N(3)-Na(1)-O(3)	122.85(10)	N(2)-Mg(1)-Se(1)	89.91(9)
O(1)-Na(1)-O(2)	103.37(9)	O(1)-Mg(1)-Se(1)	93.4(6)
O(1)-Na(1)-O(3)	101.78(9)	O(1)-Mg(1)-O(2)	84.9(10)
O(2)-Na(1)-O(3)	71.58(10)	O(2)-Mg(1)-Se(1)	126.80(10)
C(37)-N(3)-C(38)	125.1(3)	C(37)-N(3)-C(38)	124.9(4)
N(3)-C(37)-Se(1)	130.3(2)	N(3)-C(37)-Se(1)	126.9(3)
Angle [°]	**13**	Angle [°]	**13**
N(1)-Mg(1)-N(2)	83.9(3)	N(3)-Mg(2)-N(4)	83.5(2)
N(1)-Mg(1)-O(1)	74.4(2)	N(3)-Mg(2)-O(2)	74.4(2)
N(2)-Mg(1)-O(1)	146.1(2)	N(4)-Mg(2)-O(2)	144.9(3)
N(1)-Mg(1)-N(5)	137.0(3)	N(3)-Mg(2)-N(6)	143.3(3)
N(2)-Mg(1)-N(5)	97.2(3)	N(4)-Mg(2)-N(6)	99.2(2)
O(1)-Mg(1)-N(5)	82.4(2)	N(6)-Mg(2)-O(2)	83.8(2)
N(1)-Mg(1)-Se(2)	114.44(19)	N(3)-Mg(2)-Se(1)	114.7(2)
N(2)-Mg(1)-Se(2)	117.58(18)	N(4)-Mg(2)-Se(1)	113.6(2)
O(1)-Mg(1)-Se(2)	95.19(17)	O(2)-Mg(2)-Se(1)	100.44(16)
N(5)-Mg(1)-Se(2)	103.1(2)	N(6)-Mg(2)-Se(1)	97.9(2)
N(1)-C(1)-Se(1)	121.3(6)	N(3)-C(33)-Se(2)	122.2(6)

NMR spectra

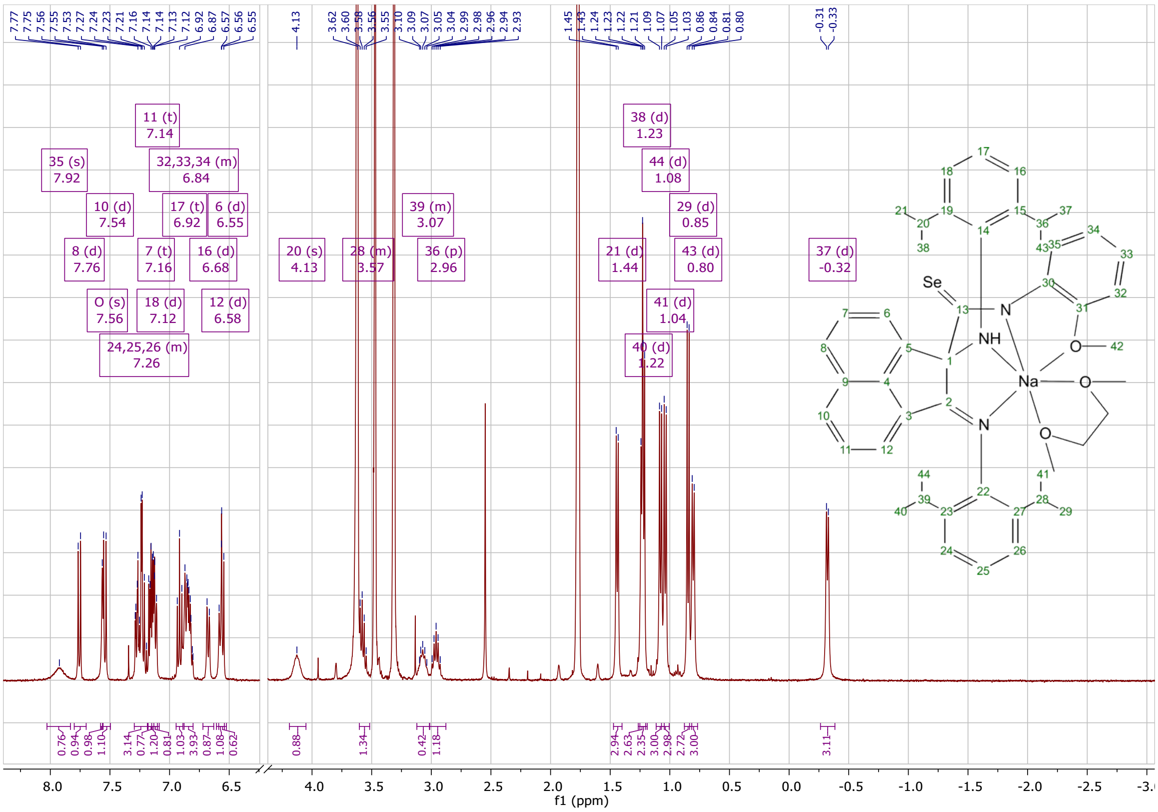

Figure S9. ^{1}H NMR spectrum of compound **2** in THF-d_8.

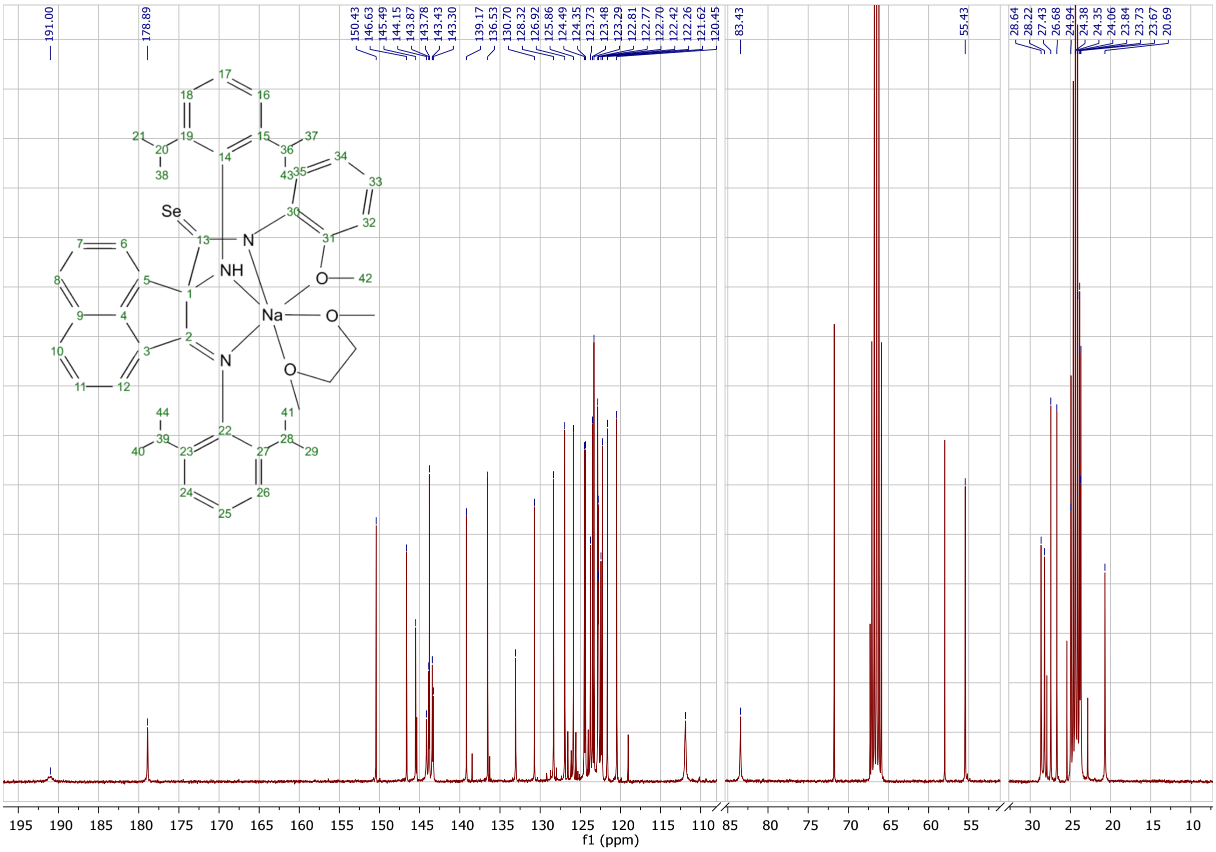

Figure S10. ^{13}C NMR spectrum of compound **2** in THF-d_8.

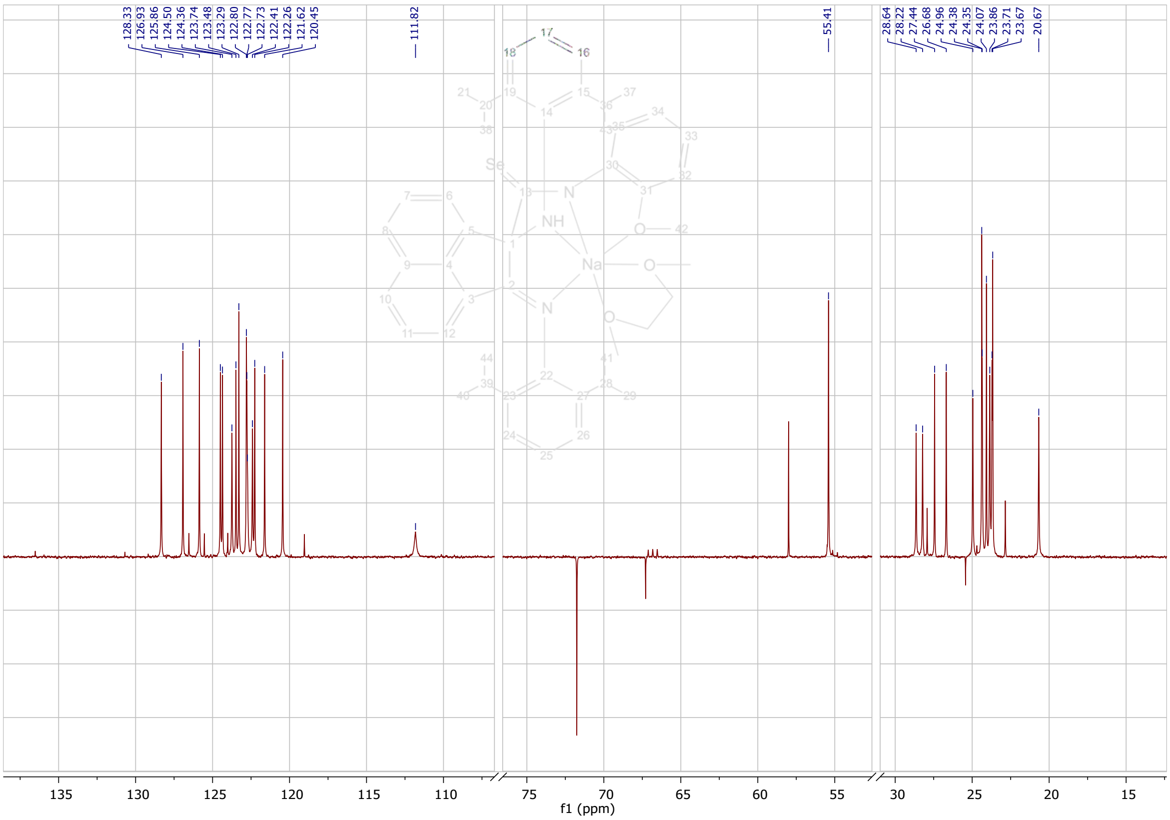

Figure S11. DEPT135 NMR spectrum of compound **2** in THF-d_8.

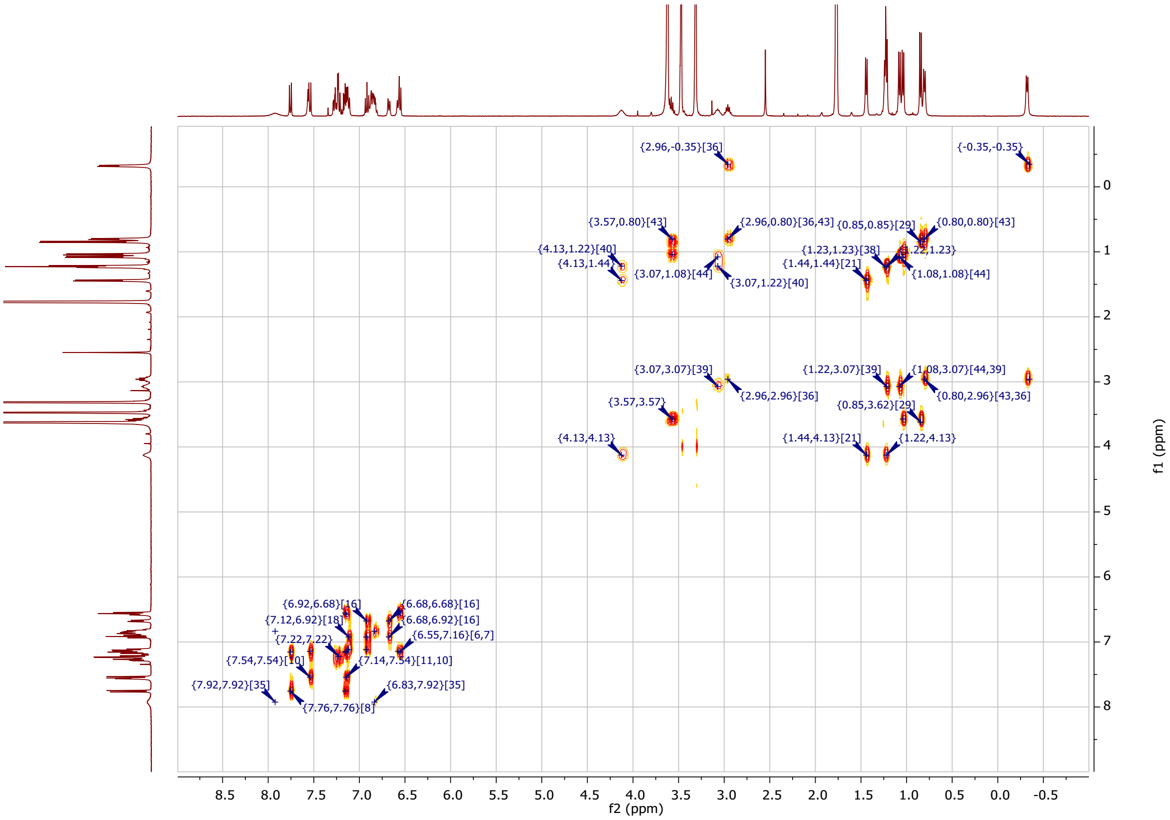

Figure S12. ^1H-^1H COSY NMR spectrum of compound **2** in THF-d_8.

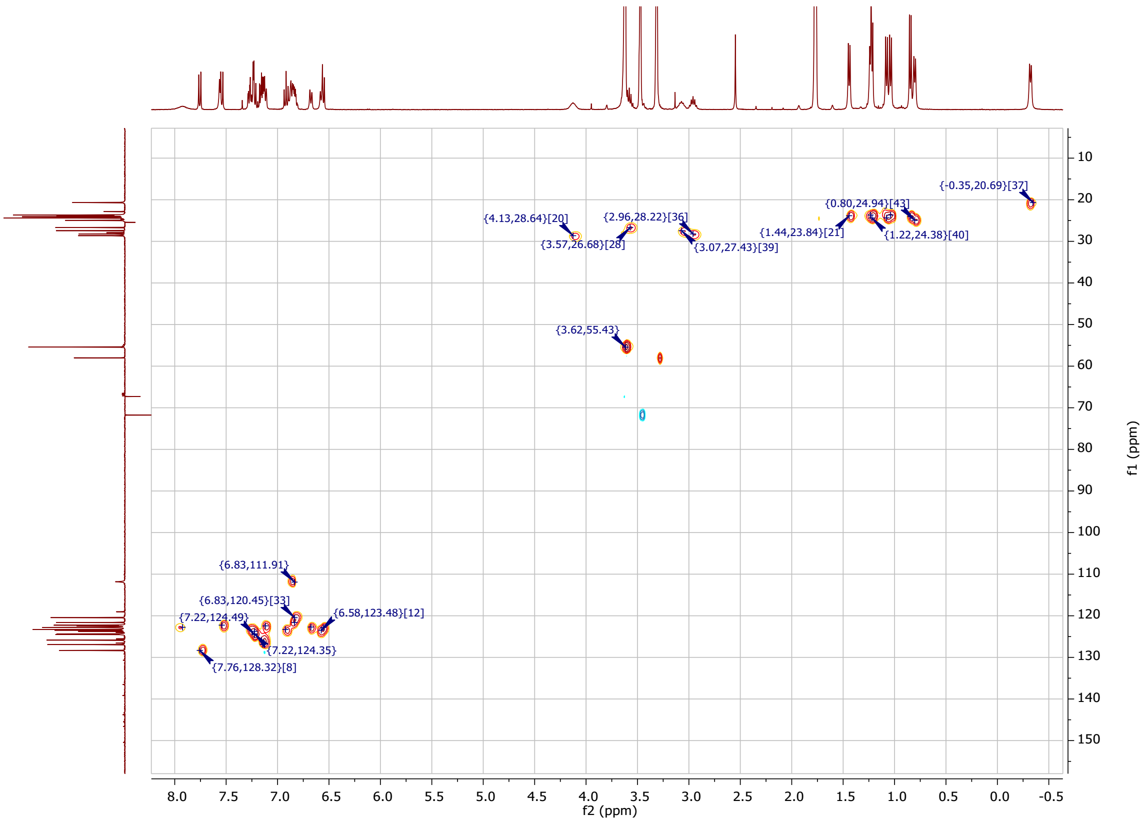

Figure S13. ^{1}H-^{13}C HSQC NMR spectrum of compound **2** in THF-d_8.

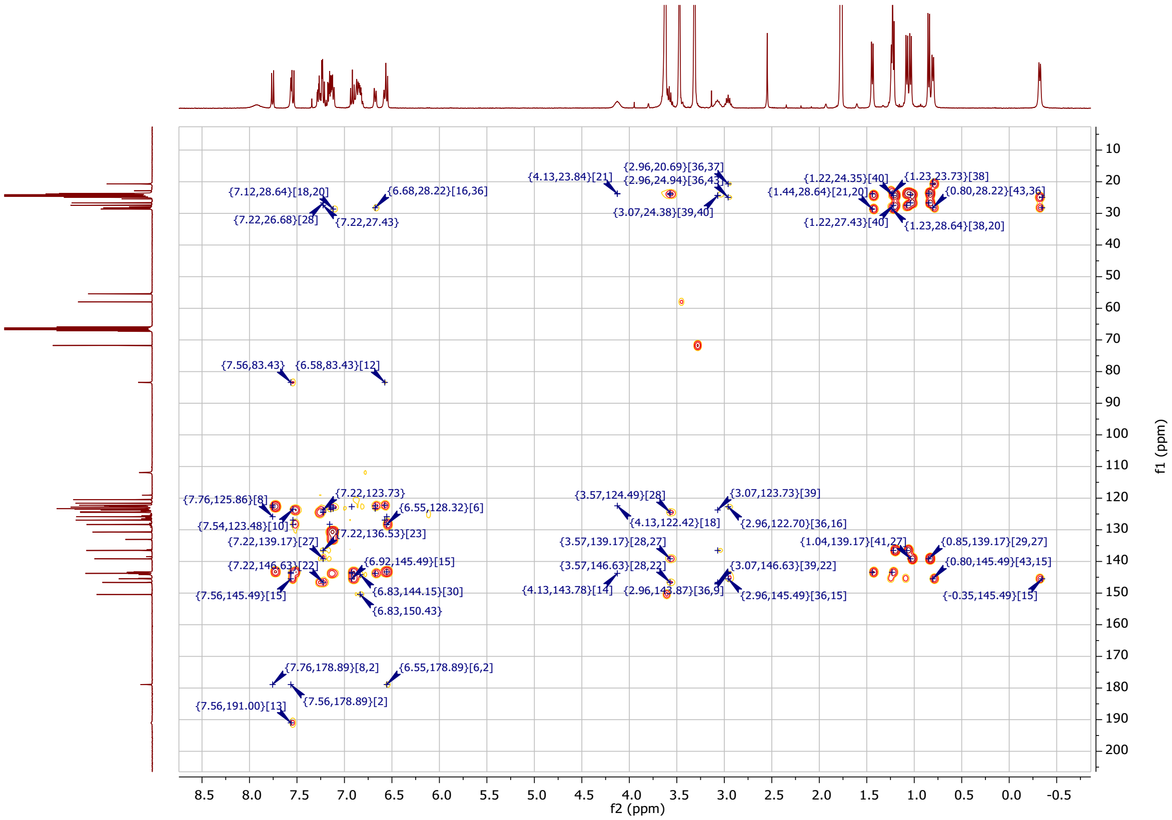

Figure S14. ^{1}H-^{13}C HMBC NMR spectrum of compound **2** in THF-d_8.

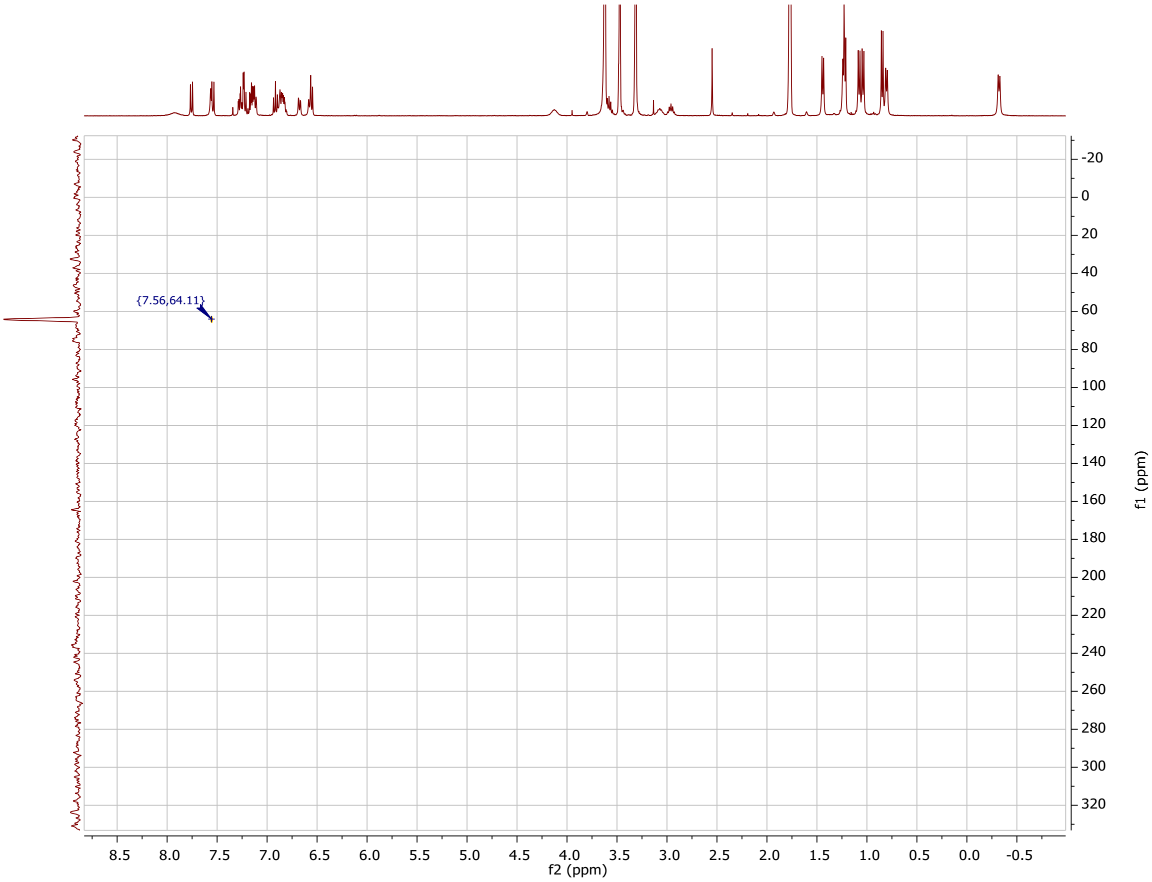

Figure S15. ^{1}H-^{15}N HSQC NMR spectrum of compound **2** in THF-d_8.

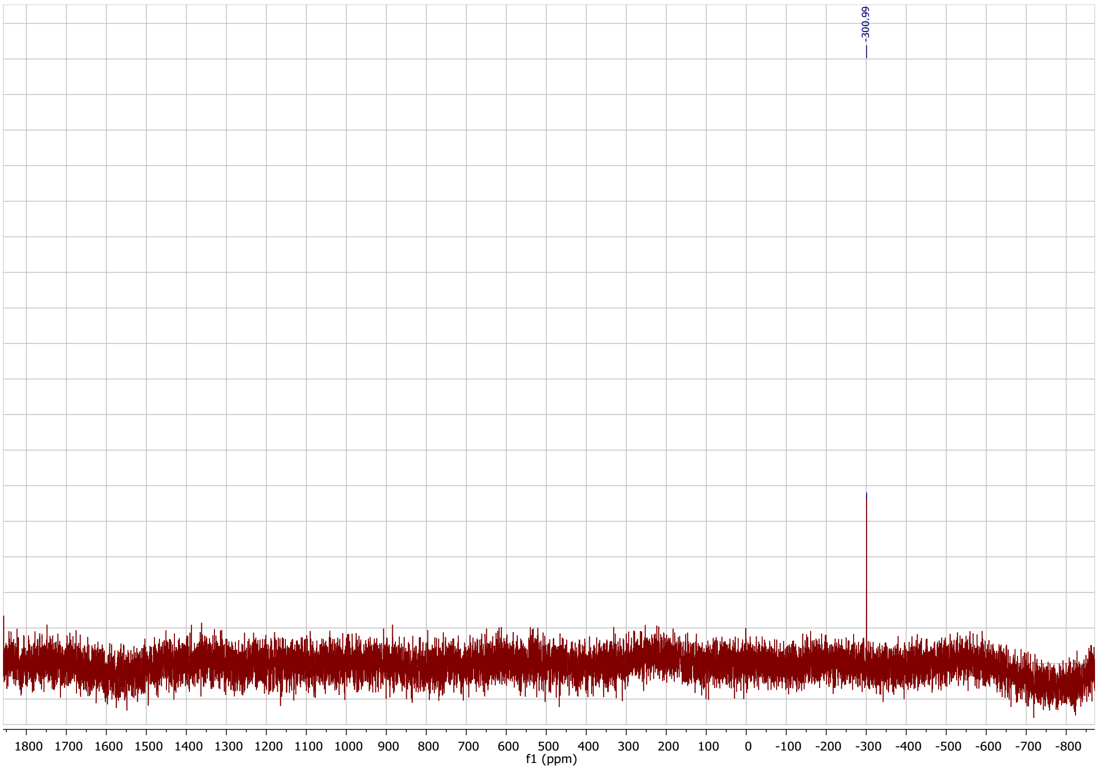

Figure S16. ^{77}Se NMR spectrum of compound **2** in C_6D_6.

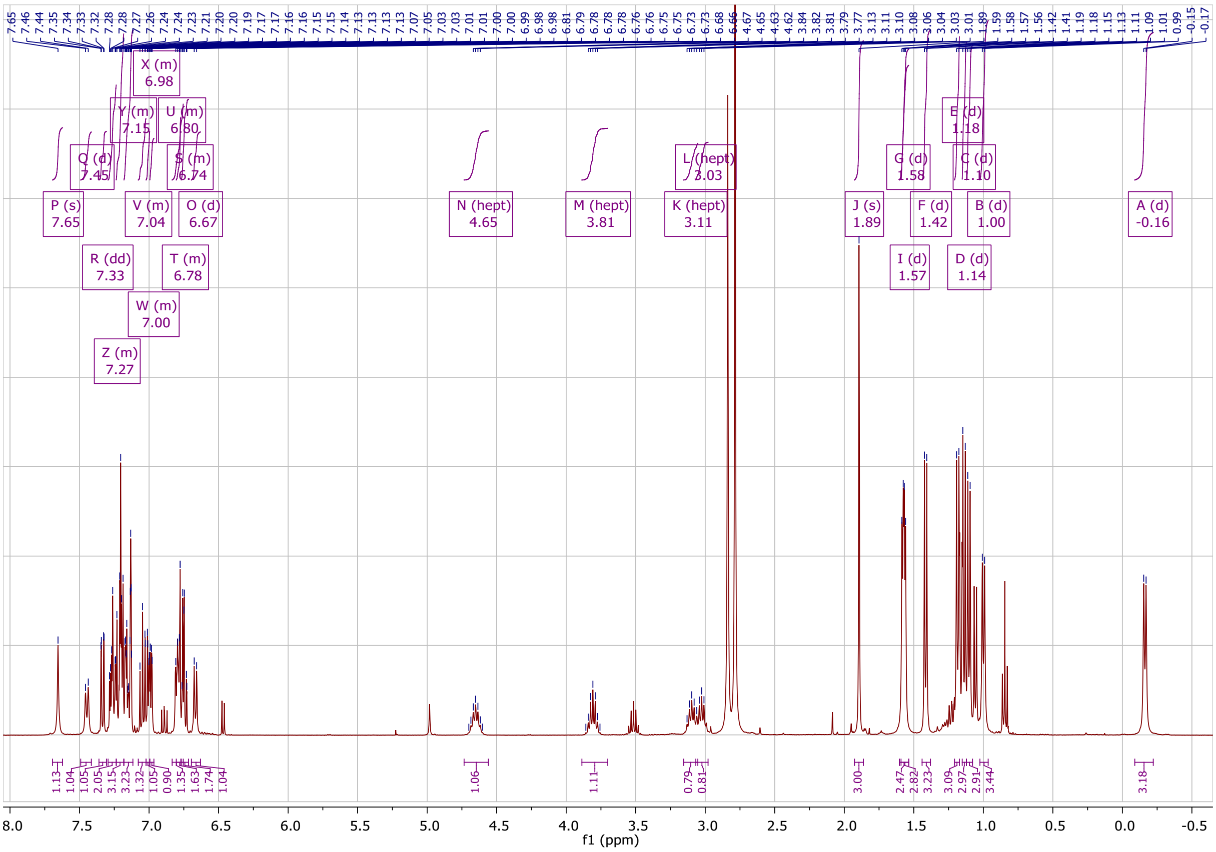

Figure S17. ^{1}H NMR spectrum of compound **3** in C_6D_6.

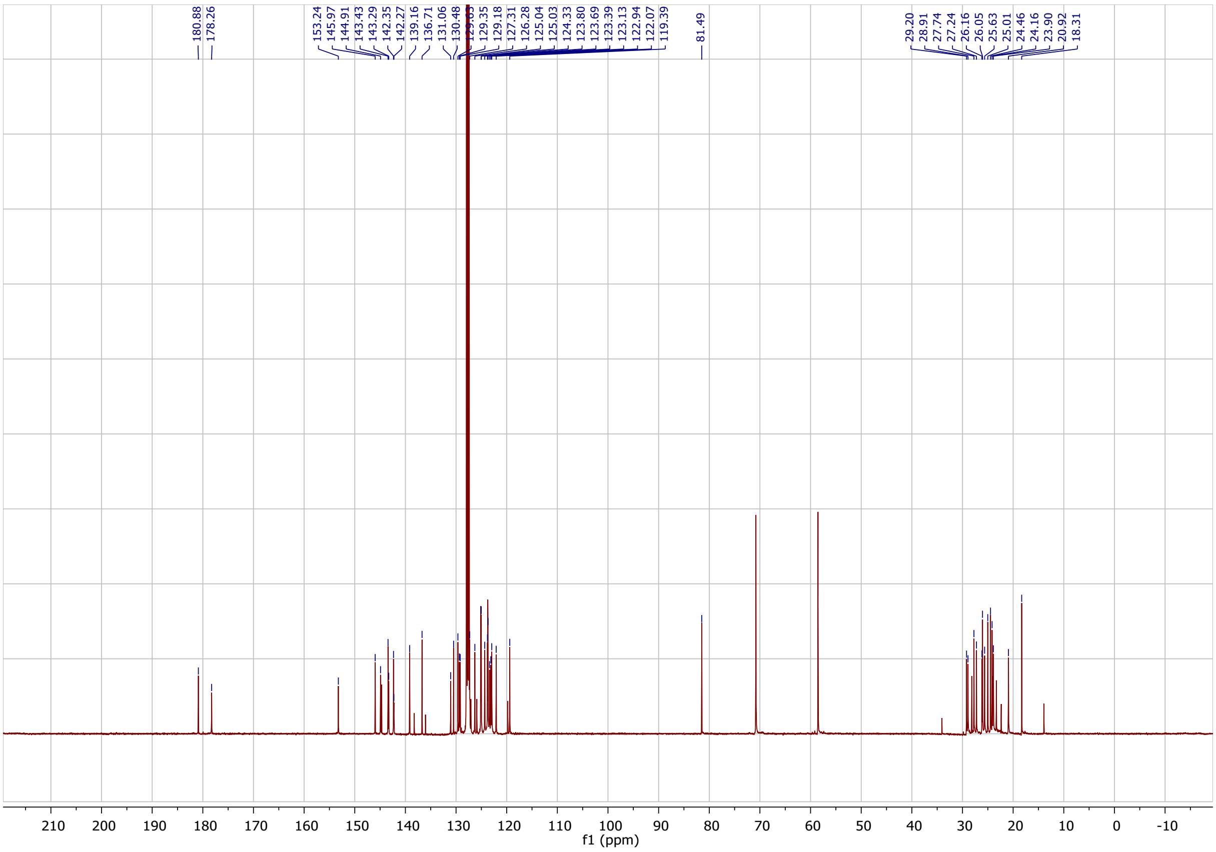

Figure S18. ^{13}C NMR spectrum of compound **3** in C_6D_6.

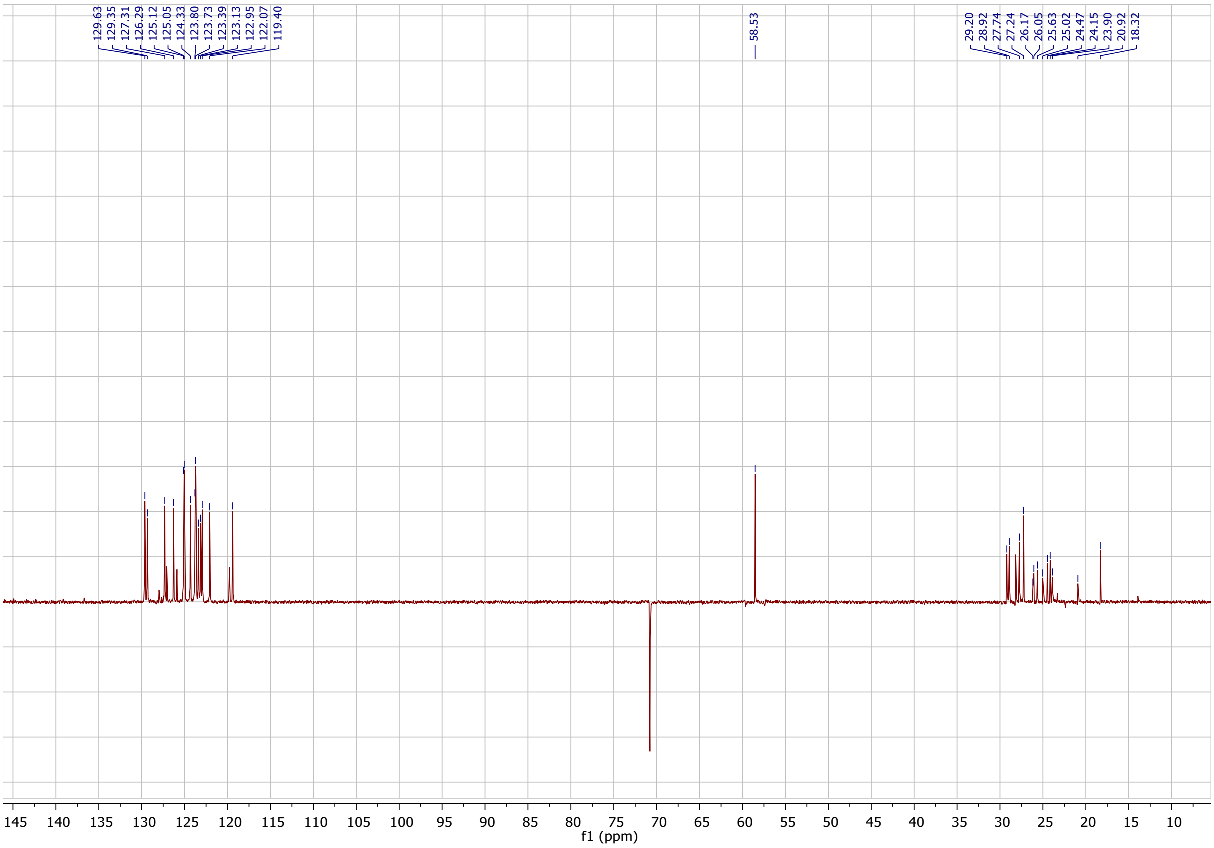

Figure S19. DEPT135 NMR spectrum of compound **3** in C_6D_6.

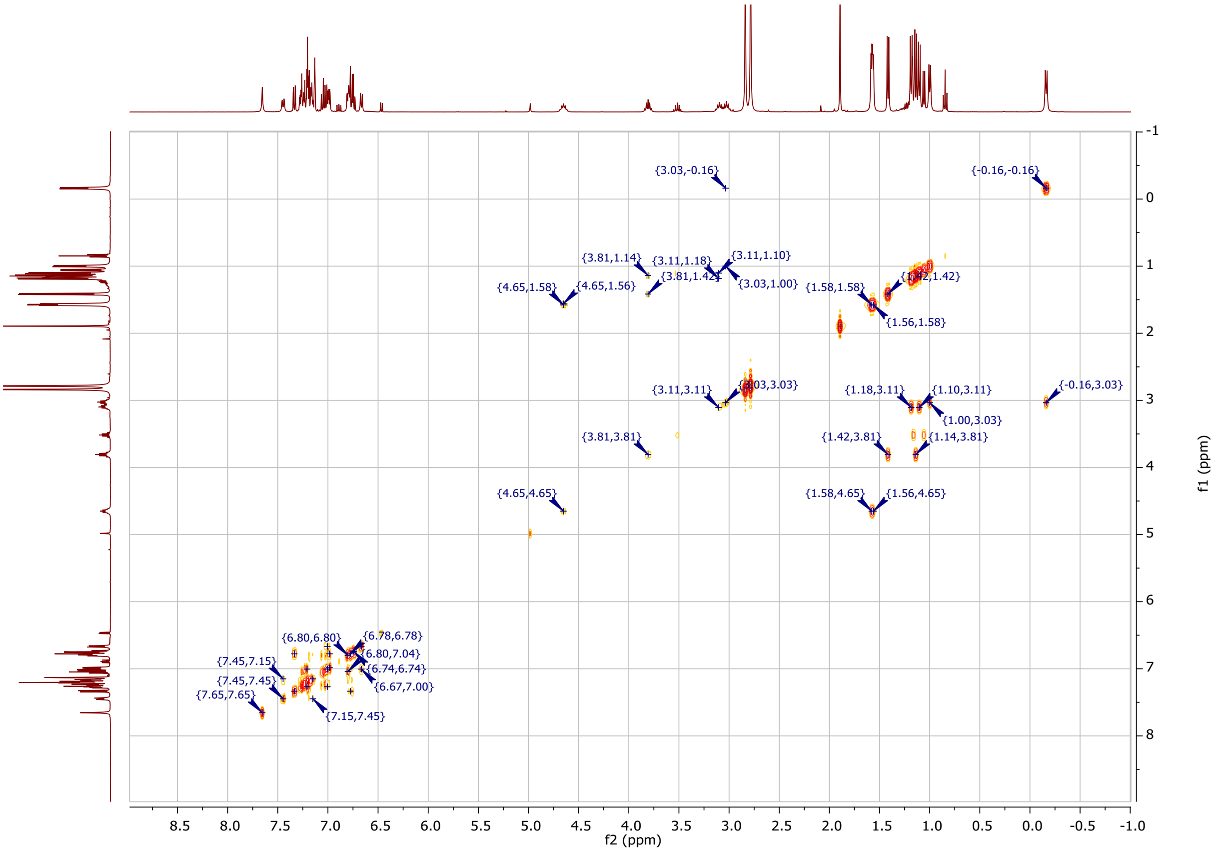

Figure S20. ^1H-^1H COSY NMR spectrum of compound **3** in C_6D_6.

Figure S21. ^{1}H-^{13}C HSQC NMR spectrum of compound **3** in C_6D_6.

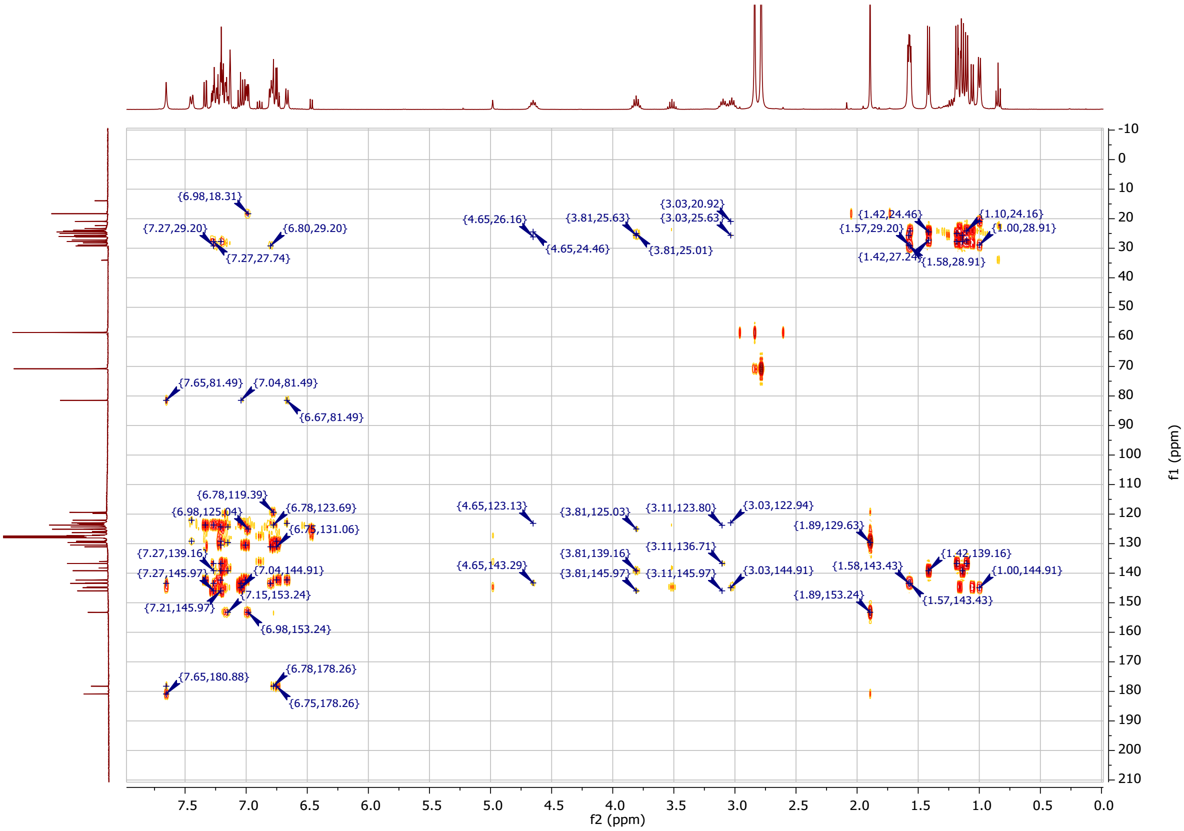

Figure S22. ^{1}H-^{13}C HMBC NMR spectrum of compound **3** in C_6D_6.

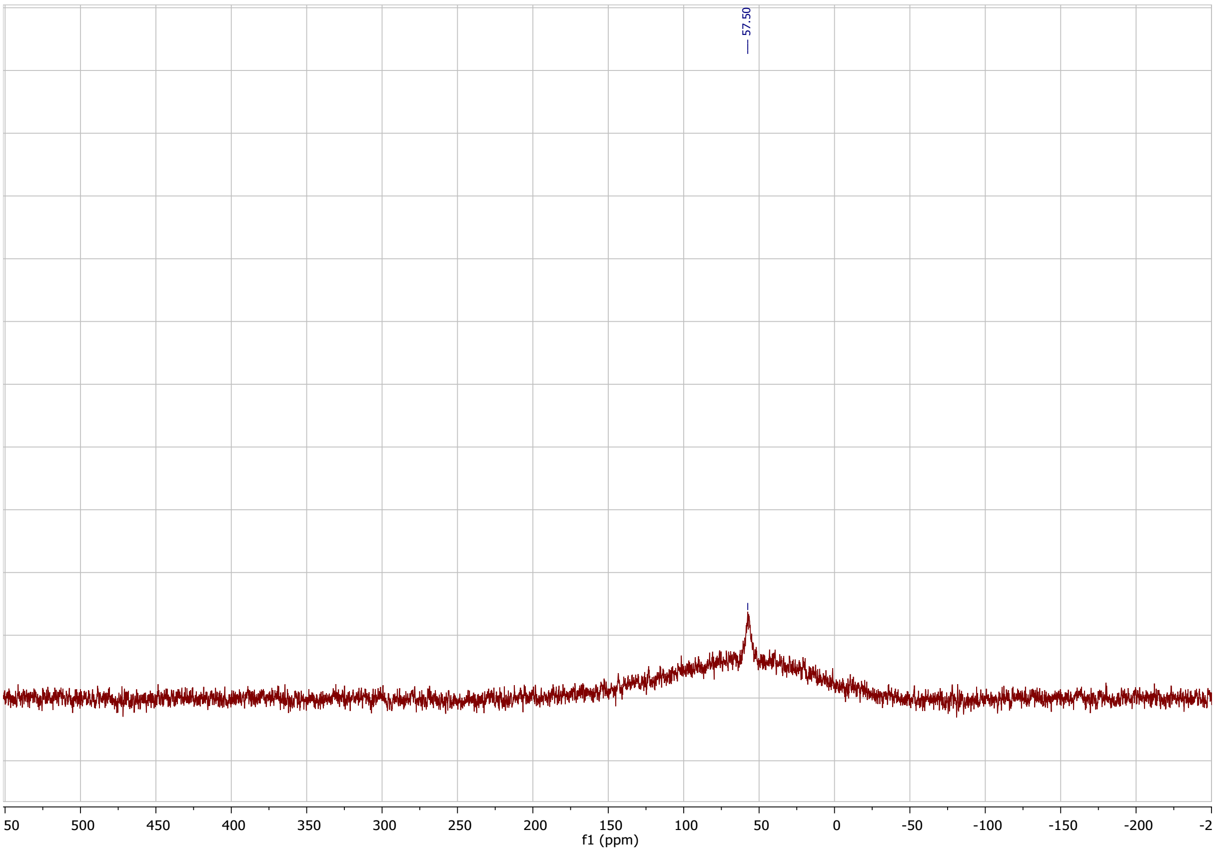

Figure S23. ^{1}H-^{13}C HMBC NMR spectrum of compound **3** in C_6D_6.

Figure S24. ^{1}H-^{15}N HSQC NMR spectrum of compound **3** in C_6D_6.

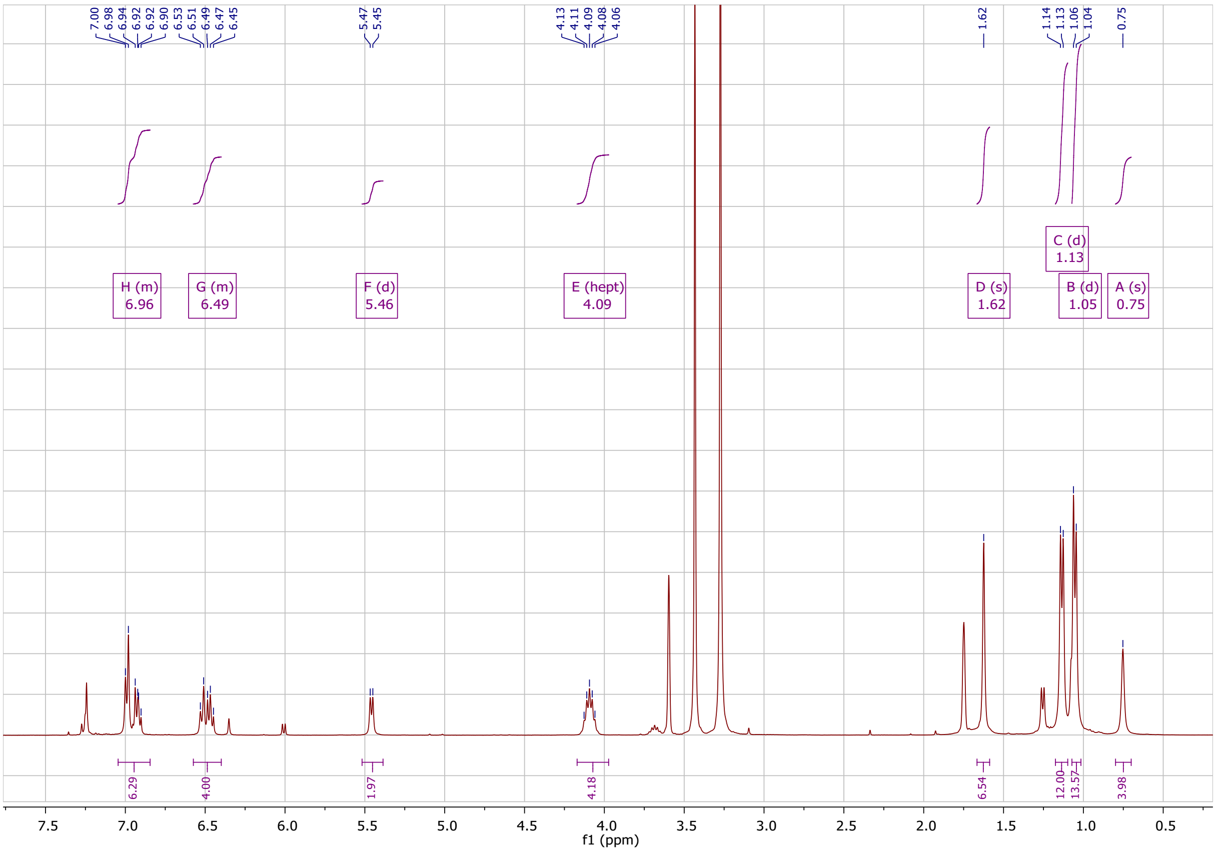

Figure S25. ^{1}H NMR spectrum of compound **9** in THF-d$_8$.

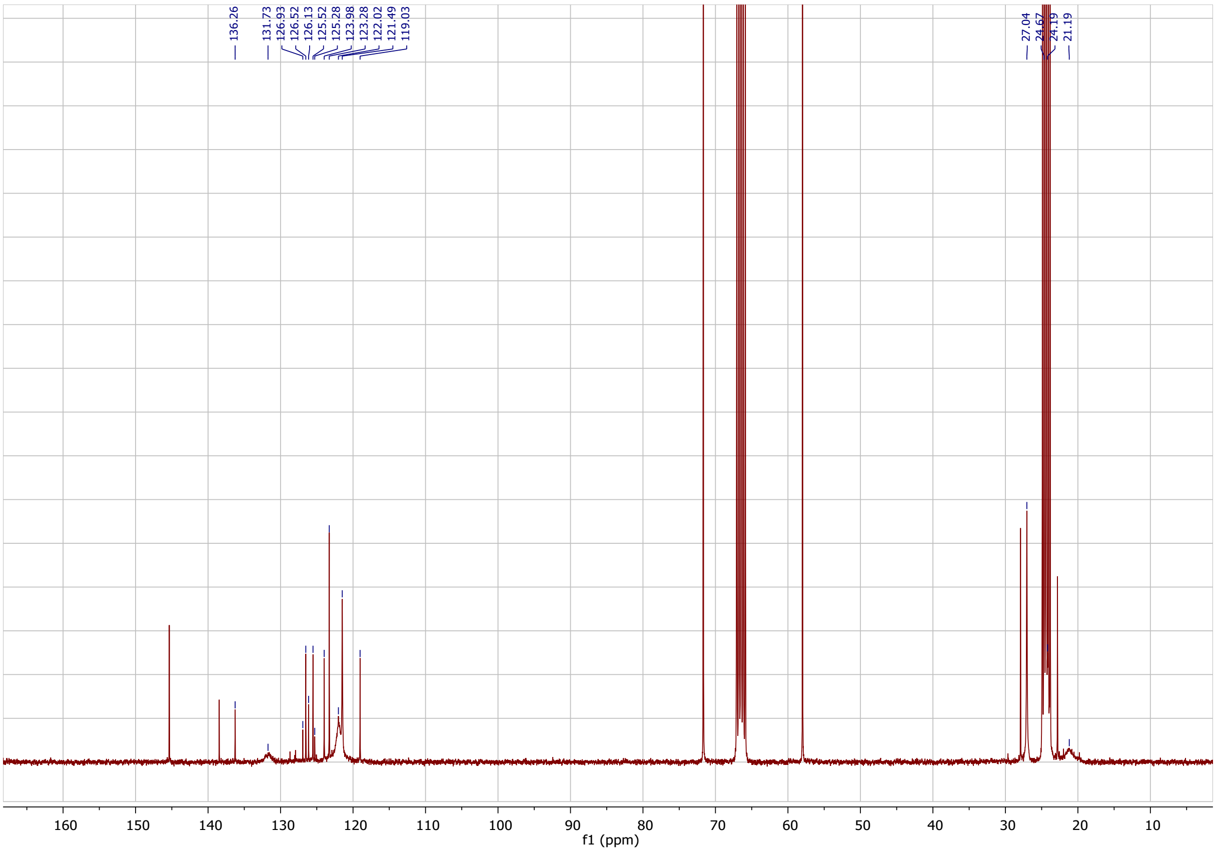

Figure S26. ^{13}C NMR spectrum of compound **9** in THF-d$_8$.

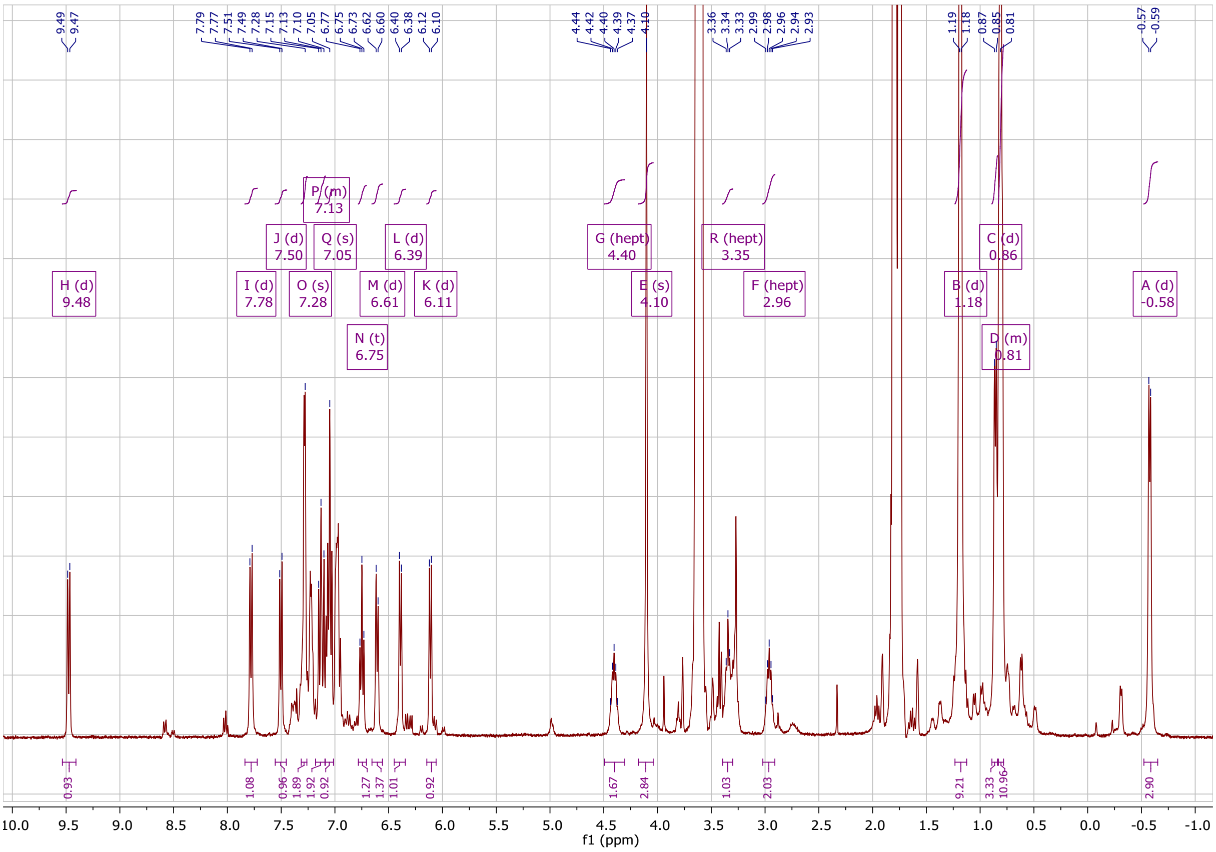

Figure S27. ^{1}H NMR spectrum of compound **11** in THF-d$_8$.

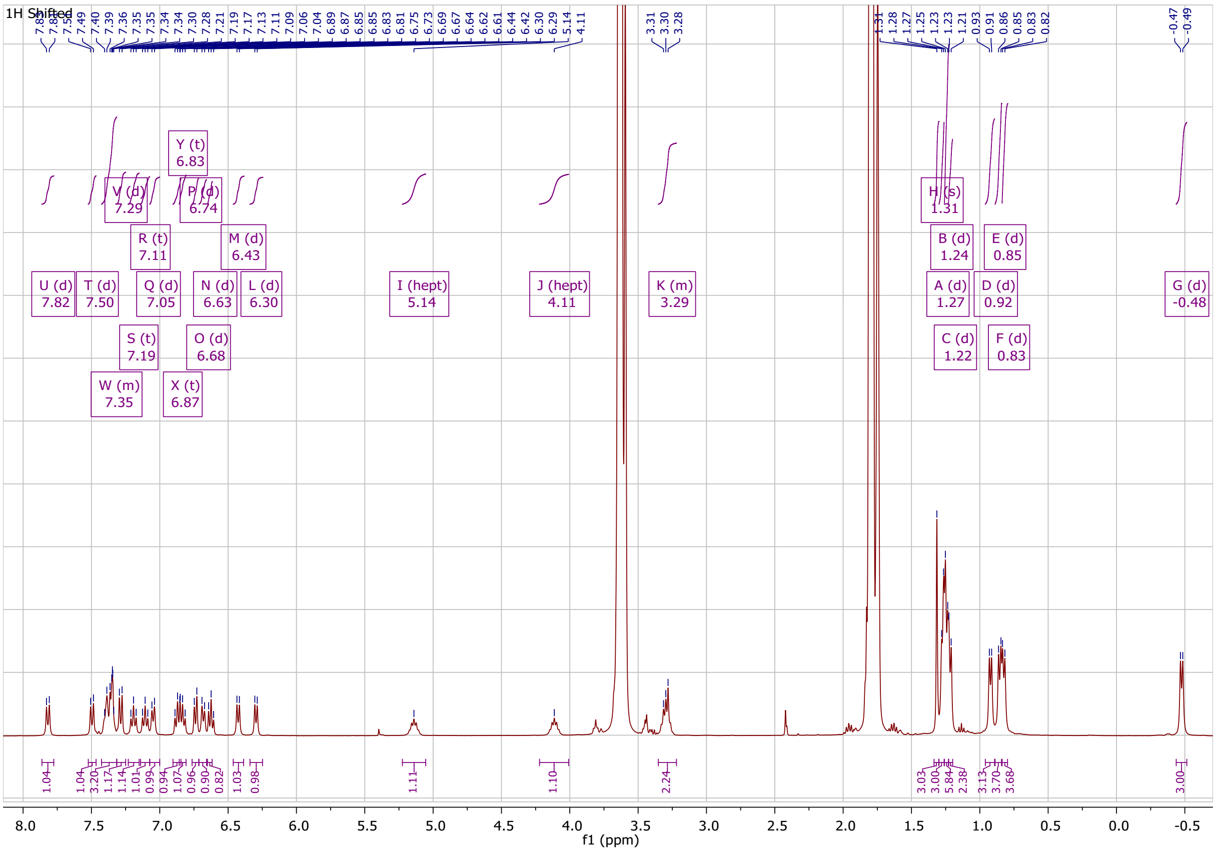

Figure S28. ^{1}H NMR spectrum of compound **12** in THF-d$_8$.

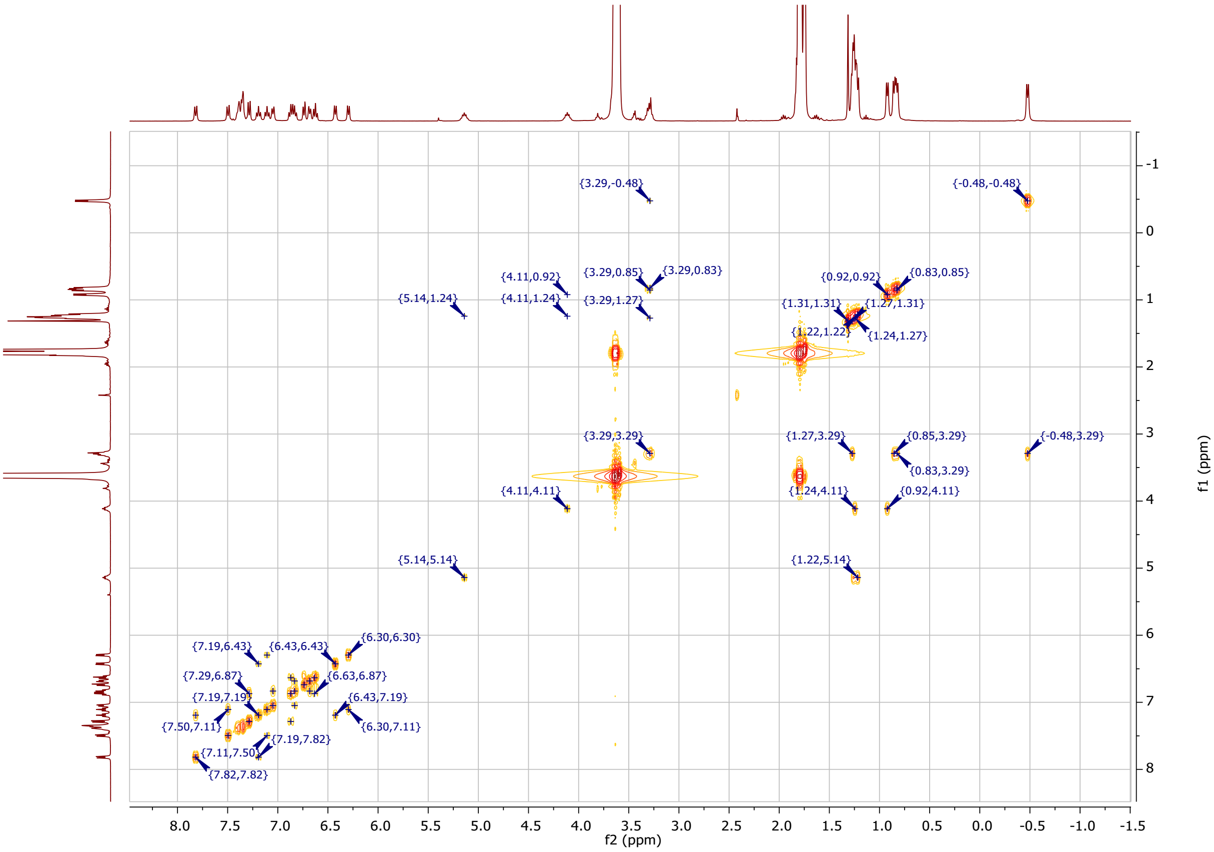

Figure S29. ^{1}H-^{1}H COSY NMR spectrum of compound **12** in THF-d$_8$.

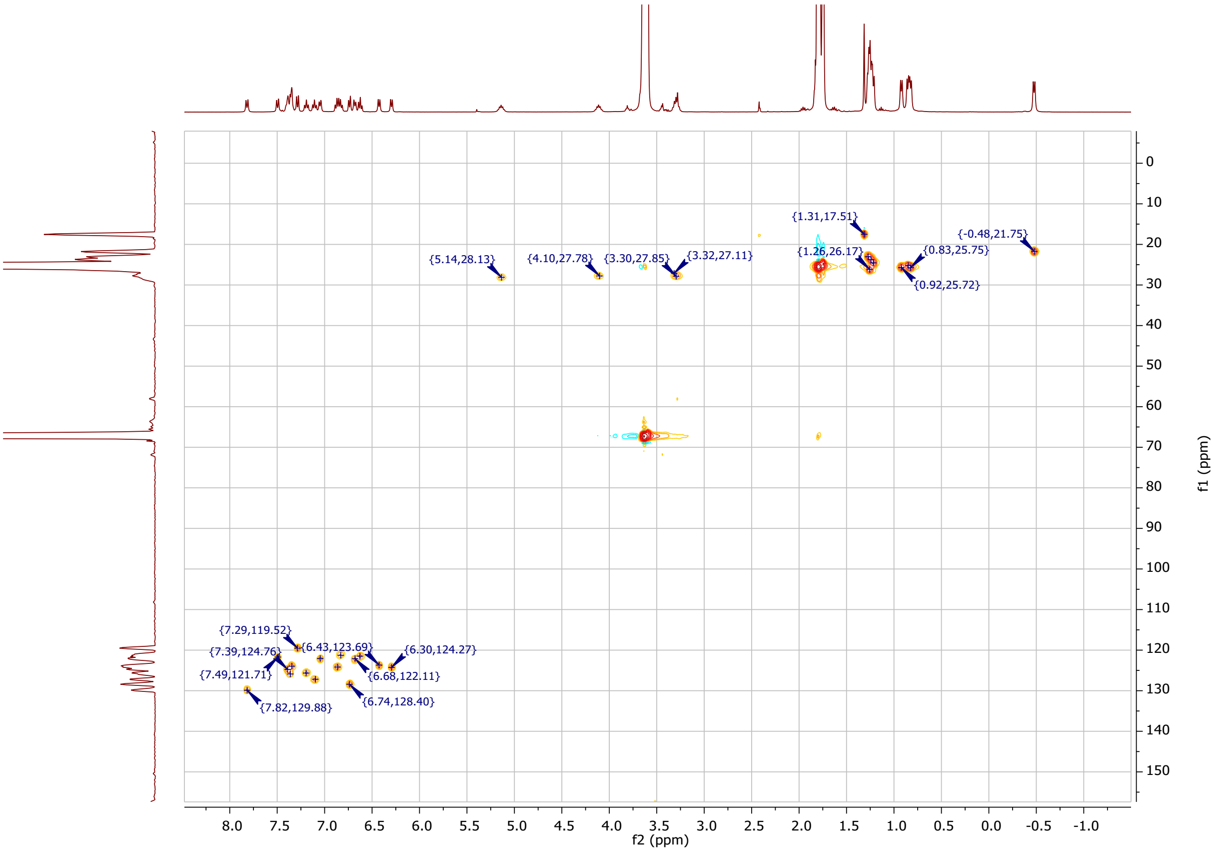

Figure S30. ^{1}H-^{13}C HSQC NMR spectrum of compound **12** in THF-d$_8$.

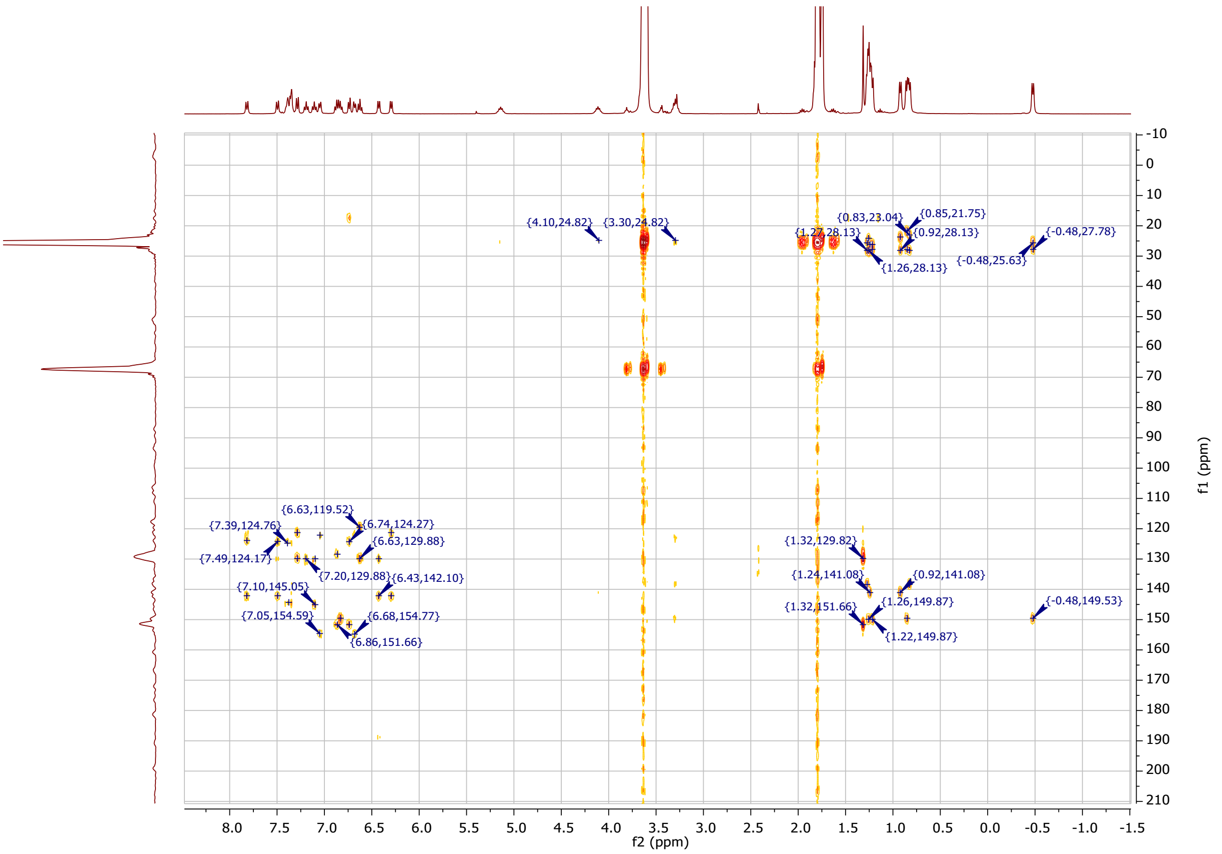

Figure S31. ^{1}H-^{13}C HMBC NMR spectrum of compound **12** in THF-d$_8$.

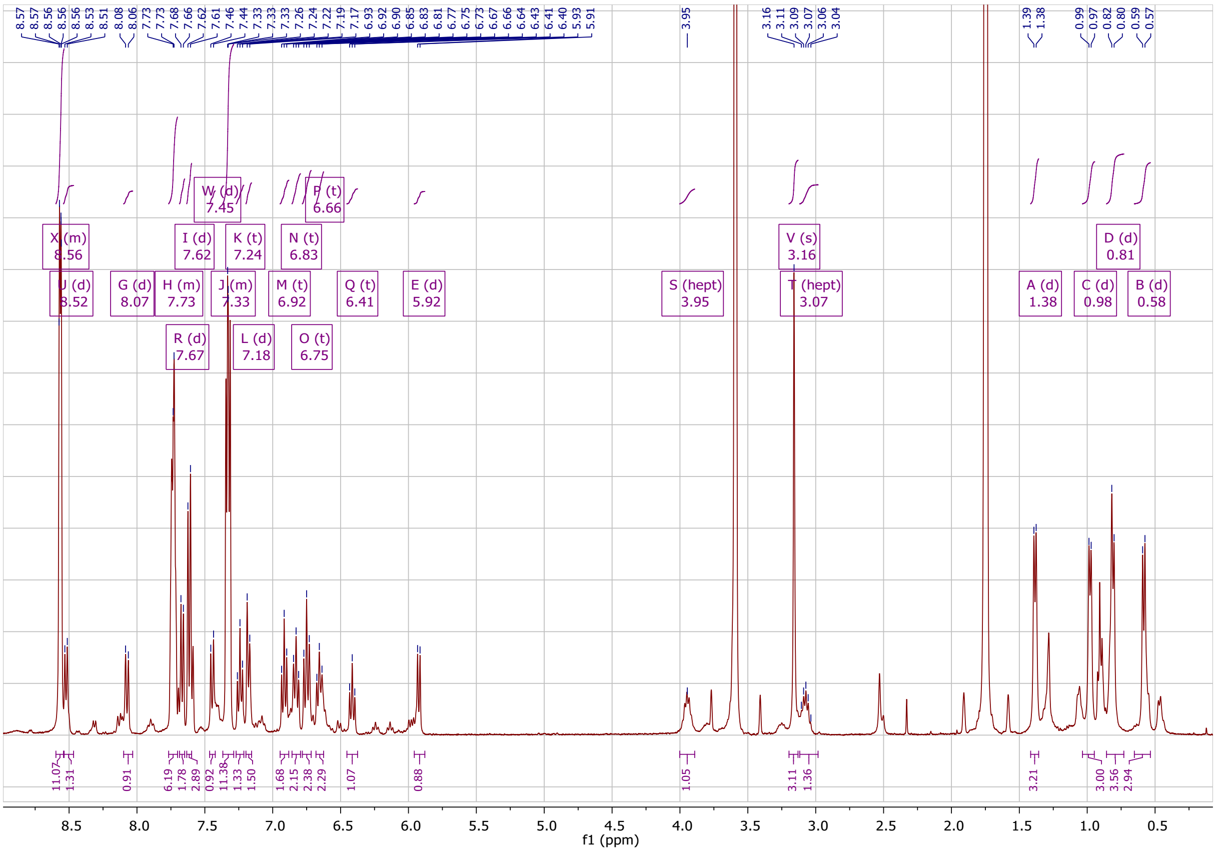

Figure S32. ^{1}H NMR spectrum of compound **13** in THF-d$_8$.

Figure S33. ^{1}H-^{1}H COSY NMR spectrum of compound **13** in THF-d_8.

DFT computations

The full geometry optimization of all model structures was carried out at the B3LYP/6-31G* level of theory with the help of Gaussian-09 program package.[18] The spin restricted approximation for the model structures with closed electron shells and unrestricted method for the model structures with open electron shells were employed. No symmetry restrictions have been applied during the geometry optimization procedure in all cases. The Hessian matrices were calculated analytically for all optimized model structures to prove the location of correct minimum on the potential energy surface (no imaginary frequencies were found in all cases, except transition state **2TS**, which is featuring only one imaginary frequency (the saddle point) and to estimate the thermodynamic parameters, the latter being calculated at 298.150 K and 1 atm. The Fuzzy bond order analysis[19] and QTAIM analysis[20] were performed by using the Multiwfn program (version 3.7)[21] and AIMALL.[22] Poincare-Hopf relationship was satisfied during the QTAIM analysis, and all critical points were successfully found. The natural bond orbital (NBO) analysis was carried out in accordance with the methodology proposed by Weinhold et al.[23] The low magnitude of the electron density (0.006–0.035 a.u.), positive values of the Laplacian of electron density (0.016–0.116 a.u.), and zero or very close to zero positive energy density (0.000–0.005 a.u.) in the found bond critical points (3, –1) were typical for closed shell contacts (noncovalent interactions).[24] The balance between the Lagrangian kinetic energy G(**r**) and potential energy density V(**r**) at the bond critical points (3, –1) revealed that a covalent contribution in all these contacts was absent.[25] Strength of Na···O, Na···N, N–H···N, and C–H···Se contacts in the optimized equilibrium model structure **2H** and transition state **2TS** was estimated on the basis of the empirical correlation between the interaction energy and the potential energy density of electrons at the bond critical points (3, –1) proposed by Espinosa at al for hydrogen bonds.[26] The molecular orbitals were plotted in the Chemcraft program (http://www.chemcraftprog.com). The Cartesian atomic coordinates for all optimized equilibrium model structures are presented in the attached xyz-file.

Table S4. Optimized structures of model compounds and transition states labelled with selected interatomic distances.

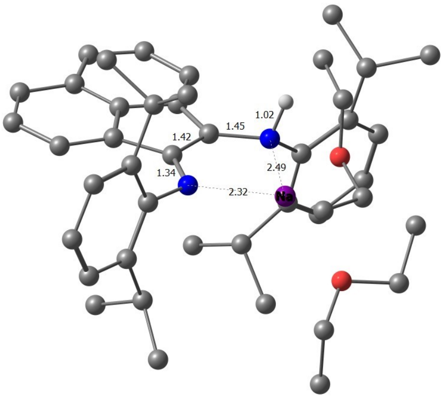	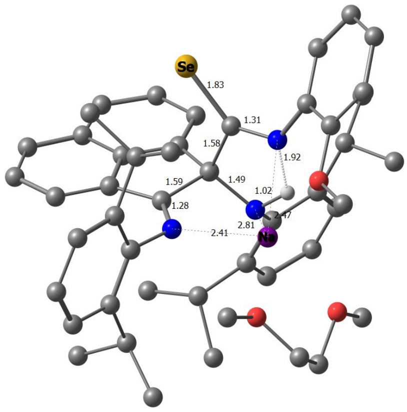
1H	**2H**
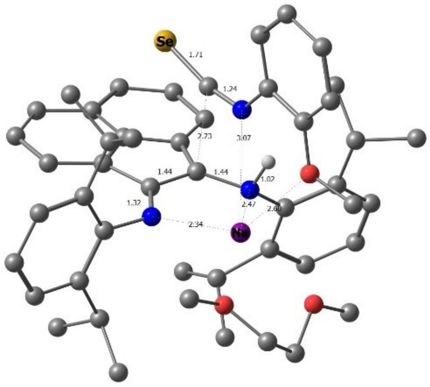	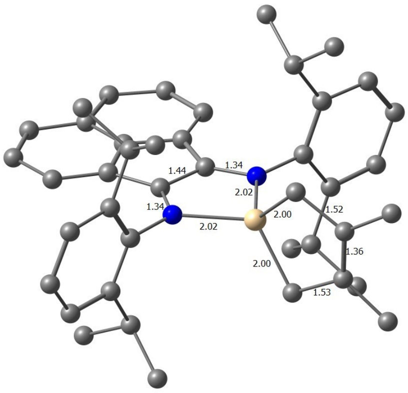
2TS	**6H**
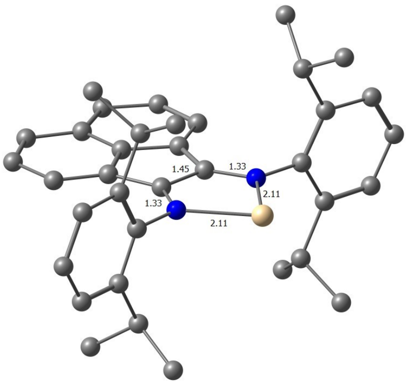	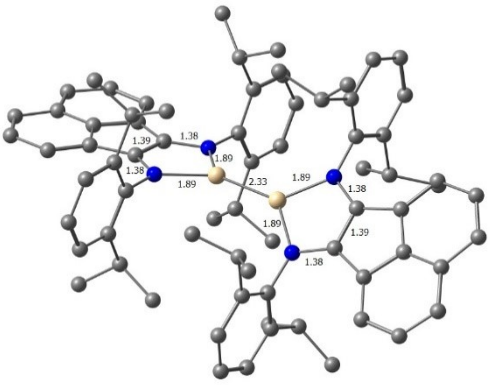
8H	**7H**
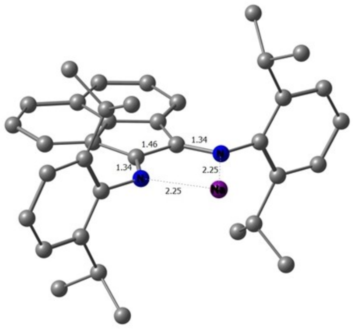	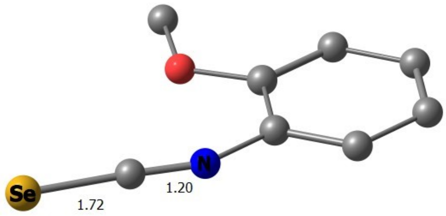
[(dpp-bian)$^{1-}$Na^{1+}]	**2-MeOC$_6$H$_4$N=C=Se**

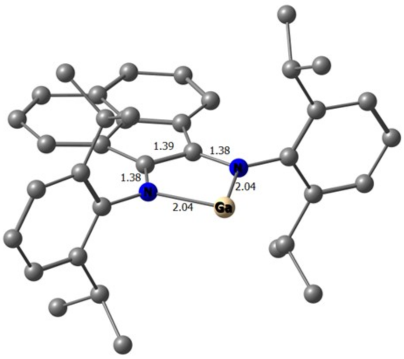

4H

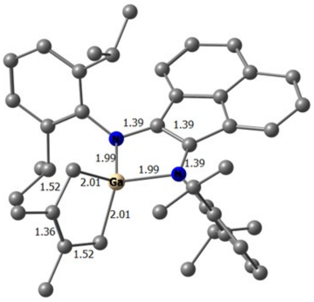

9H

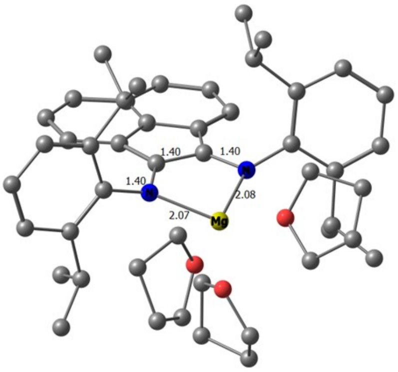

10H

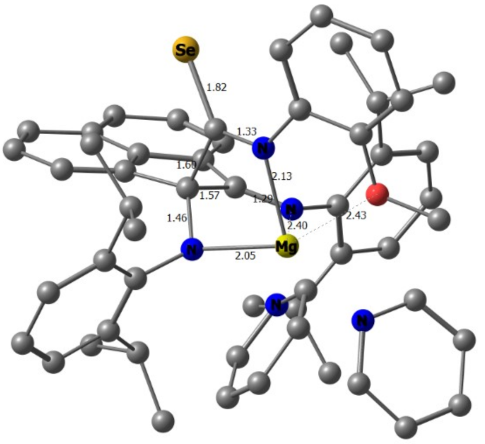

11H

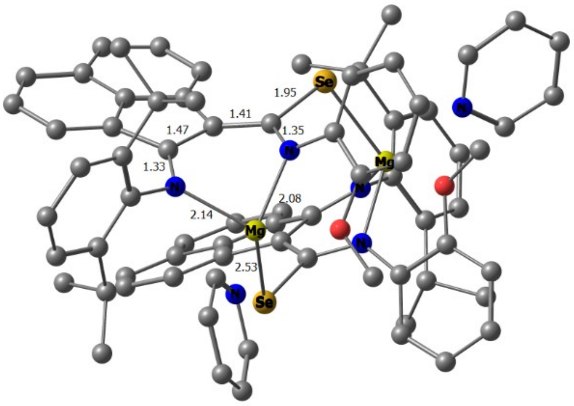

13H

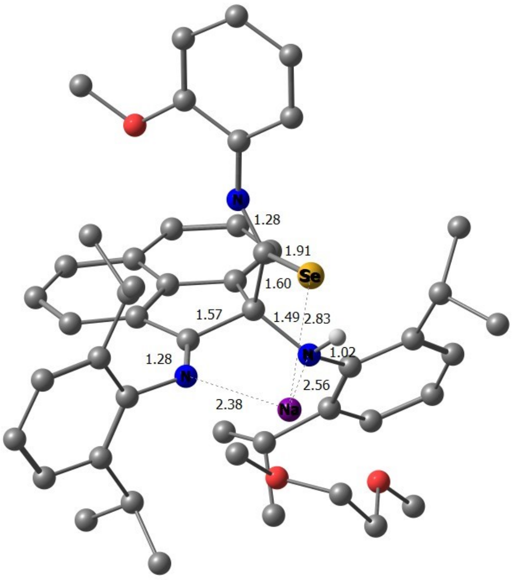

2H_Se-isomer

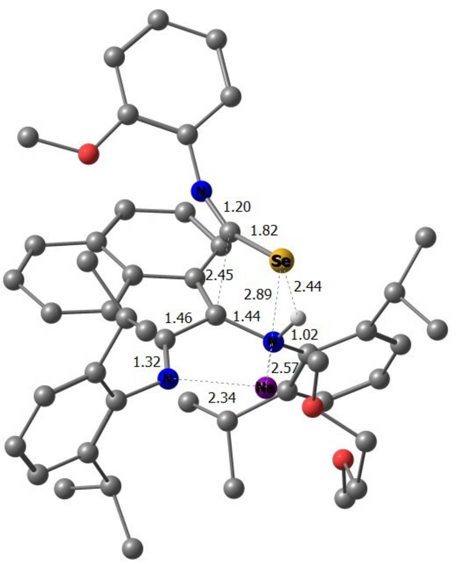

2H_se-isomer_TS

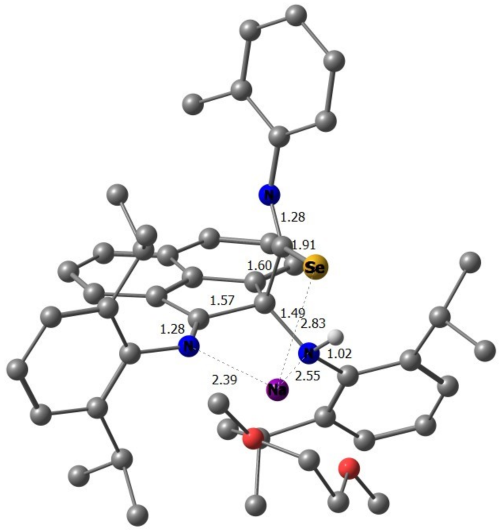

3H

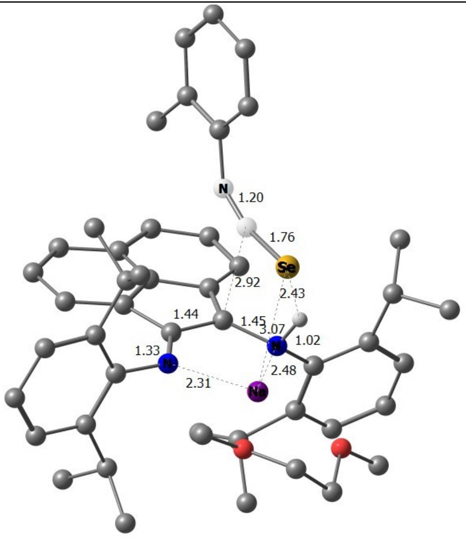

3H_TS

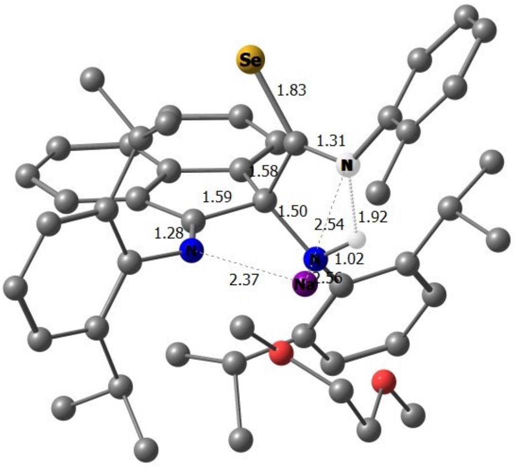

3H_N-isomer

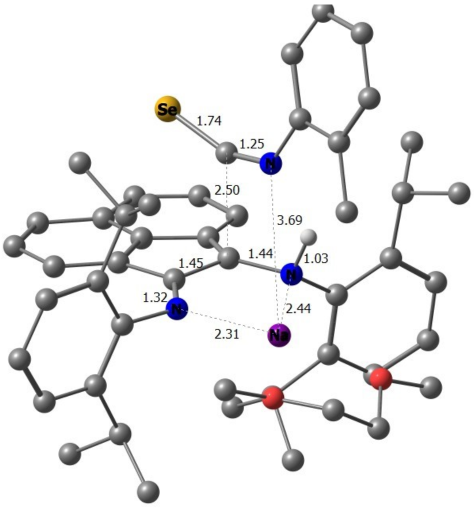

3H_N-isomer_TS

Table S5. Calculated total energies, enthalpies, Gibbs free energies (in Hartree), and entropies (in cal/mol•K) for optimized equilibrium model structures (E, H, G, and S, respectively).

Model structure	E	H	G	S
2-MeOC_6H_4N=C=Se	-2838.39818795	-2838.253013	-2838.302162	103.444
2-MeC_6H_4N=C=Se	-2763.19563292	-2763.056370	-2763.104185	100.633
1H	-2135.74334265	-2134.725341	-2134.874936	314.849
2H	-3663.11303010	-3662.250839	-3662.377524	266.632
7H	-6856.96612148	-6855.538721	-6855.726863	395.977
6H	-4815.71376240	-4814.688796	-4814.843236	325.047
8H	-3428.44642514	-3427.735169	-3427.847044	235.461
[(dpp-bian)$^{-1}$Na^{+1}]	-1667.79445912	-1667.084844	-1667.198309	238.806
butadiene_s-cis	-234.609493459	-234.462008	-234.496619	72.846
2TS	-4815.68268470	-4814.659925	-4814.814991	326.364
1H_DME	-1977.27786527	-1976.401617	-1976.534478	279.629
4H	-3428.50412322	-3427.795394	-3427.906825	234.525
9H	-3663.16967834	-3662.309290	-3662.431951	258.160
10H	-2402.99563490	-2401.908334	-2402.057037	312.972
11H	-5040.63663056	-5039.584653	-5039.739011	324.873
13H	-8540.28507657	-8538.934638	-8539.136493	424.840
2H_Se-isomer	-4815.72874359	-4814.703749	-4814.858304	325.290
2H_Se-isomer2	-4815.72110146	-4814.695999	-4814.850540	325.258
2H_Se-isomer_TS	-4815.68871713	-4814.666130	-4814.822319	328.727
3H	-4740.52756135	-4739.508306	-4739.661343	322.094
3H_N-isomer	-4740.50111737	-4739.482224	-4739.634126	319.704
3TS	-4740.48852064	-4739.471922	-4739.628167	328.846
3H_N-isomer_TS	-4740.47188806	-4739.455389	-4739.609644	324.658

Table S6. Calculated values of Gibbs free energies of hypothetical transformations (ΔG, in kcal/mol).

Hypothetical transformation	ΔG
7H → 2 **8H**	20.6
7H + 2 **butadiene_s-cis** → 2 **6H**	-21.9
8H + **butadiene_s-cis** → **6H**	-21.2
1H_DME + 2-MeOC$_6$H$_4$N=C=Se → 2TS	13.6*
1H_DME + 2-MeOC$_6$H$_4$N=C=Se → 2H	-4.1
4H + **butadiene_s-cis** → **9H**	-17.9
1H_DME + 2-MeC$_6$H$_4$N=C=Se → 3H	-14.2
1H_DME + 2-MeC$_6$H$_4$N=C=Se → 3TS	6.6*
1H_DME + 2-MeC$_6$H$_4$N=C=Se → 3H_N-isomer	2.8
1H_DME + 2-MeC$_6$H$_4$N=C=Se → 3H_N-isomer_TS	18.2*

* In fact, this is activation barrier.

Table S7. Frontier molecular orbitals of model compounds

HOMO	LUMO
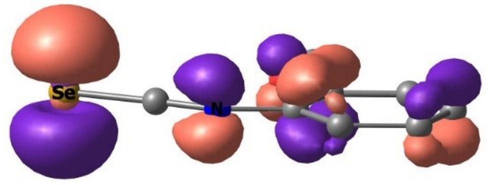	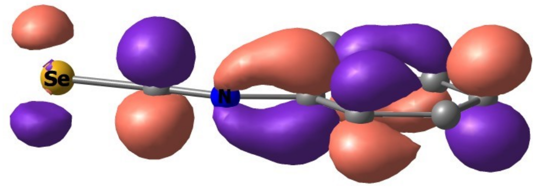
2-MeOC_6H_4N=C=Se HOMO –5.72 eV	**2-MeOC_6H_4N=C=Se LUMO –1.09 eV**
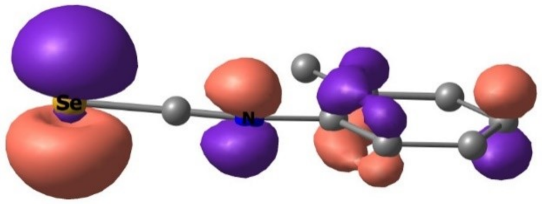	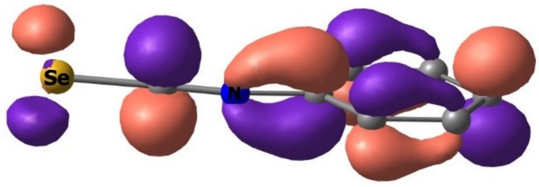
2-MeC_6H_4N=C=Se HOMO –5.96 eV	**2-MeOC_6H_4N=C=Se LUMO –1.26 eV**
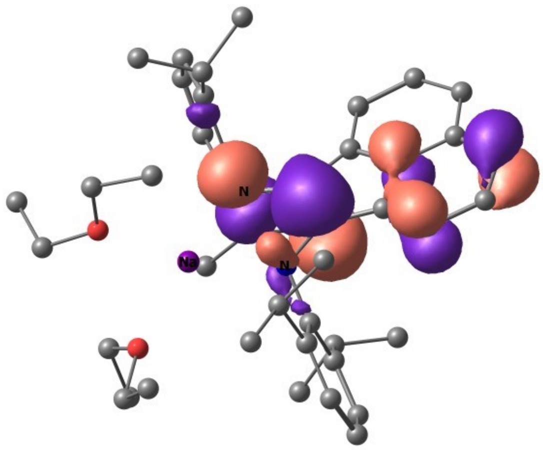	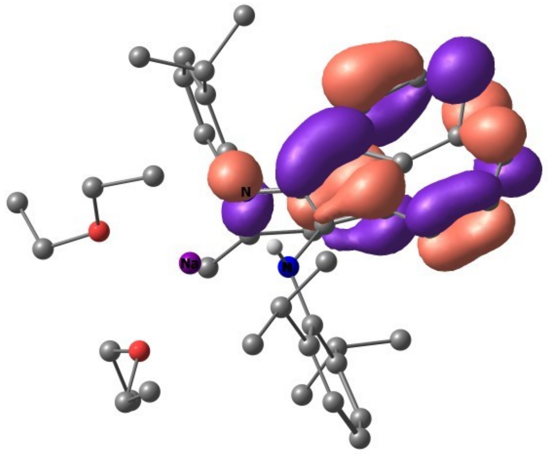
1H HOMO –3.42 eV	**1H LUMO –0.71 eV**
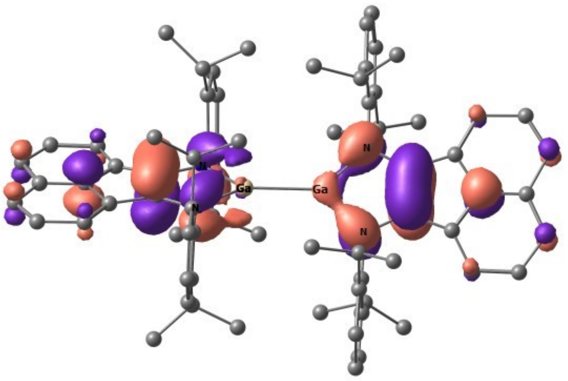	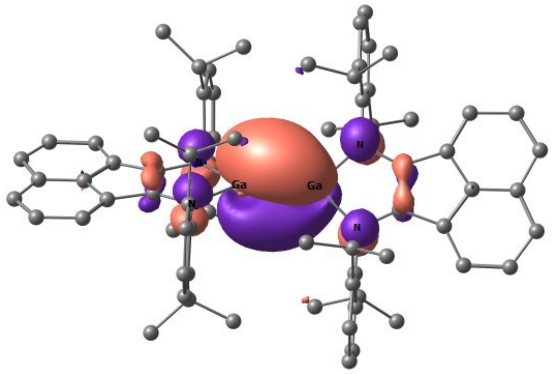
7H HOMO –4.13 eV	**7H LUMO –1.58 eV**

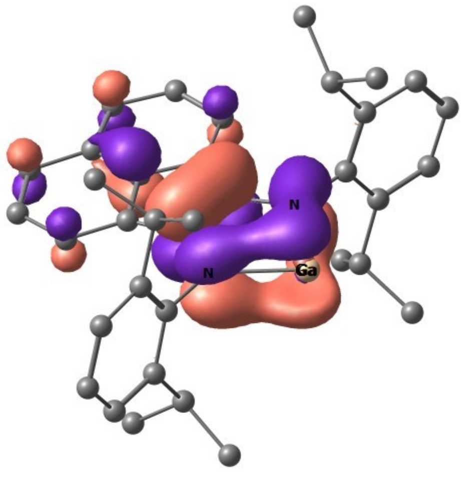

8H SOMO –2.58 eV

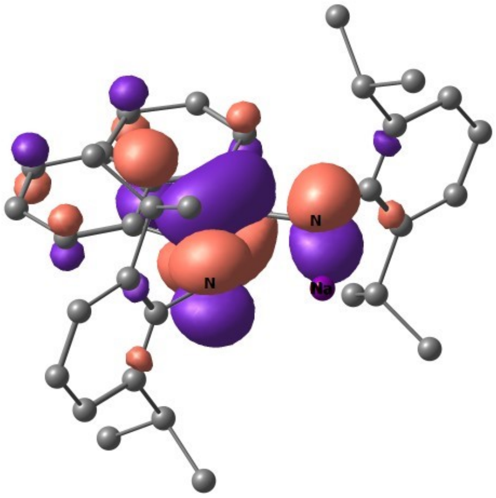

[(dpp-bian)Na] SOMO –1.49 eV

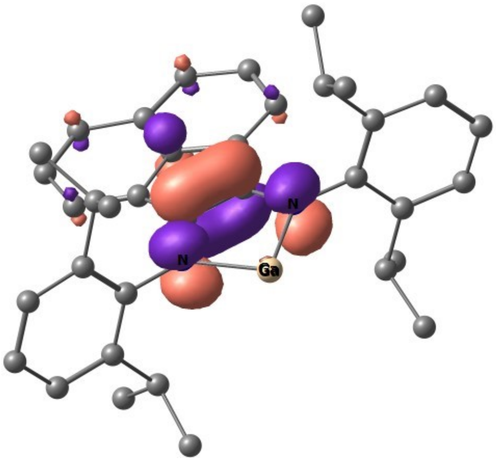

4H HOMO –0.57 eV

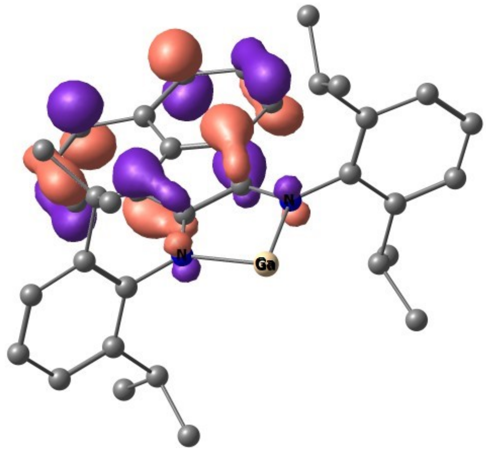

4H LUMO 1.43 eV

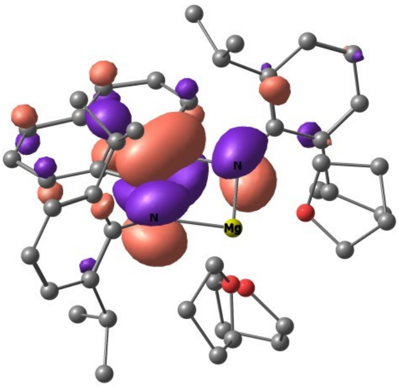

10H HOMO –2.69 eV

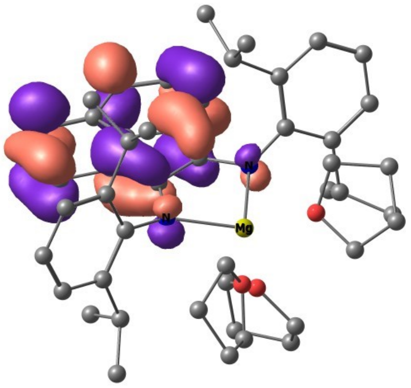

10H LUMO –0.56 eV

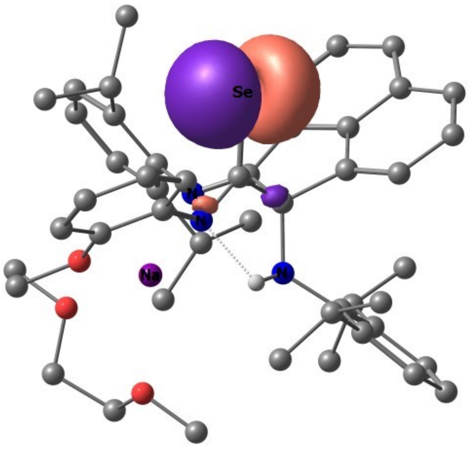	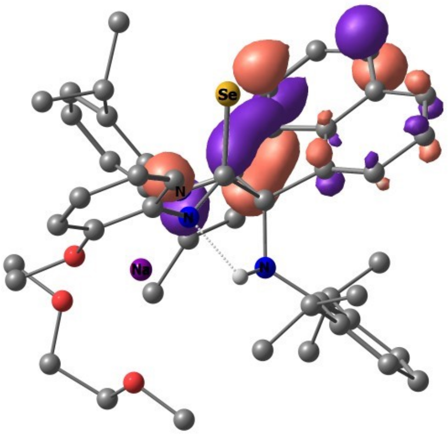
2H HOMO -3.93 eV	**2H LUMO -1.57 eV**
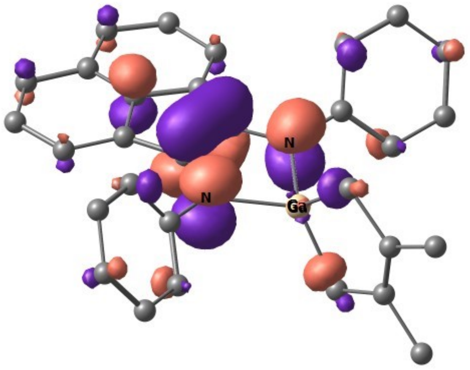	
9H SOMO -0.64 eV	

Table S8. Values of the density of all electrons – $\rho(\mathbf{r})$, Laplacian of electron density – $\nabla^2\rho(\mathbf{r})$ and appropriate λ_2 eigenvalues, energy density – H_b, potential energy density – $V(\mathbf{r})$, and Lagrangian kinetic energy – $G(\mathbf{r})$ (a.u.) at the bond critical points (3, –1), corresponding to six formal coordination bonds involving Na cation, intramolecular hydrogen bonds N–H···N and C–H···Se in the optimized equilibrium model structure **2H** as well as estimated strengths E_{int} (kcal/mol) of these noncovalent interactions.

Contact*	$\rho(\mathbf{r})$	$\nabla^2\rho(\mathbf{r})$	λ_2	H_b	$V(\mathbf{r})$	$G(\mathbf{r})$	$E_{int} = -V(\mathbf{r})/2$
Na1···O5 2.510 Å	0.013	0.072	-0.013	0.003	-0.013	0.015	4.1
Na1···O4 2.493 Å	0.013	0.074	-0.013	0.003	-0.013	0.016	4.1
Na1···O3 2.387 Å	0.017	0.100	-0.017	0.004	-0.017	0.021	5.3
Na1···N9 2.468 Å	0.018	0.093	-0.018	0.004	-0.016	0.020	5.0
Na1···N8 2.406 Å	0.020	0.112	-0.020	0.005	-0.019	0.023	6.0
Na1···N6 2.805 Å	0.008	0.038	-0.008	0.001	-0.007	0.008	2.2
N6–H7···N9 1.919 Å	0.035	0.116	-0.035	0.000	-0.030	0.030	9.4
C76–H77···Se2 2.756 Å	0.012	0.035	-0.012	0.001	-0.007	0.008	2.2
C88–H89···Se2 2.888 Å	0.011	0.038	-0.011	0.002	-0.006	0.008	1.9

* The numeration of atoms corresponds to their ordering in the attached xyz-file for optimized equilibrium model structure **2H**.

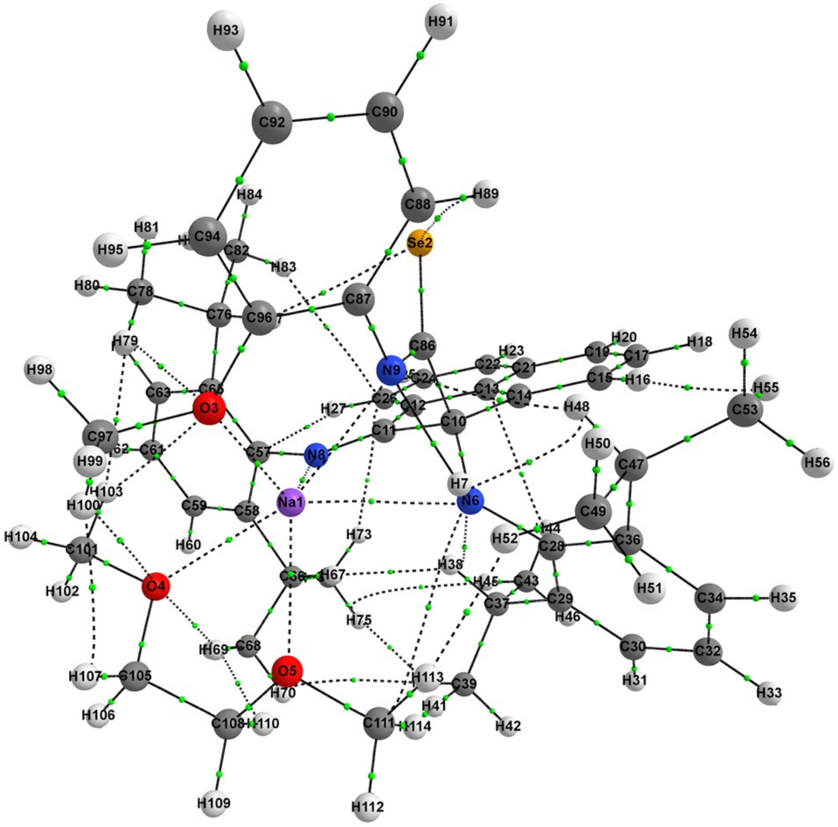

Figure S34. Molecular graph from QTAIM analysis of optimized equilibrium model structure **2H**. Bond critical points (3, -1) are shown in green.

Table S9. Values of the density of all electrons – $\rho(\mathbf{r})$, Laplacian of electron density – $\nabla^2\rho(\mathbf{r})$ and appropriate λ_2 eigenvalues, energy density – H_b, potential energy density – $V(\mathbf{r})$, and Lagrangian kinetic energy – $G(\mathbf{r})$ (a.u.) at the bond critical points (3, –1), corresponding to Na···O and Na···N noncovalent attractive interactions in the optimized equilibrium model structure **2TS** as well as estimated strengths E_{int} (kcal/mol) of these noncovalent interactions.

Contact[*]	$\rho(\mathbf{r})$	$\nabla^2\rho(\mathbf{r})$	λ_2	H_b	$V(\mathbf{r})$	$G(\mathbf{r})$	$E_{int} = -V(\mathbf{r})/2$
Na1···O99 2.596 Å	0.010	0.055	-0.010	0.002	-0.010	0.012	3.1
Na1···O90 2.548 Å	0.012	0.064	-0.012	0.002	-0.012	0.014	3.8
Na1···O81 2.421 Å	0.016	0.091	-0.016	0.003	-0.016	0.019	5.0
Na1···N2 2.341 Å	0.024	0.137	-0.024	0.006	-0.023	0.029	7.2
Na1···N3 2.474 Å	0.018	0.091	-0.018	0.004	-0.016	0.019	5.0
N102···H4 2.099 Å	0.023	0.073	-0.023	0.000	-0.017	0.018	5.3
C8···Se98 3.348 Å	0.010	0.028	-0.010	0.001	-0.005	0.006	1.6
C97···C6 2.730 Å	0.023	0.042	-0.023	0.001	-0.009	0.010	2.8

[*] The numeration of atoms corresponds to their ordering in the attached xyz-file for optimized equilibrium model structure **2TS**.

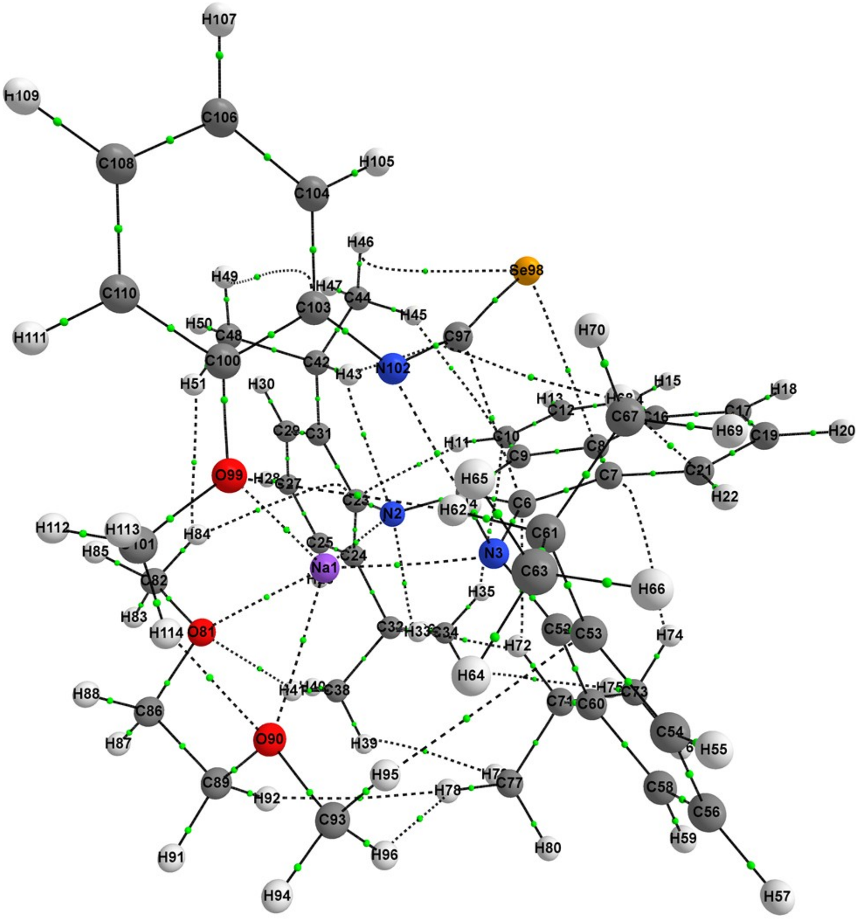

Figure S35. Molecular graph from QTAIM analysis of optimized equilibrium model structure **2TS**. Bond critical points (3, -1) are shown in green.

Table S10. Values of the density of all electrons – ρ(**r**), Laplacian of electron density – $\nabla^2\rho(\mathbf{r})$ and appropriate λ_2 eigenvalues, energy density – H_b, potential energy density – V(**r**), and Lagrangian kinetic energy – G(**r**) (a.u.) at the bond critical points (3, –1), corresponding to Na···O and Na···N noncovalent attractive interactions in the optimized equilibrium model structure **2H_se-isomer** as well as estimated strengths E_{int} (kcal/mol) of these noncovalent interactions.

Contact*	ρ(**r**)	$\nabla^2\rho(\mathbf{r})$	λ_2	H_b	V(**r**)	G(**r**)	$E_{int} = -V(\mathbf{r})/2$
Na1···Se109 2.829 Å	0.017	0.073	-0.017	0.002	-0.013	0.016	4.1
H5···Se109 2.313 Å	0.029	0.069	-0.029	-0.002	-0.022	0.019	6.9
Na1···N4 2.556 Å	0.014	0.072	-0.014	0.003	-0.012	0.015	3.8
Na1···O3 2.374 Å	0.018	0.105	-0.018	0.004	-0.018	0.022	5.6
Na1···O2 2.380 Å	0.018	0.106	-0.018	0.004	-0.019	0.023	6.0
Na1···N6 2.380 Å	0.022	0.122	-0.022	0.005	-0.020	0.025	6.3

* The numeration of atoms corresponds to their ordering in the attached xyz-file for optimized equilibrium model structure **2H_se-isomer**.

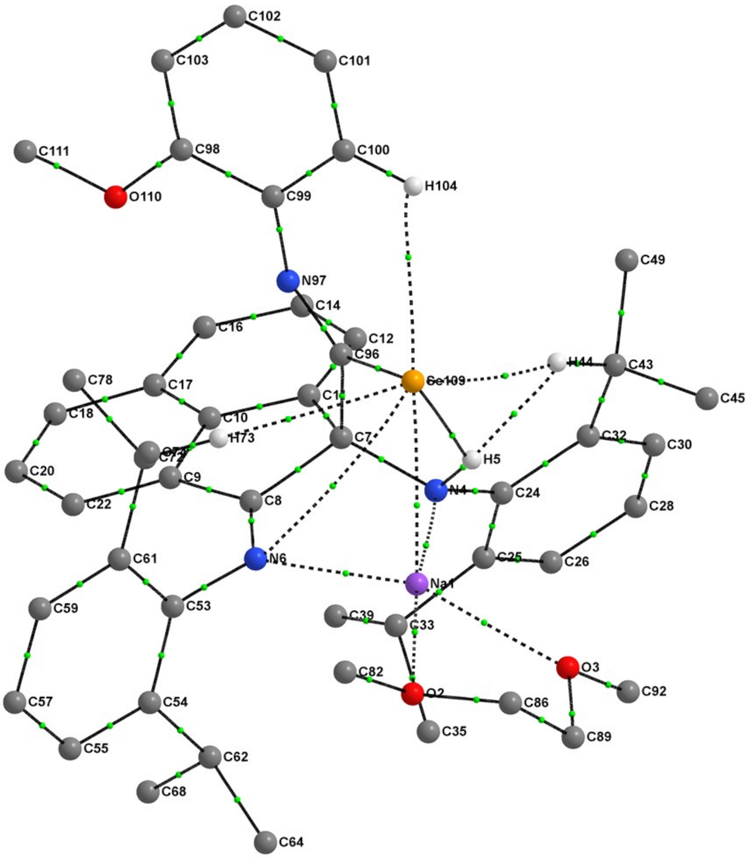

Figure S36. Molecular graph from QTAIM analysis of optimized equilibrium model structure **2H_Se-isomer_TS**. Bond critical points (3, -1) are shown in green.

Table S11. Values of the density of all electrons – ρ(**r**), Laplacian of electron density – $\nabla^2\rho(\mathbf{r})$ and appropriate λ_2 eigenvalues, energy density – H_b, potential energy density – V(**r**), and Lagrangian kinetic energy – G(**r**) (a.u.) at the bond critical points (3, –1), corresponding to Na···O and Na···N noncovalent attractive interactions in the optimized equilibrium model structure **2H_Se-isomer_TS** as well as estimated strengths E_{int} (kcal/mol) of these noncovalent interactions.

Contact*	ρ(**r**)	$\nabla^2\rho(\mathbf{r})$	λ_2	H_b	V(**r**)	G(**r**)	E_{int} = –V(**r**)/2
Na1···Se109 2.891 Å	0.014	0.060	-0.014	0.002	-0.011	0.013	3.5
H5···Se109 2.891 Å	0.022	0.056	-0.022	0.000	-0.015	0.014	4.7
Na1···N4 2.573 Å	0.014	0.067	-0.014	0.002	-0.012	0.014	3.8
Na1···O3 2.381 Å	0.018	0.104	-0.018	0.004	-0.018	0.022	5.6
Na1···O2 2.444 Å	0.016	0.086	-0.016	0.003	-0.015	0.018	4.7
Na1···N6 2.341 Å	0.024	0.137	-0.024	0.006	-0.023	0.028	7.2

[*] The numeration of atoms corresponds to their ordering in the attached xyz-file for optimized equilibrium model structure **2H_Se-isomer_TS**.

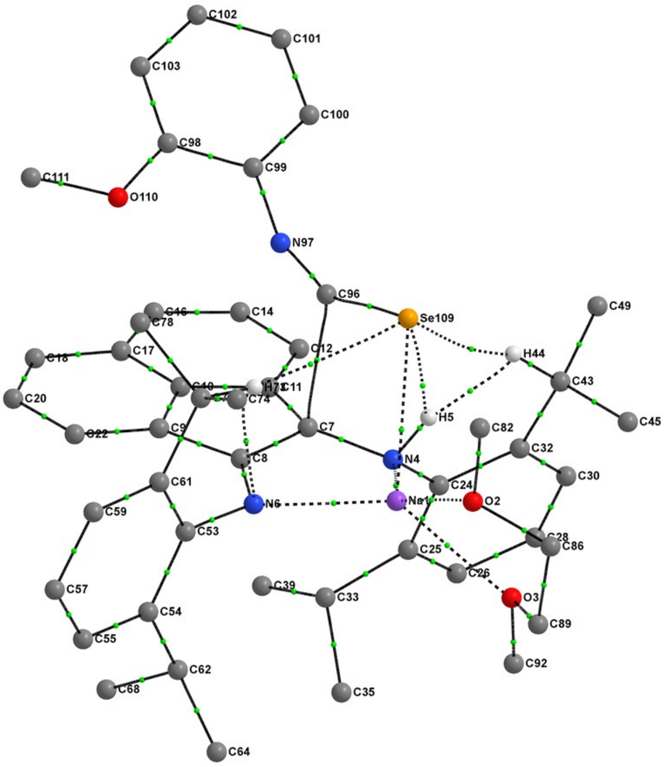

Figure S37. Molecular graph from QTAIM analysis of optimized equilibrium model structure **2H_se-isomer**. Bond critical points (3, -1) are shown in green.

Table S12. Values of the density of all electrons – ρ(**r**), Laplacian of electron density – $\nabla^2\rho(\mathbf{r})$ and appropriate λ_2 eigenvalues, energy density – H_b, potential energy density – V(**r**), and Lagrangian kinetic energy – G(**r**) (a.u.) at the bond critical points (3, –1), corresponding to Na···O and Na···N noncovalent attractive interactions in the optimized equilibrium model structure **3H** as well as estimated strengths E_{int} (kcal/mol) of these noncovalent interactions.

Contact*	ρ(**r**)	$\nabla^2\rho(\mathbf{r})$	λ_2	H_b	V(**r**)	G(**r**)	$E_{int} = -V(\mathbf{r})/2$
Na1···Se109 2.830 Å	0.017	0.073	-0.017	0.002	-0.013	0.016	4.1
H5···Se109 2.310 Å	0.029	0.069	-0.029	-0.002	-0.022	0.019	6.9
Na1···N4 2.552 Å	0.014	0.073	-0.014	0.003	-0.013	0.015	4.1
Na1···O3 2.373 Å	0.018	0.105	-0.018	0.004	-0.018	0.022	5.6
Na1···O2 2.372 Å	0.019	0.109	-0.019	0.004	-0.019	0.023	6.0
Na1···N6 2.386 Å	0.021	0.120	-0.021	0.005	-0.020	0.025	6.3

[*] The numeration of atoms corresponds to their ordering in the attached xyz-file for optimized equilibrium model structure **3H**.

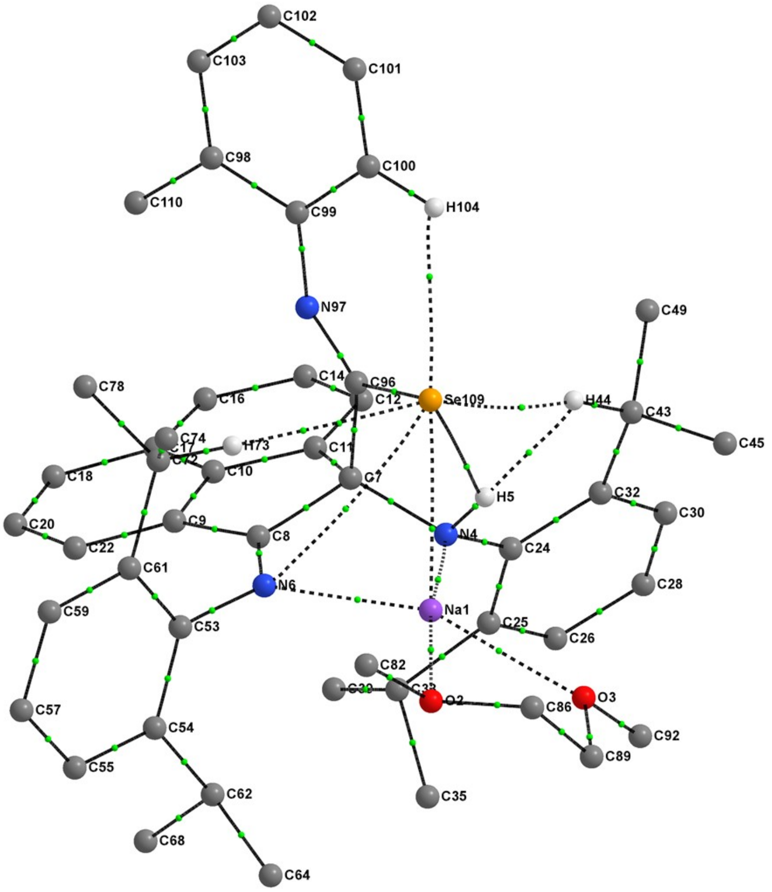

Figure S38. Molecular graph from QTAIM analysis of optimized equilibrium model structure **3H**. Bond critical points (3, -1) are shown in green.

Table S13. Values of the density of all electrons – ρ(**r**), Laplacian of electron density – $\nabla^2\rho(\mathbf{r})$ and appropriate λ_2 eigenvalues, energy density – H_b, potential energy density – V(**r**), and Lagrangian kinetic energy – G(**r**) (a.u.) at the bond critical points (3, –1), corresponding to Na···O and Na···N noncovalent attractive interactions in the optimized equilibrium model structure **3Ts** as well as estimated strengths E_{int} (kcal/mol) of these noncovalent interactions.

Contact*	ρ(**r**)	$\nabla^2\rho(\mathbf{r})$	λ_2	H_b	V(**r**)	G(**r**)	$E_{int} = -V(\mathbf{r})/2$
Na1···Se109 3.069 Å	0.009	0.037	-0.009	0.002	-0.006	0.008	1.9
H5···Se109 2.426 Å	0.022	0.057	-0.022	0.000	-0.015	0.015	4.7
Na1···N4 2.483 Å	0.018	0.089	-0.018	0.003	-0.016	0.019	5.0
Na1···O3 2.399 Å	0.017	0.098	-0.017	0.004	-0.017	0.021	5.3
Na1···O2 2.384 Å	0.018	0.103	-0.018	0.004	-0.018	0.022	5.6
Na1···N6 2.307 Å	0.026	0.153	-0.026	0.006	-0.025	0.032	7.8
C96···C7 2.919 Å	0.016	0.031	-0.016	0.001	-0.005	0.007	1.6

[*] The numeration of atoms corresponds to their ordering in the attached xyz-file for optimized equilibrium model structure **3TS**.

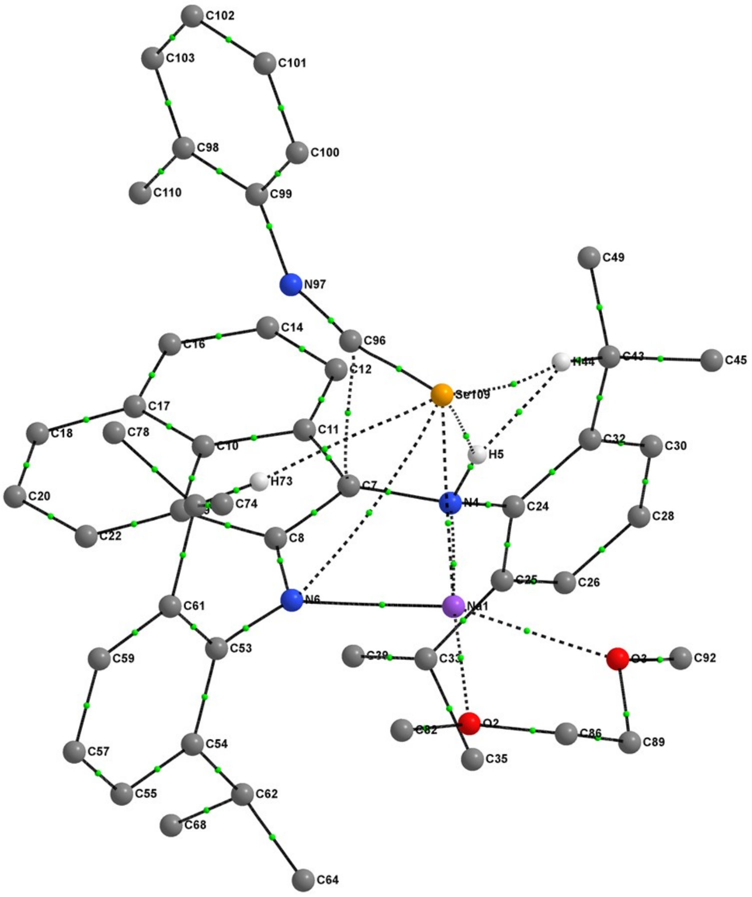

Figure S39. Molecular graph from QTAIM analysis of optimized equilibrium model structure **3TS**. Bond critical points (3, -1) are shown in green.

Table S14. Values of the density of all electrons – ρ(**r**), Laplacian of electron density – $\nabla^2\rho(\mathbf{r})$ and appropriate λ_2 eigenvalues, energy density – H_b, potential energy density – V(**r**), and Lagrangian kinetic energy – G(**r**) (a.u.) at the bond critical points (3, –1), corresponding to Na···O and Na···N noncovalent attractive interactions in the optimized equilibrium model structure **3H_N-isomer** as well as estimated strengths E_{int} (kcal/mol) of these noncovalent interactions.

Contact*	ρ(**r**)	$\nabla^2\rho(\mathbf{r})$	λ_2	H_b	V(**r**)	G(**r**)	E_{int} = –V(**r**)/2
Na1···O4 2.440 Å	0.016	0.087	-0.016	0.003	-0.016	0.019	5.0
Na1···O5 2.430 Å	0.016	0.089	-0.016	0.003	-0.016	0.019	5.0
Na1···N9 2.541 Å	0.016	0.076	-0.016	0.003	-0.014	0.016	4.4
Na1···N6 2.556 Å	0.014	0.070	-0.014	0.003	-0.012	0.015	3.8
Na1···N8 2.368 Å	0.022	0.126	-0.022	0.005	-0.021	0.026	6.6
H7···N9 1.915 Å	0.036	0.116	-0.036	-0.001	-0.031	0.030	9.7

* The numeration of atoms corresponds to their ordering in the attached xyz-file for optimized equilibrium model structure **3H_N-isomer**.

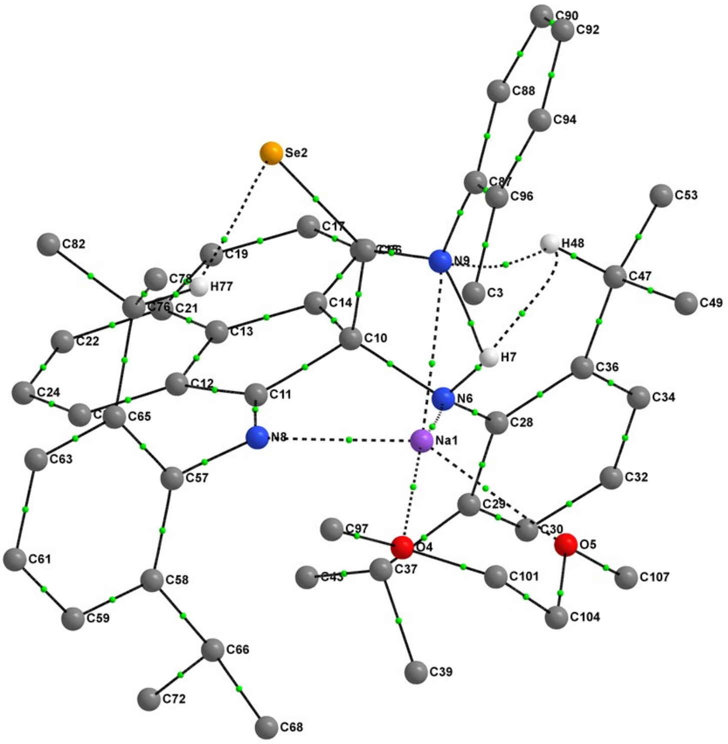

Figure S40. Molecular graph from QTAIM analysis of optimized equilibrium model structure **3H_N-isomer**. Bond critical points (3, -1) are shown in green.

Table S15. Values of the density of all electrons – ρ(**r**), Laplacian of electron density – $\nabla^2\rho(\mathbf{r})$ and appropriate λ_2 eigenvalues, energy density – H_b, potential energy density – V(**r**), and Lagrangian kinetic energy – G(**r**) (a.u.) at the bond critical points (3, –1), corresponding to Na···O and Na···N noncovalent attractive interactions in the optimized equilibrium model structure **3H_N-isomer_TS** as well as estimated strengths E_{int} (kcal/mol) of these noncovalent interactions.

Contact[*]	ρ(**r**)	$\nabla^2\rho(\mathbf{r})$	λ_2	H_b	V(**r**)	G(**r**)	E_{int} = –V(**r**)/2
Na1···O4 2.382 Å	0.018	0.104	-0.018	0.004	-0.018	0.022	5.6
Na1···O5 2.402 Å	0.017	0.097	-0.017	0.004	-0.017	0.021	5.3
Na1···N6 2.441 Å	0.020	0.103	-0.020	0.004	-0.018	0.022	5.6
Na1···N8 2.313 Å	0.026	0.150	-0.026	0.006	-0.025	0.031	7.8
N9···H7 2.004 Å	0.029	0.084	-0.029	-0.001	-0.022	0.022	6.9
C86···C10 2.502 Å	0.035	0.049	-0.035	-0.002	-0.016	0.014	5.0

[*] The numeration of atoms corresponds to their ordering in the attached xyz-file for optimized equilibrium model structure **3H_N-isomer_TS**.

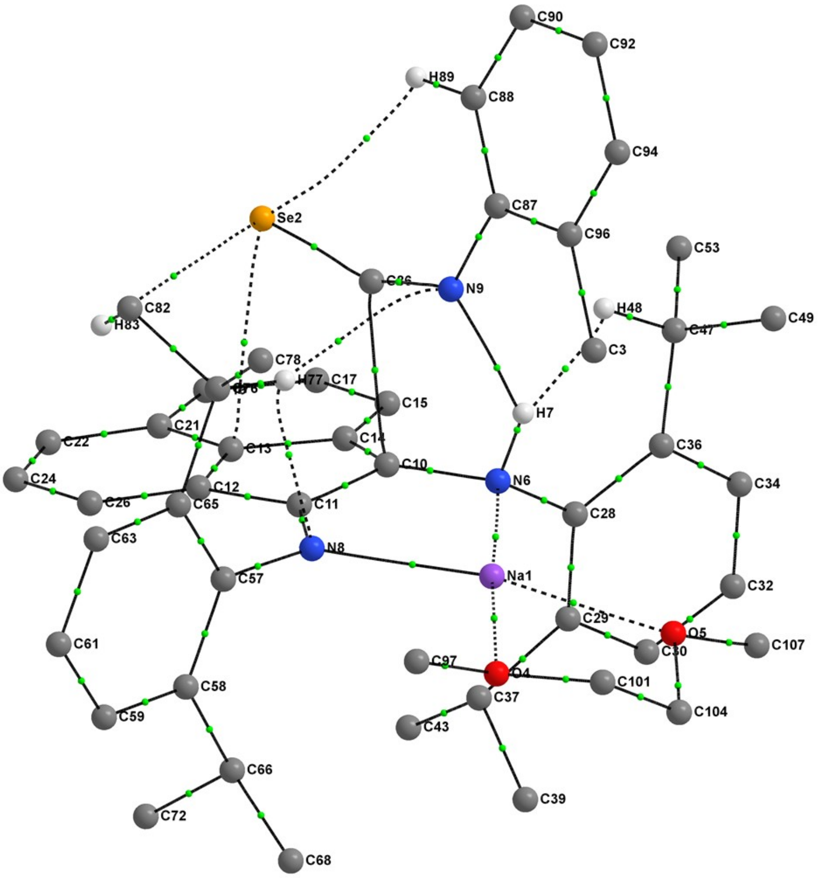

Figure S41. Molecular graph from QTAIM analysis of optimized equilibrium model structure **3H_N-isomer_TS**. Bond critical points (3, -1) are shown in green.

Table S16. Values of the density of all electrons – ρ(**r**), Laplacian of electron density – $\nabla^2\rho(\mathbf{r})$ and appropriate λ_2 eigenvalues, energy density – H_b, potential energy density – V(**r**), and Lagrangian kinetic energy – G(**r**) (a.u.) at the bond critical points (3, –1), corresponding to Na···O and Na···N noncovalent attractive interactions in the optimized equilibrium model structure **11H** as well as estimated strengths E_{int} (kcal/mol) of these noncovalent interactions.

Contact*	ρ(**r**)	$\nabla^2\rho(\mathbf{r})$	λ_2	H_b	V(**r**)	G(**r**)	E_{int} = – V(**r**)/2
Mg1···O3 2.426 Å	0.015	0.077	-0.015	0.002	-0.016	0.018	5.0
Mg1···N4 2.050 Å	0.046	0.307	-0.046	0.009	-0.059	0.068	18.5
Mg1···N5 2.402 Å	0.020	0.098	-0.020	0.002	-0.020	0.022	6.3
Mg1···N6 2.132 Å	0.039	0.240	-0.039	0.007	-0.046	0.053	14.4
Mg1···N7 2.322 Å	0.024	0.128	-0.024	0.004	-0.024	0.028	7.5
Mg1···N8 2.300 Å	0.025	0.137	-0.025	0.004	-0.025	0.030	7.8
Se2···H55 2.946 Å	0.009	0.024	-0.009	0.001	-0.004	0.005	1.3
Se2···H82 3.234 Å	0.006	0.016	-0.006	0.001	-0.002	0.003	0.6
Se2···H88 2.546 Å	0.019	0.056	-0.019	0.001	-0.012	0.013	3.8

* The numeration of atoms corresponds to their ordering in the attached xyz-file for optimized equilibrium model structure **11H**.

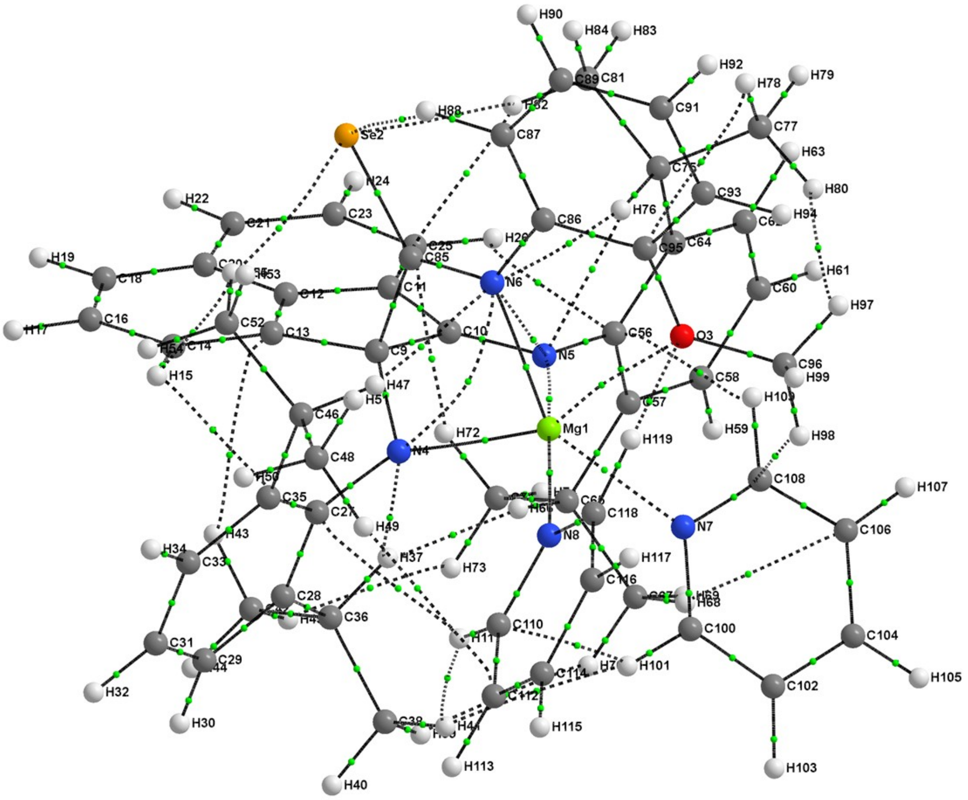

Figure S42. Molecular graph from QTAIM analysis of optimized equilibrium model structure **11H**. Bond critical points (3, -1) are shown in green.

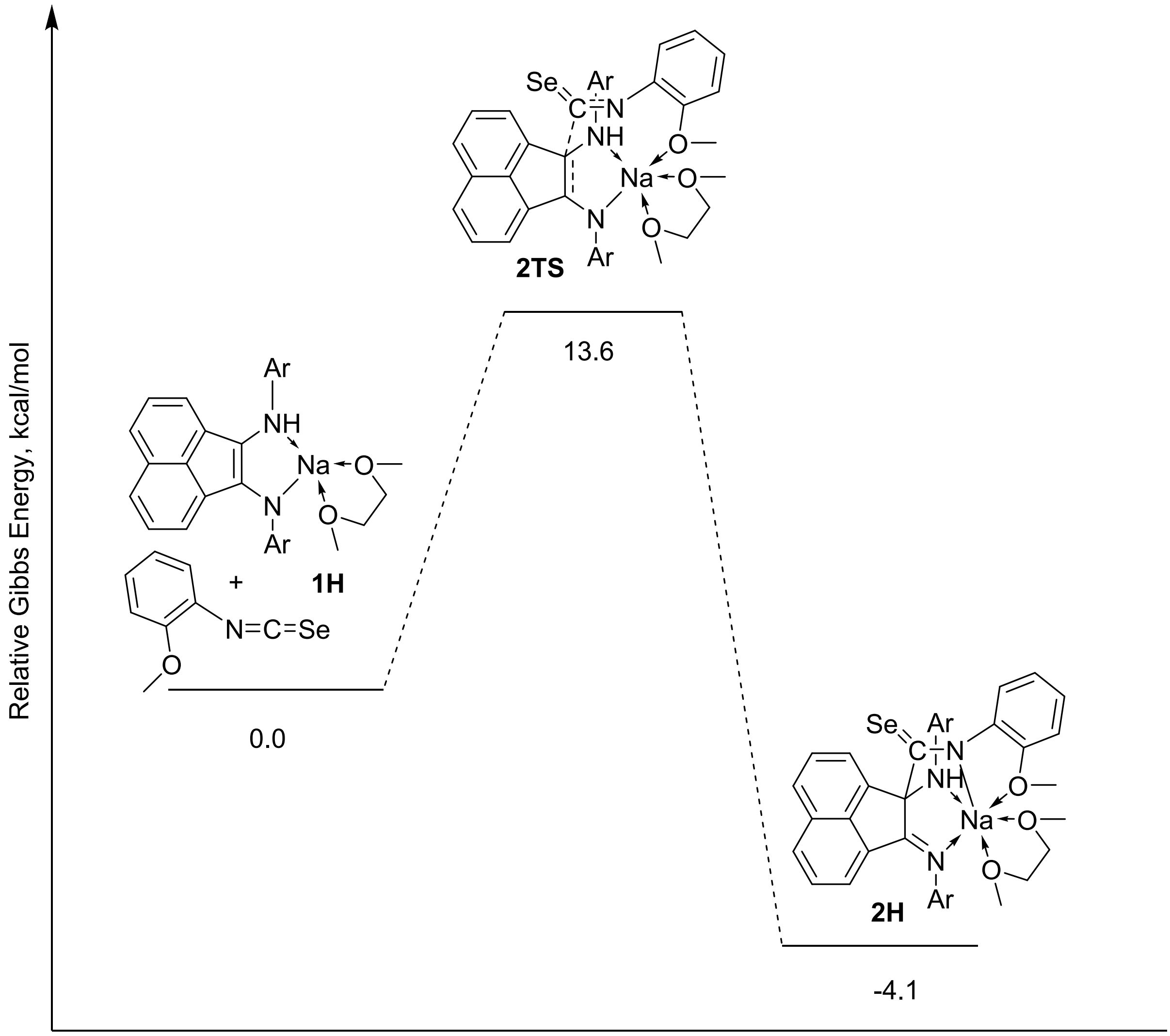

Figure S43. Energy profile (kcal/mol) for the reaction of **1H** + 2-MeOC$_6$H$_4$N=C=Se.

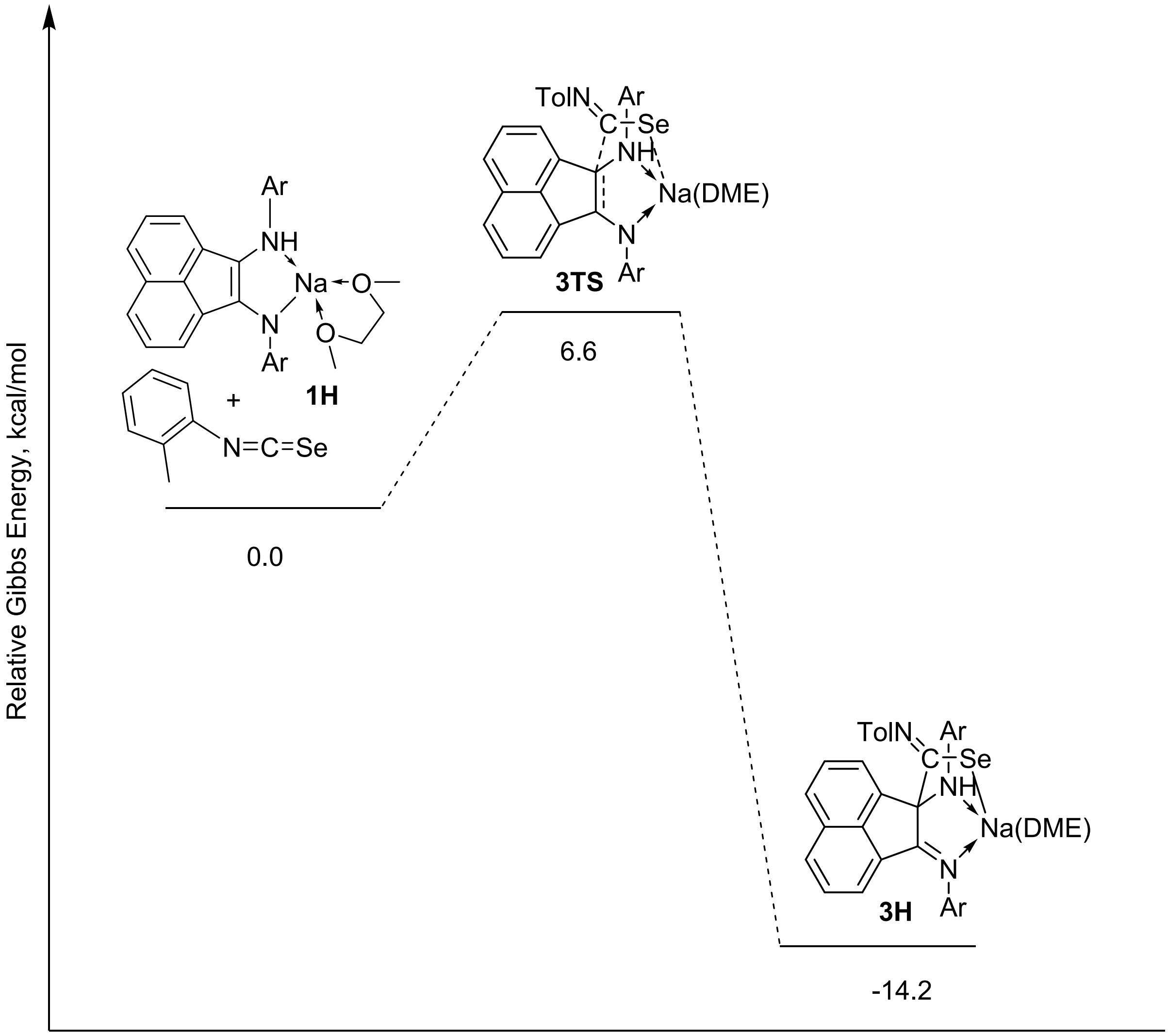

Figure S44. Energy profile (kcal/mol) for the reaction of **1H** + 2-MeC$_6$H$_4$N=C=Se.

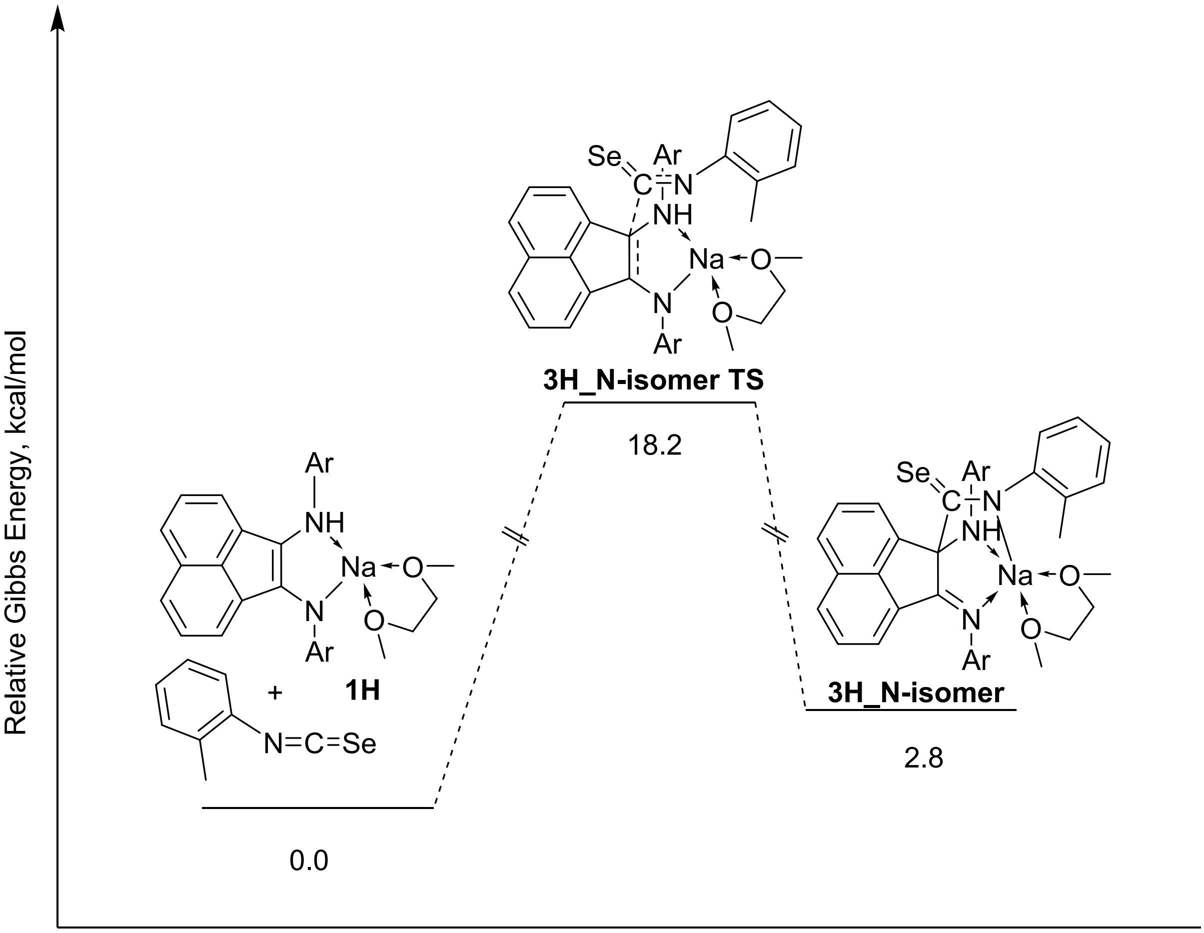

Figure S45. Energy profile (kcal/mol) for the reaction of **1H** + 2-$MeOC_6H_4N=C=Se$ for formation of **3H_N-isomer**.

References

[1] I. L. Fedushkin, A. N. Lukoyanov, A. N. Tishkina, G. K. Fukin, K. A. Lyssenko, M. Hummert, *Chem. Eur. J.* **2010**, *16*, 7563-7571.

[2] I. L. Fedushkin, V. A. Chudakova, G. K. Fukin, S. Dechert, M. Hummert, H. Schumann, *Russ. Chem. Bull.* **2004**, *53*, 2744-2750.

[3] a) V. A. Dodonov, W. Chen, Y. Zhao, A. A. Skatova, P. W. Roesky, B. Wu, X. J. Yang, I. L. Fedushkin, *Chem. Eur. J.* **2019**, *25*, 8259-8267; b) W. Zhang, V. A. Dodonov, W. Chen, Y. Zhao, A. A. Skatova, I. L. Fedushkin, P. W. Roesky, B. Wu, X.-J. Yang, *Chem. Eur. J.* **2018**, *24*, 14994-15002.

[4] I. L. Fedushkin, A. A. Skatova, V. A. Chudakova, G. K. Fukin, S. Dechert, H. Schumann, *Eur. J. Inorg. Chem.* **2003**, *2003*, 3336-3346.

[5] J. Zakrzewski, B. Huras, A. Kiełczewska, *Synthesis* **2016**, *48*, 85-96.

[6] S. Stoll, A. Schweiger, *J. Magn. Reson.* **2006**, *178*, 42-55.

[7] Bruker (2017) SAINT Data Reduction and Correction Program v. 8.38A, Bruker AXS, Madison, Wisconsin, USA.

[8] Data Collection, Reduction and Correction Program, CrysAlisPro 1.171.40.67a - Software Package, Rigaku OD (2019).

[9] L. Krause, R. Herbst-Irmer, G. M. Sheldrick, D. Stalke, *J. Appl. Crystallogr.* **2015**, *48*, 3-10.

[10] R. C. Clark, J. S. Reid, *Acta Crystallographica Section A* **1995**, *51*, 887-897.

[11] G. Sheldrick, *Acta Crystallographica Section A* **2015**, *71*, 3-8.

[12] G. Sheldrick, *Acta Crystallographica Section C* **2015**, *71*, 3-8.

[13] H. Flack, *Acta Crystallographica Section A* **1983**, *39*, 876-881.

[14] Guzei, I.A., Wendt, M. Program Solid-G, UW-Madison, WI, USA, 2004.

[15] O. V. Dolomanov, L. J. Bourhis, R. J. Gildea, J. A. K. Howard, H. Puschmann, *J. Appl. Crystallogr.* **2009**, *42*, 339-341.

[16] a) W.-J. Chang, M. V. Kulkarni, C.-M. Sun, *RSC Adv.* **2015**, *5*, 97113-97120; b) G. Chennakrishnareddy, G. Nagendra, H. P. Hemantha, U. Das, T. N. Guru Row, V. V. Sureshbabu, *Tetrahedron* **2010**, *66*, 6718-6724; c) R. T. Yu, T. Rovis, *J. Am. Chem. Soc.* **2008**, *130*, 3262-3263.

[17] a) S. J. Grabowski, *Tetrahedron* **1998**, *54*, 10153-10160; b) L. Lo Presti, R. Soave, R. Destro, *The Journal of Physical Chemistry B* **2006**, *110*, 6405-6414.

[18] M. J. Frisch, G. W. Trucks, H. B. Schlegel, G. E. Scuseria, M. A. Robb, J. R. Cheeseman, G. Scalmani, V. Barone, B. Mennucci, G. A. Petersson, H. Nakatsuji, M. Caricato, X. Li, H. P. Hratchian, A. F. Izmaylov, J. Bloino, G. Zheng, J. L. Sonnenberg, M. Hada, M. Ehara, K. Toyota, R. Fukuda, J. Hasegawa, M. Ishida, T. Nakajima, Y. Honda, O. Kitao, H. Nakai, T. Vreven, J. A. Montgomery Jr., J. E. Peralta, F. Ogliaro, M. Bearpark, J. J. Heyd, E. Brothers, K. N. Kudin, V. N. Staroverov, T. Keith, R. Kobayashi, J. Normand, K. Raghavachari, A. Rendell, J. C. Burant, S. S. Iyengar, J. Tomasi, M. Cossi, N. Rega, J. M. Millam, M. Klene, J. E. Knox, J. B. Cross, V. Bakken, C. Adamo, J. Jaramillo, R. Gomperts, R. E. Stratmann, O. Yazyev, A. J. Austin, R. Cammi, C. Pomelli, J. W. Ochterski, R. L. Martin, K. Morokuma, V. G. Zakrzewski, G. A. Voth, P. Salvador, J. J. Dannenberg, S. Dapprich, A. D. Daniels, O. Farkas, J. B. Foresman, J. V. Ortiz, J. Cioslowski and D. J. Fox, in Gaussian 09, Revision C.01, Gaussian, Inc., Wallingford, CT, 2010.

[19] I. Mayer, P. Salvador, *Chem. Phys. Lett.* **2004**, *383*, 368-375.

[20] R. F. W. Bader, *Chem. Rev.* **1991**, *91*, 893-928.

[21] T. Lu, F. Chen, *J. Comput. Chem.* **2012**, *33*, 580-592.

[22] T. A. Keith, AIMAll (version 17.11.14), TK Gristmill Software, Overland Park KS, USA, 2017 (aim.tkgristmill.com).

[23] E. D. Glendening, C. R. Landis, F. Weinhold, *WIREs Computational Molecular Science* **2012**, *2*, 1-42.

[24] a) V. N. Mikhaylov, V. N. Sorokoumov, K. A. Korvinson, A. S. Novikov, I. A. Balova, *Organometallics* **2016**, *35*, 1684-1697; b) T. V. Serebryanskaya, A. S. Novikov, P. V. Gushchin, M. Haukka, R. E. Asfin, P. M. Tolstoy, V. Y. Kukushkin, *Physical Chemistry Chemical Physics* **2016**, *18*, 14104-14112; c) K. I. Kulish, A. S. Novikov, P. M. Tolstoy, D. S. Bolotin, N. A. Bokach, A. A. Zolotarev, V. Y. Kukushkin, *J. Mol. Struct.* **2016**, *1111*, 142-150; d) A. A. Melekhova, A. S. Novikov, K. V. Luzyanin, N. A. Bokach, G. L. Starova, V. V. Gurzhiy, V. Y. Kukushkin, *Inorg. Chim. Acta* **2015**, *434*, 31-36; e) A. S. Novikov, M. L. Kuznetsov, A. J. L. Pombeiro, *Chem. Eur. J.* **2013**, *19*, 2874-2888.

[25] E. Espinosa, I. Alkorta, J. Elguero, E. Molins, *The Journal of Chemical Physics* **2002**, *117*, 5529-5542.

[26] E. Espinosa, E. Molins, C. Lecomte, *Chem. Phys. Lett.* **1998**, *285*, 170-173.